Nancy-Université INPL

en co-tutelle avec Zhejiang University

Ecole **D**octorale

Ressources **P**rocédés **P**roduits **E**nvironnement

(RP2E)

Ecole **N**ationale **S**upérieure des

Industries **C**himiques

(ENSIC)

Laboratoire des **S**ciences

du **G**énie **C**himique

(LSGC-CNRS UPR 6811)

Simulation par CFD et mesure en ligne de la distribution des temps de séjour et la qualité de mélange dans une extrudeuse bi-vis

THESE

présentée en vue de l'obtention du

DOCTORAT DE L'INSTITUT NATIONAL POLYTECHNIQUE DE LORRAINE

Spécialité : Génie des Procédés et des Produits

par

Xian-Ming ZHANG

Master en génie des procédés d'élaboration des matériaux

Tianjin University of Science and Technology

Soutenance prévue le 10 novembre 2008 à 14h

Composition du jury :

Rapporteurs :	M. Bruno VERGNES	Directeur de recherche (Mines ParisTech)
	M. Jia-Jun WANG	Professeur (Zhejiang Sci-Tech University, Chine)
Examinateurs :	M. Guo-Hua HU	Professeur (Nancy-Université, INPL) et membre de l'IUF
	M. Lian-Fang FENG	Professeur (Zhejiang University, Chine)

Abstract

The development of new materials with improved properties seems to rely nowadays more on blending and compounding than on the synthesis of chemically new polymers. Mixing may have a great effect on the morphology and structure of multi-component polymer materials. Therefore, the selection of mixing devices and optimization of processing parameters are two important issues in polymer processing. The twin-screw extruders (TSE) have a modular geometry, which allows adjusting the screw profile to control the axial, dispersive and distributive mixing. TSE are widely used as mixers/reactors for blending, compounding, and reactive processing. Study on mixing in twin-screw extruders has been one of the challenges due to the complex geometry configuration and transient flow pattern. Flow visualization provides qualitative analysis for shearing, stretching, and tearing motions of polymers. Morphological analysis of samples obtained from stopping extruders can not necessarily characterize the dynamic feature in extrusion processing. In-line measurement with numerical simulation is used to study mixing in TSE. Polymer processing is an interdisciplinary field with many unsolved, challenging fundamental research topics and practical applications related to polymer rheology, polymer chemistry and physics, instrument science, mechanical engineering, chemical engineering and computational fluid dynamics (CFD).

This work aimed at developing a new instrument to measure in real time the residence time distribution (RTD) which characterizes the axial mixing and transport abilities of different screw elements based on the analysis of the transient flow pattern and systematic evaluation of mixing theory in TSE. Distributive mixing of polymer melts is characterized by the generation of interfacial area, which is experimentally much more difficult to measure. This 3D numerical simulation based on CFD is adopted. Most relevant results obtained in this work are summarized as follows.

First, we developed a new instrument to measure in real time the RTD in screw extruders based on fluorescent excitation and emission. It possessed two light paths/two optical probes, allowing simultaneous measurement of the RTD at two different locations. The evaluation of the set-up was done in terms of the reproducibility, on the one hand; the linearity between the amplitude of the response signal and the amount of the tracer, on the other hand. Results showed that this device was accurate and reliable for in-line monitoring of the RTD in screw extruders. The

effect of different kneading discs and one special mixing element on local RTD was studied and the screw configurations were designed to match the in-line measurement. The axial mixing quality was characterized by the width of the RTD curve. The result showed that the local RTD of a kneading zone depended very much on the staggering angle of the kneading discs.

Secondly, it was confirmed theoretically and experimentally that specific throughput Q/N, defined as a ratio of throughput (Q) over screw speed (N), was indeed a key process parameter for controlling the dimensionless time distribution, residence revolution distribution (RRD) and residence volume distribution (RVD). For a given value of Q/N, the overall, partial and local RTD were different when Q and N varied. However the corresponding dimensionless RTD as well as the RRD and RVD all fell on single master curves, respectively. The relationship among those three different distributions was established. It was concluded that the mean degree of fill and complete fill length were the same for a given value of Q/N, leading to the superposition of RRD, RVD and dimensionless RTD curves.

Finally, the flow mechanisms and distributive mixing in the kneading disc domain of co-rotating twin screw extruders were studied by the 3-D finite element method. The Mesh Superposition Technique (MST) was introduced to modeling intermeshing twin-screw extruders without calling upon remeshing. A rigorous validation of the model was carried out. Comparison of the 3D model against experimental RTD data is presented. Results confirmed the ability of the model to predict the flow and mixing behavior. Initially, these particles are randomly distributed in an inlet vertical plane and their trajectories between the inlet and outlet are calculated from the velocity profiles. Along each trajectory, the residence time is obtained. The residence time distribution is then obtained based on the residence time of each of those particles. Simulated results are compared with experimental ones obtained by an in-line measurement. The distributive mixing parameters such as the area stretch ratio of material surface η, instantaneous mixing efficiency e_η and time-averaged mixing efficiency $\langle e_\eta \rangle$ are calculated using the interface tracking techniques. These parameters are then used to compare the distributive mixing performance and efficiency of different kneading discs.

Résumé

Aujourd'hui le développement de nouveaux matériaux polymères ayant de bonnes propriétés repose de plus en plus sur des procédés de mélange ou de compoundage de polymères au lieu de recourir à la synthèse de nouvelles molécules. L'action du mélange peut fortement influer sur la morphologie des matériaux polymères multi-constituants. Elle dépend du type de mélangeur et des conditions du procédé. Les extrudeuses bi-vis (TSE) ont une géométrie modulable permettant d'adapter leurs profils de vis aux besoins des mélanges dispersif et distributif. Elles sont souvent utilisées comme mélangeurs/réacteurs pour des procédés de mélange, de compoundage et d'extrusion réactive. Cependant, l'étude sur la qualité du mélange dans les TSE demeure un grand défi en raison de la complexité géométrique et du caractère transitoire de l'écoulement. La visualisation de l'écoulement offre une analyse qualitative de la qualité du mélange. La morphologie des échantillons obtenus par l'arrêt de l'extrudeuse ne permet pas d'analyser le caractère dynamique des procédés d'extrusion. Il serait préférable d'étudier la qualité du mélange dans des TSE à l'aide de mesures en ligne couplées à des simulations numériques. Le " polymer processing" est un domaine de recherche pluridisciplinaire qui fait appel à la rhéologie, à la chimie, à la physique, à l'instrumentation, au génie des procédés et à la mécanique des fluides numérique et qui présente beaucoup de problèmes fondamentaux à résoudre et beaucoup d'applications pratiques à exploiter.

Cette thèse a pour objet de développer un nouvel instrument en line pour mesurer en temps réel la distribution des temps de séjour (DTS) qui caractérise la performance du mélange axial et la capacité de convoyage de différents types d'éléments de vis basées sur l'analyse de l'écoulement transitoire et l'évaluation systématique de la théorie de mélange dans les TSE. Le mélange distributif des polymères fondus est caractérisé par la génération de l'aire des interfaces, un paramètre difficile à mesurer expérimentalement. Alors on fait appel à des simulations numériques de type CFD. Les principaux résultats obtenus dans ce travail se résument de la manière suivante :

Tout d'abord, un nouvel appareil a été mis au point. Il permet de mesurer en temps réel la DTS dans une extrudeuse bi-vis sur la base du principe d'excitation et d'émission fluorescentes. Il est muni de deux chemins lumineux / deux sondes optiques permettant la mesure simultanée de la DTS à deux endroits différents. La performance de cet appareil a été évaluée en termes de reproductibilité, d'une part; et

de la linéarité entre l'amplitude du signal et la concentration du traceur, d'autre part. Il a été démontré que cet appareil est précis et robuste. L'influence de différents types de disques de mélange et celle d'un élément spécifique sur les DTS locales ont été étudiées. La qualité du mélange axial est caractérisée par la largeur de la courbe de la DTS. Il s'est avéré que la DTS locale d'une zone composée de disques de mélange dépend fortement de leur angle d'hélice.

En deuxième lieu, il a été confirmé théoriquement et expérimentalement que le débit spécifique Q/N, défini comme le rapport entre le débit (Q) et la vitesse de rotation des vis (N), est un paramètre clé du procédé pour contrôler la distribution des temps de séjour adimensionnels, celle des révolutions de séjour (DRS) ainsi que celle des volumes de séjour (DVS). Pour une valeur de Q/N donnée, les DTS globale, partielle et locale varient avec Q et N. Cependant, les DTS adimensionnelles correspondantes ainsi que les DRS et DVS se superposent sur les courbes maîtrises respectives. La relation entre ces trois différentes distributions a été développée. Il a été conclu que lorsque le rapport Q/N est fixe, le taux de remplissage moyen et la longueur remplie sont également fixes. Ce qui conduit à la superposition des courbes de DRS, DVS et DTS adimensionnelles.

Enfin, les mécanismes de l'écoulement ainsi que le mélange distributif dans la zone de mélange d'une extrudeuse bi-vis ont été étudiés par une méthode d'éléments finis 3-D. Une technique de superposition de maillages (MST) est employée pour modéliser l'écoulement dans une extrudeuse bi-vis sans remaillage. Ce modèle a été validé avec des données expérimentales de la DTS. Les résultats confirment la capacité de ce modèle à prédire l'écoulement et la qualité du mélange. D'abord, les particules sont réparties de manière aléatoire sur le plan vertical de l'entrée and leurs trajectoires entre l'entrée et la sortie sont calculés à partir des profils de vitesse. Le temps de séjour est obtenu pour chaque trajectoire. La DTS est alors obtenue à partir du temps de séjour de chacune de ces particules. Les résultats simulés sont comparés avec ceux des expériences obtenues à l'aide de l'appareil de mesure en ligne. Les paramètres du mélange distributif tels que le rapport de l'aire d'étirement de la surface du fluide η, l'efficacité instantanée du mélange e_η et la moyenne de l'efficacité du mélange par rapport au temps de mélange $\langle e_\eta \rangle$ sont calculées en utilisant les techniques de suivi des interfaces. Ces paramètres sont ensuite utilisés pour comparer la performance et l'efficacité du mélange distributif de différents types de disques de mélange.

Acknowledgements

I would like to take this opportunity to recognize the support and contributions of some special individuals without whom I would not have been successful in my research. Most important is the continued instructions, patience, insight and great inspiration for me throughout the entire project made by my advisors, Professors Guo-Hua HU and Lian-Fang FENG. They trained me a lot of important skills necessary for a PhD student. Following your vision of reactive extrusion, I was able to achieve my academic and scientific goals.

I deeply appreciate Dr. Jia-Jun WANG, Ms. Xu-Ping GU, whose expertise, helpful suggestions and friendly guidance in all phase of my study are essential to the accomplishment of this work.

I also like to thank my friends: Guang-Zan LI, Cai-Liang ZHANG, Lu-Gang WANG, Xiao-Bo SONG, Feng-Yong LI, Yu-Hua XUE, Jing CHANG, Wen-Feng ZHANG, Yan-Fei TANG, Jin-Xia LI and Penu CHRISTIAN, who made my experience an enjoyable one. Thank you for your friendship and assisting me with assignments.

I am grateful for the financial support from the China Scholarship Council (CSC) enabled me to complete my study in France in 2007. Without the financial support, it would have been impossible for me to complete my academic pursuits smoothly.

I own a debt of gratitude to my wife, my parents, and my brother, for their patience and understanding. They put my interests above their own needs and desires, yet they still supported me and encouraged me throughout this four-year period.

Table of Contents

List of Figures

List of Tables

CHAPTER 1 Introduction

The melt blending of different existing homopolymers is an important route to obtain the specific material properties that homopolymers often cannot accomplish. The mixing of polymer melts is a critical process because the final product properties depend on its uniformity[1]. However, turbulent mixing is usually unobtainable in polymer processing due to the sufficiently high viscosity of polymer and diffusion coefficients for even very small molecules are exceedingly low. Most polymers in melt processing exhibit "viscoelastic" behavior, meaning that they exhibit not only viscous behavior but also elastic behavior in the liquid state. Viscous energy dissipation during mixing can cause significant temperature variation throughout a vessel, thus contributing to further viscosity nonuniformity, and possibly product degradation[2]. The above limitations are great challenges for polymer processing. Selection of a mixing device can be complex such as the relationship between the mixing impeller and its position in a mixing vessel is critical to process results.

1.1 Classification of Extruders

Screw extruders are the most important piece of polymer processing equipment. They are divided into two main types: single and twin screw extruders. The key advantages of twin-screw extruders are higher functionality, lower energy consumption and flexibility, which have been widely used for extruding, mixing, and kneading for various polymer materials. Meanwhile, they often used as continuous reactors for preparing multiphase polymer materials such as polymer blends and polymer composites. Twin screw extruders are divided into three types according to the intermeshing structure. These are non-intermeshing, tangential and intermeshing twin screw machines. There are also classified into many types by their rotational direction: co-rotating twin screw extruders and counter rotating twin screw extruders. Fig. 1.1 shows a number of twin screw extruders' designs which combine the features mentioned above[3]. Generally speaking twin-screw extruders used in industries are three predominant designs which are intermeshing co-rotating, intermeshing

counter-rotating and non-intermeshing counter-rotating. The advantage of the co-rotating extruders is more flexible and stable extrusion characteristics against fluctuations of pressure and the temperature. The higher output rate can be obtained from the intermeshing counter-rotating extruders, although its extrusion stability is inferior to that of co-rotating extruders[4].

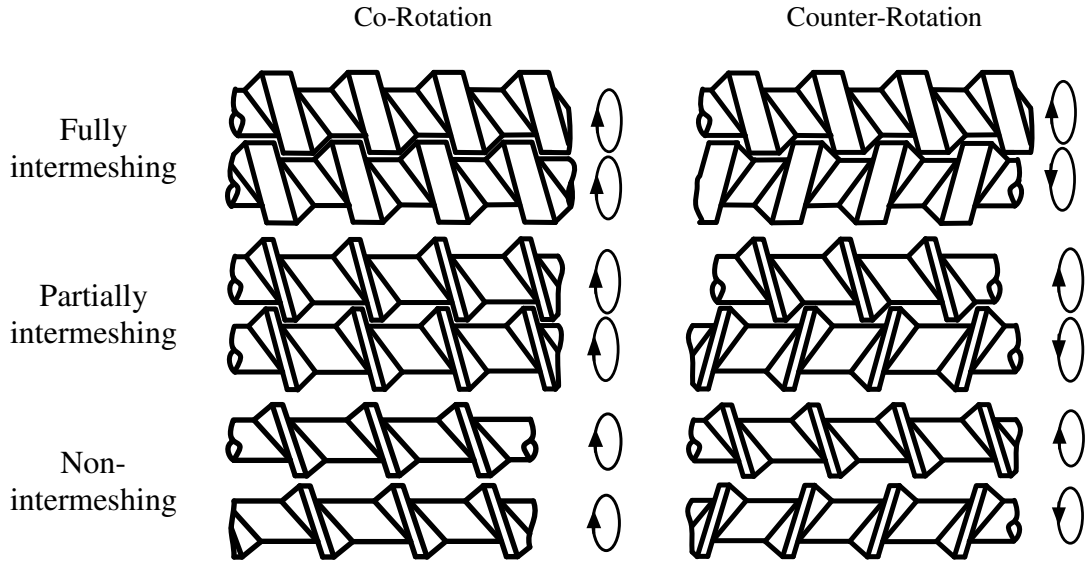

Fig. 1.1 Twin-screw extruders of various kinds

Co-rotation twin-screw extruders are built in a modular fashion to meet the diversity of tasks such as mixing, reaction extrusion and devolatilization. Screw elements are assembled on shafts. They are three main types of elements: full flight conveying elements, kneading discs mixing elements and special mixing elements which are presented in Fig. 1.2.

Full flight conveying elements can have right-handed or left-handed shapes which are characterized by its pitch and length, Right-handed screws are so defined that screw rotation pumps material forward from hopper to the die, and left-handed elements convey material back toward the feed throat. Screw conveying elements can have various numbers of thread starts. Screws with two thread starts are most common (Fig. 1.2a).

The second elements, the kneading discs, are characterized by individual disc length, number of discs and stagger angle between successive discs. The kneading discs can provide the different distributive and dispersive mixing according to the combination of kneading discs. The kneading discs very frequently work under a fully filled channel condition.

Manufacturers of intermeshing co-rotating twin-screw extruders offer various special mixing elements as alternatives to kneading discs to achieve certain mixing function. These included the efforts by Kobe Steel and Farrel Inc., Werner&Pfleiderer, and Berstorff[5, 6]. The elements can be arranged by the machine user in anyway that is desired to carry out the proposed manufacturing process. Fig. 1.2c shows one classic construction of special element. The purpose of these elements is to provide better mixing due to multiple division, reorientation and recombinations of the flow fluid with less energy consumption. These gear mixing elements are defined by the number of gear around the circumference and the angle of inclination along the axial direction. The gear used to split the flow liquid to generate the interfacial surface; different inclination angles contributed to the different conveying capacity.

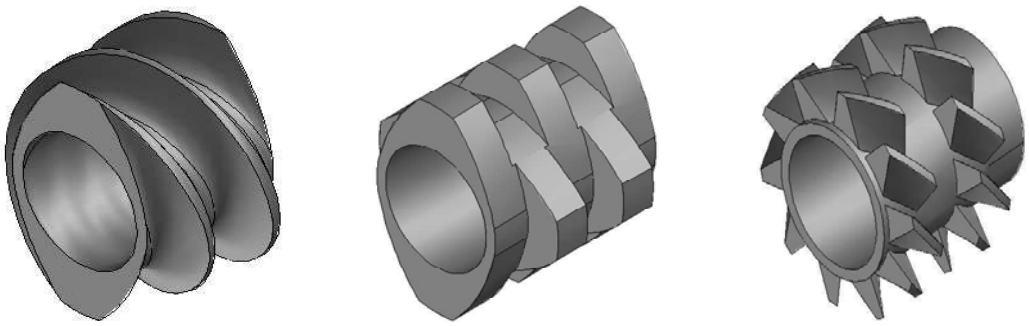

(a) Conveying elements (b) Kneading disc (c) Special mixing element

Fig. 1.2 Common elements in co-rotating twin screw extruders.

1.2 The Residence Time Distribution in Extruders

The axial mixing in extruders is connected to the residence time distribution (RTD). The RTD has the following applications in extrusion processes:

a) An important use of residence time measurements is to diagnose abnormalities in flow. If the average residence time is lower than expected value (the ratio of fill volume to throughput), it suggests the extruder used has stagnancy. A higher average residence time is more likely to be caused by experimental error[7]. Therefore, the RTD data are useful for guidance in the selection of appropriate mixing devices and the combination of screw elements.

b) Extrusion of polymers in a screw extruder is composed of a series of thermal, physical and eventually chemical histories/changes occurring in a simultaneous and/or consecutive manner inside the extruder. The time a flow element spends in the extruder can be a measure of the extent of these histories/changes. Thus the RTD provides an aspect of the heating and shearing histories in the screw channel and is helpful for understanding the effects of extrusion variables and screw geometry.

c) For reactive extrusion processes where the reaction time is the same order of mean residence time, for example some types of grafted reaction for polyethylene and polypropylene, the RTD is of interest since the length of time that the material remains in extruder should be closely coupled to the reaction kinetics and hence greatly impact product quality. For example, if a reaction is first order with rate constant k, the knowledge of the RTD allows the reaction yield to be calculated.

d) Although the one dimension (1-D) reactor models and computational fluid dynamic (CFD) methods are increasing popular in the simulation of extrusion processes, experimental validation of simulated results is a big challenge. Velocity measurements are difficult; pressure drop measurements are easy but insensitive to the details of the flow. The global, partial and local RTDs in a twin-screw extruder will be a useful tool for the validation.

1.2.1 Off-line Measurements

Typically the RTD is measured when the extrusion process has reached a steady state. A tracer is injected to the flow stream (usually at the hopper) as a pulse, the time interval being so short that the input can be considered as a Dirac function. The RTD can be measured off-line, on-line or in-line. Off-line methods are relatively simple in device. A review of off-line measurement in different extruders is presented in Table 1.1. However, measurements are done in a discrete manner. Thus, they are often very time-consuming and generally cannot be performed automatically. Moreover, the resulting data points may not be numerous enough and/or may lack accuracy. Shon et al. [8] used off-line method to measure the RTDs of co-rotating twin-screw extruders. The experimental data are presented in Fig. 1.3 which has small numbers of points and greater scatter in the tail region. This reduces the confidence in the calculated

average residence time and variance. With the development of measurement methods, the off-line will be replaced by in-line or on-line methods step by step.

Table 1.1 Summary of the literature on off-line RTD measurement in extruders

Measurement method	Tracer	Extruder type	Reference	Date
Spectrophoto-mer	Color dye	Single screw	Bigg et al.[9]	1974
		Co-rotating	Todd[10]	1975
		Single screw	Weiss et al.[11]	1989
UV	Carbon Black	Co-rotating	Kao et al.[12]	1984
	Phenyl, Anthracene grafted PVC	Co-rotating Counter-rotating	Cassagnau et al.[13]	1991
	Anthracenemethanol	Co-rotating	Oberlehner et al.[14]	1994
	1-Aminoanthraquinone	Co-rotating	Sun et al.[15]	1995
			Hu et al[16]	1996
	Free anthracene, Anthracene grafted PS	Buss cokneader	Hoppe et al.[17]	2002
Radioactivity	Manganese dioxide	Counter-rotating	Janssen et al.[18]	1979
		Single screw	Tzoganakis et al.[19]	1989
Particles count	NaCl crystal	Single screw	Kemblowski et al.[20]	1981
	Aluminum flakes	Buss kneader Co-rotating Counter-rotating	Shon et al.[8]	1999
X-ray fluorescence	Sb oxide	Co-rotating Counter-rotating	Rauwendaal[21]	1981
Calcinate	Silica	Co-rotating	Carneiro et al.[22]	1999

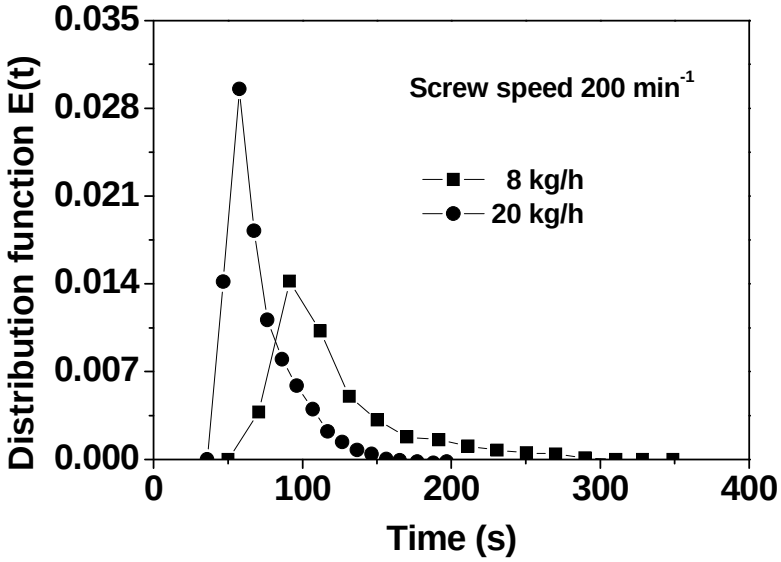

Fig. 1.3 Comparison of residence time distribution at different feed rate in a co-rotating twin screw extruder (off-line)

1.2.2 In-line Measurements

By contrast, in-line measurements continuously analyze the flow material in real time and have no need to collect samples like off-line methods do. Thus, in-line measurements have many advantages over off-line ones[23]. On-line methods slightly differ from in-line ones in that sample are collected through a bypass and then analyzed. Thus the flow stream is more or less perturbed. However, both sample collection and analysis are done in a continuous manner. Recent studies developed on-line and in-line methods for the RTD measurement that used different tracers and detection devices. Detection principles are based on properties such as radioactivity (MnO2, La2O3, etc.), ultrasound reflectivity (filling, carbon black, etc.), optical reflectivity (TiO2), electrically conductivity (KNO3, NaNO3, KCl, etc.), light transmission (carbon black), and fluorescence emission (anthracene). Advantages and weaknesses of those measurements will be reviewed in the following sections.

1.2.2.1 Radioactive Methods

The radioactive method has a high sensitivity, and even with the low tracer concentrations required which depends on the neutron flux to which the manganese is subjected to during irradiation and the specific isotope used. Wolf and White[24] introduced this measurement technology to study the RTDs of a single screw extruder

and counterrotating twin-screw extruders. The tracer used was a masterbatch of 1% manganese dioxide ($Mn^{55} \xrightarrow{(n,\gamma)} Mn^{56}$) in PE. The detection of the γ rays emitted by the radioactive tracer was made with a sodium iodide probe. The intensity of the radioactivity of the radioisotope in the sample is a function of radiation time and other parameters by using the following equation:

$$I_A = \frac{N_0 \sigma_0 \phi a W}{3.7 \times 10^7 M} (1 - e^{-0.693 \frac{t_i}{t_{1/2}}})(e^{-0.693 \frac{t_c}{t_{1/2}}}) \qquad (1.1)$$

in which N_0 is the Avogadros numbers, σ_0 is the cross section of isotope to nuclear reaction, Φ is neutron flux, a is the natural abundance of active isotope, W is weight of irradiated sample, $t_{1/2}$ is the half-life of the radioisotope. Thompson et al.[25] used the radioactive technique to measure the RTDs of a counter-rotating non-intermeshing twin screw extruder. Manganese was chosen for the tracer species. The measuring system (detector and shielding) is similar to that used by Wolf and White[24].

Kiani et al.[26, 27] designed a special measuring plate to study the RTD and morphology simultaneously. The radionuclide Indium-113m with a half time of 100 min are used as labeling agents. Only small amount of these tracers (10^{-8} - 10^{-6} gm) are needed as labeling agents due to the high sensitivity. Gamma radiation penetrates the barrel walls of the extruder and enables detection of radiotracer concentration at nearly any point along the length of the machine. The effect of operating parameters on RTD was investigated such as screw speed, screw configuration and feed rate.

As far as the radioactive method is concerned, the sensor must be shielded very carefully to reduce background noise, and the extrudate must be removed immediately. The limitation of this method is that the alpha ray is harmful to our health, and the measurement devices are ponderous.

1.2.2.2 Ultrasound Reflection

Ultrasound method has found numerous uses in widely different fields of application, in particular to characterize composition of polymer blends, the extrusion flow instabilities, the filler concentration, and molecular weight distribution, etc. Gendron et al.[28] proposed ultrasound method for in-line determination of the RTD in twin-screw extruders. The method is based on the polymer filled by solid particles induced the ultrasound attenuation. Particle concentration is correlated with the intensity of the ultrasound. The result showed that the ultrasound technique is suitable

to monitor RTD in extruders due to its nonintrusive nature and good sensitivity. Chalamet and Taha[29] used the same method to research the RTD of reactive extrusion in extruders. The slit die was equipped with two pressure transducers, a thermocouple and ultrasound probe used in the experiment (Fig. 1.4). The effect of the filler nature on RTD, viscosity evolution and condensation reaction were investigated. Comparing the RTDs obtained using the different particle tracers showed the particles have great influence on the results because the tracers change the viscosity of the system.

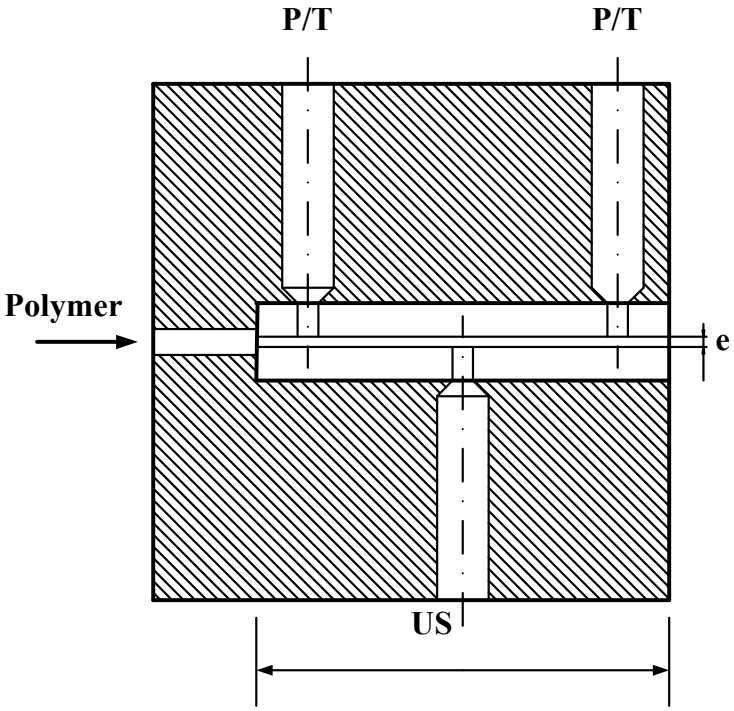

Fig. 1.4 Extrusion die designed for the ultrasonic method

Lee et al.[30] carried out RTD measurement in a co-rotating twin-screw extruder using a non-destructive ultrasonic monitoring system and used CaCO3 as ultrasonic tracer. RTD measurements were carried out with various tracer concentrations, screw speeds, feed rates and screw configurations. The flow in the extruder approached plug flow as the feed rate increased, whereas an increase in the screw speed resulted in the flow approaching mixed flow.

1.2.2.3 Electrical Conductivity

Choudhary and Goutam[31] developed a technique of the measuring the RTD in-line based on the electrical conductivity of material in the die and used a series

circuit. Change in the current flow was measured by an electrical sensor. Results of this method were reported to be well correlated with those of the well established colored tracer method. Unlu and Faller[32, 33] investigated the effects of feed rate screw speed on the RTD and the barrel degree of fill based on electrical conductivity method. The tracer was the Potassium chloride (KCL). The electrical circuit configuration was similar to the one designed by Choudhury and Gautam. Two electrodes were inserted into the extrusion die as probes. The 2V DC-voltage and a 10 Ω resistor composed the circuit and connected with electrodes (Fig. 1.5). The proportional voltage response on the 10R resistance was measured by a digital multimeter and the melt electrical conductivity was obtained from the voltage measurement across the10 Ω resistor using circuit analysis and Ohm's Law expressed as:

$$I_s = \frac{V_s}{R_s} = \frac{V_t}{R_t} = \frac{V_t}{R_s + R_d} \tag{1.2}$$

$$R_d = \frac{V_t R_s}{V_s} - R_s \tag{1.3}$$

$$K_d = \frac{1}{R_d} \tag{1.4}$$

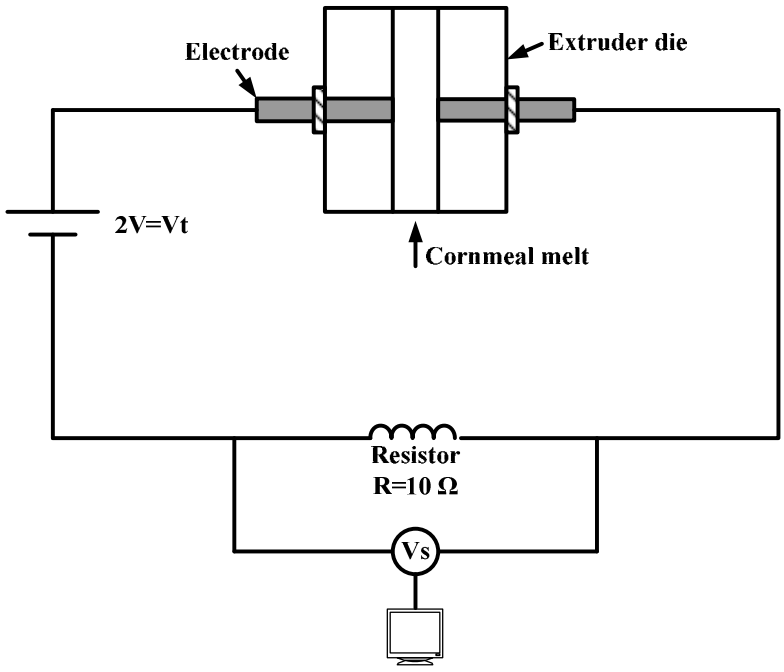

Fig. 1.5 Series circuit configuration for measuring melt conductivity response during extrusion

Van den Einde et al.[34] used the electrical conductivity to measure the partial RTD

at two points in the extruder. The material used for extrusion was a solution of waxy cornstarch in water. The tracer was the mixture of this starch solution, NaCl and water. The extruder used was a transparent model of a corotating twin-screw extruder. The concluded the type and position of mixing elements affected the upstream and downstream RTD and flow pattern.

The electrical conductivity mainly used in food industries with low viscosity and temperature which cannot be used to measure the RTD of polymer melt in extruders.

1.2.2.4 Light Reflection

Wetzel et al.[35] used the light reflection method to determine the local RTD in a small section of a co-ratoting twin-screw extruder. A dual probe can be inserted into various positions along the extruder. The working principle of this reflective probe is shown in Fig. 1.6. A bifurcated optical fiber was mounted in a stainless steel shell with a transparent sapphire window. A pulse of a titanium oxide tracer was injected at the feeder and the concentration of the tracer was detected by optical probes at two positions. This measurement gives great flexibility to the research of RTD but relies heavily on the light scattering of the tracer. Polybutene was used as the model fluid which is a Newtonian fluid at the normal shear rate.

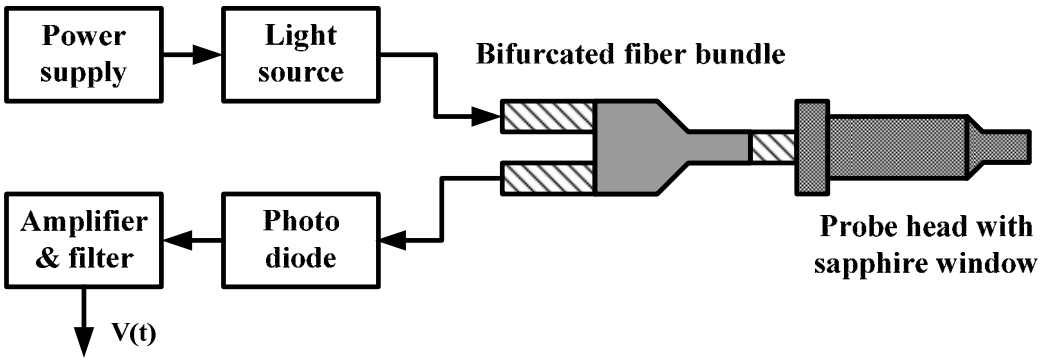

Fig. 1.6 Reflective optical probe configuration

Gao et al.[36, 37] used the same device to research the mean residence time and RTD in co-ratotaing extruders. According to the results, a predictive model for mean residence time was developed which can be used to explain the experimental results. Elkouss et al.[38] investigated the influence of polymer viscoelasticity on the RTD using light reflection method. Based on the detail analysis, they concluded viscoelastic nature of the polymer must be taken into account in analyzing extrusion processes.

However, the probes are sensitive to screw surface reflections and screw rotation which must be excluded from the signal by data processing. Also the correlation between the probe single and tracer concentration is quite difficult and the proper calibration is a great drawbacks.

1.2.2.5 Light Transmission

When an in-line measurement is required, it is necessary to develop a suitable sensor to detect the tracer concentration continuously under extrusion processes. Chen et al.[39] selected light transmission method to study the RTD in extruders. A He-Ne laser was used as the light source. A photomultiplier mounted in die was selected to detect the concentration variation of carbon black in PP. From the experimental results, they concluded that light transmission method works well and gives good RTD curves with an error range of less that 6 % of the mean residence time.

Mélo et al.[40, 41] presented an in-line transmission light device to measure the RTD curves under continuously extrusion. The measurement system is composed of a slit die with transparent windows (Fig. 1.7). The light source was incandescent W filament microbulb. The polymer used as flow media was PP and the tracer was a masterbatch of organic pigment (blue phthalocyanme) and PP. Measurements were taken from a W&P ZSK 30 twin-screw extruder operating with various screw speeds, feed rate and screw configurations.

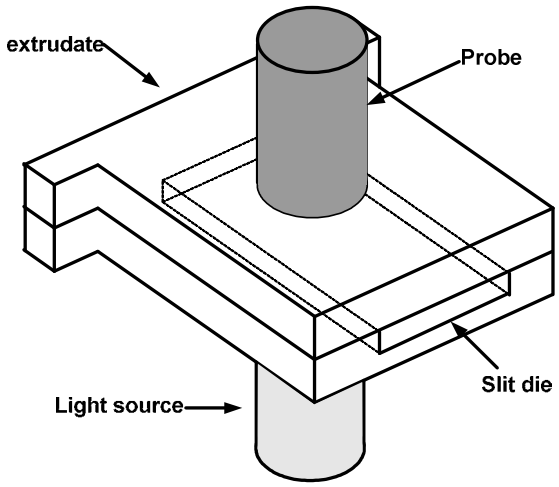

Fig. 1.7 Extrusion die designed for the light transmission method

1.2.2.6 Fluorescence Emission

Bur et al.[42] employed the fluorescence spectroscopy method to measure the flow instability and quality-of-mix of highly filled polymeric systems using a small-molecule fluorescent dye. They hypothesized that the mixing uniform mixing is achieved when the fluorescence intensity is constant with time. Hu et al.[23, 43] used the method to measure the RTD in co-rotating extruders. The set-up of the measuring system is shown in Fig. 1.8. The guide/support system was used to guide and support the extrudate and to prevent it from exposure to the daylight. The optical fiber probe can transfer the UV-light generated by mercury lamp and fluorescence emission excited by 9-(methylaminomethyl) anthracene. The tracer was previously incorporated in PS and PMMA backbones, which guarantee the molecular tracers have same rheological and miscible behavior with the extrudate.

Poulesquen et al.[44] reported the results of RTD measurements carried out in different extruders with various operating conditions using an in-line fluorescence emission and off-line methods. In order to be able to predict RTD for extrusion processes, a new model without adjustable parameters was presented and validated by the experimental RTD. Cassagnau et al.[45] studied the distributive mixing in batch mixers based on the fluorescence monitoring method. Hydroxymethyl anthracene was used as fluorescence tracer and was preliminarily dispersed in the minor component. Structure development during mixing of miscible polymers blends and immiscible polymer blends was investigated by this method. Cassagnau et al.[46] used fluorescence emission method to reveal the mixing process of two phases of strongly different viscosity in a co-rotating twin-screw extruder. For miscible binary systems, the RTD of each phase is basically the same. For immiscible binary systems, when the flow rate is high, the shape of the RTD of both phases may be different. Carneiro et al.[47] developed an in-line measurement device of RTD based on the light emission. The in-line RTDs in single and co-rotating twin screw extruders were compared with off-line measurements, the agreement is good.

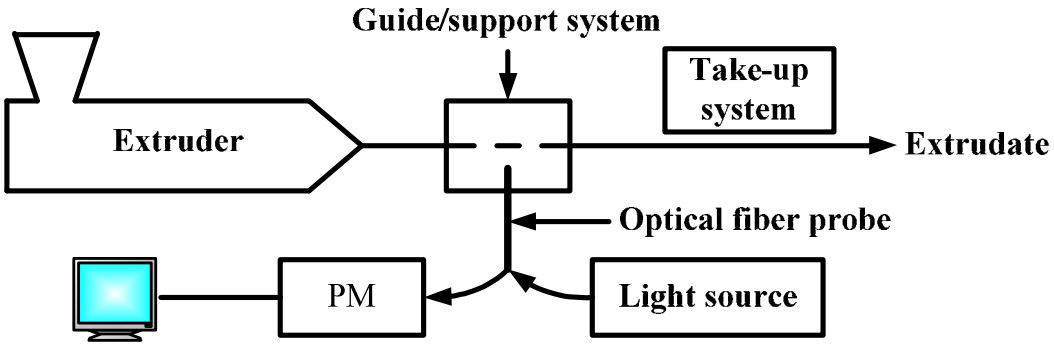

Fig. 1.8 A schematic diagram of the fluorescence-monitoring device for on-line measurement of the RTD

1.2.2.7 Magnetic Susceptibility and Other Methods

The magnetic susceptibility of iron powder for in-line measurement of RTD were used by Puaux et al.[48]. The described technique demands a relatively simple measurement set-up and is easily adaptable for computer data acquisition. The main purpose of the investigation is to test the one and two-parameter models which can be used to simulate the reactive extrusion. The results showed that the back-flow cell model and ADM model are suitable to fit the experimental data and to explain the physical features of the corotating twin-screw extruder.

Razaviaghjeh et al.[49] introduced an in-line method for measuring the RTD of twin screw extruders based on the free radical modification of PE. When a free radical initiator was added into PE melt, the chain branching and crosslinking of PE will increase the viscosity of reaction system, thus lead to an increase of torque of the extruder which can be recorded by a computer. The results measured by this method are in good agreement with that of off-line method. Gilmor et al.[50] used spectrometer to quantitatively monitor, in-line, the color of the polymer melt. The variation of color concentration with time can be used to calculate the RTD.

1.3 The RTD Simulation Using One Dimension Reactor Models

A profound understanding of flow and mixing behavior is necessary to produce the satisfactory products and design the screw configurations. One dimension reactor

model is a method used to predict the RTD, temperature, pressure and the degree of fill. The modeling of flow conditions may be used to predict the extent of reaction along the extruder, to scale in and/or scale-up extruders, to optimize the processing conditions such screw speed, feed rate and operating temperature, and to study the flow instability[51, 52]. The advantage of the one dimension model is that the calculation cost is relatively small and program is simple.

1.3.1 Classic Ideal Reactor Models

In this model, the RTD during extrusion is first obtained by experiment. Then, conceptual models is used to descript the flow behavior which consist in combinations of ideal reactors such as continuous stirred tank reactors (CSTR) and plug flow reactors (PFR). Each section of the extruder can be considered as an ideal reactor (Fig. 1.9). According to the type of elements constituting the screw profile (left- and right-handed screw elements, kneading discs and special mixing elements), different reactors can be chosen to match the elements. Local RTD and mean residence time of each section can be calculated according to ideal reactors. The global residence time distribution is then done by a product of convolution of these local RTDs.

Numerous flow models have been developed to fit RTD curves in screw extruders. The axial dispersion model (AMD) and CSTR in series are the most common models. The CSTR in series is described by the number of tanks and the volume of each tank. The axial dispersion model is characterized by Peclet number. The CSTR in series can be expanded to many new models such as Gamma model, Wolf-Resnick model, the backflow cell model and the double backflow cell model.

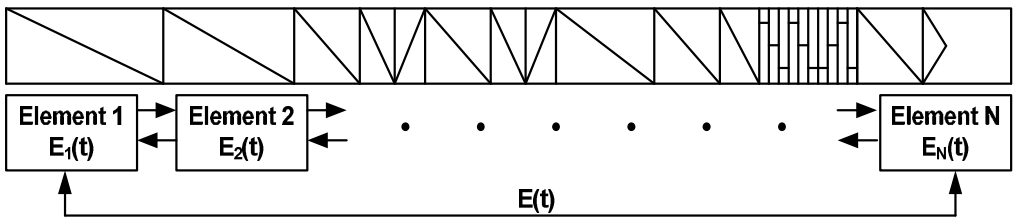

Fig. 1.9 Simulation model of screw extruder

Puaux et al.[48] fit the experimental RTD curves with the classic one-, two- and three-parameter models. According to the fitting quality, the three-parameter backflow cell model and two-parameter AMD are the most efficient models. They point out that the two models are consistent with the flow characteristics of co-rotating twin-screw

extruders. Thompson et al. used several classic models to fit the experimental data in order to characterize the material time history in the extruders. The result shows that the AMD provide the closest approach to the RTD.

Chen et al.[53, 54] presented a RTD model for intermeshing and non-intermeshing counterrotating twin-screw extruder. They assumed that two-dimensional perfect mixing exists at the boundary of two divided screw elements and treated the screw as a set of individual "C" turns connected in series. The RTDs in the adjacent zones are assumed to statistically independent of each other. The predictions are in good agreement with experimental data.

The RTD is considered as a system parameters like as velocity, pressure and temperature in the extruders which is correlated to process variables and material parameters. Hoppe et al.[17] developed a mathematical model consisting of ideal reactors such as CSTR and PFR, and fitted with the experimental data to establish the relationship between model parameters and extrusion conditions. The screw extruder was divided in seven zones and each section was link to an ideal model. The flow models used are shown in Fig. 1.10.

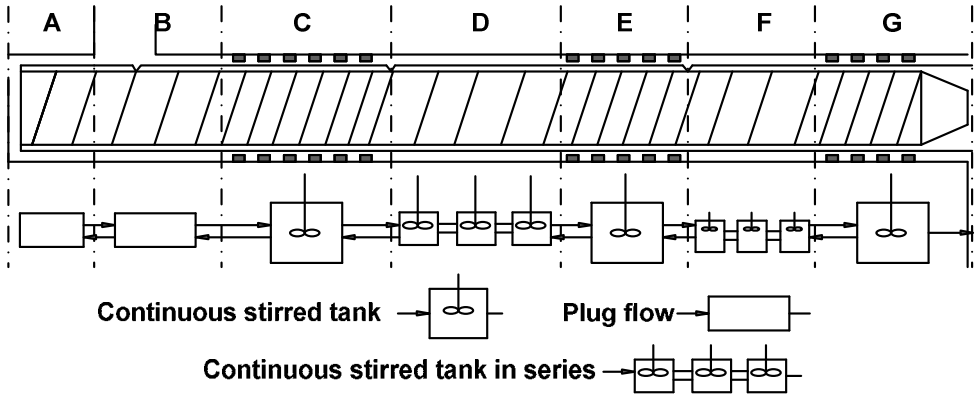

Fig. 1.10 Flow model of single screw extruder

Poulesquen et al.[44, 55] coupled the continuum mechanics and chemical engineering techniques to propose a new model for calculating the RTD in the extruders. The new model is also base on the ideal reactors but the selection and association of ideal reactors can reflect the real flow behavior within extruders. They first used the Ludovic software to calculate the mean residence times of the solid conveying, the molten fully filled and partially filled sections. In the second step, the ideal reactors were selected for three sections according to the mean residence time, and local RTD are calculated.

1.3.2 New Flow Models

The RTD is to be strongly dependent on the material parameters and process variables including the screw configurations, feed rate and screw speed. Incomplete understanding of the real flow characteristic in twin-screw extruders and multivariate adjustable parameters may lead to unsatisfactory model result. Therefore, many researchers proposed new models to descript physical features of twin-screw extruders. Kim and White[56] investigated the influence of different screw configurations, screw speed and feed rate on the RTD. The result showed that kneading discs and left-handed screw element brought about a remarkable broadening of the RTD. Increasing the feed rate or screw speed resulted in a reduced mean residence time. They used the following model to calculate the mean residence time t_m:

$$t_m = \frac{V_{occ}}{Q} = \frac{L_f A_f + \varphi(L - L_f)A_f}{Q} \tag{1.5}$$

where Q is the feed rate, V_{occ} is the occupied volume, L_f is the length of the fully filled region, L is the total length of the screw, φ is the degree of fill, A_f is the free cross sectional area of the screw.

De Graaf et al.[57] proposed a new model for RTD in a counter rotating twin-screw extruder. The model is based on physical principles without any adjustable parameters and is agreement with the experimental data. The RTD curves are calculated using the following equation:

$$C_{out}(t) = (\Re M^{\mu})^n C_{in}(t) \tag{1.6}$$

where $C_{out}(t)$ is the tracer concentration in the die exit, $C_{in}(t)$ is the input tracer concentration, $\Re$ and M are matrices describing the influence of the extruder parameters (like screw speed, feed rate, screw configuration etc.), μ is the amount of steps in a revolution, n is time index.

Gao et al.[37] presented two new models: residence revolution distribution (RRD) and residence volume distribution (RVD) which are obtained by the transformation of RTD. The RVD gives a direct measure of the physical distribution of tracer in the extrudate along the axis of the sample. The RRD gives insight into the transport behavior of an extruder. The parameters of the RTD, RRD and RVD model are specified by a least-squares method, and the result showed that the model function is

appropriate to describe the RTD experimental data of different operating conditions.

Mehranpour et al.[58, 59] established a functionality method for predicting RTD of the modular screw extruders, and named the method as cluster model. The flow model used for calculation is show in Fig. 1.11. When a tracer with concentration C_0 passes through the first element, the concentration C(t) at the exit of first element can be determined by the RTD of the element. Also C(t) is the input tracer concentration of the second elements. The output tracer concentration is determined by the second elements. Using the cluster model, they calculated the cumulative RTD of combination of several screw elements.

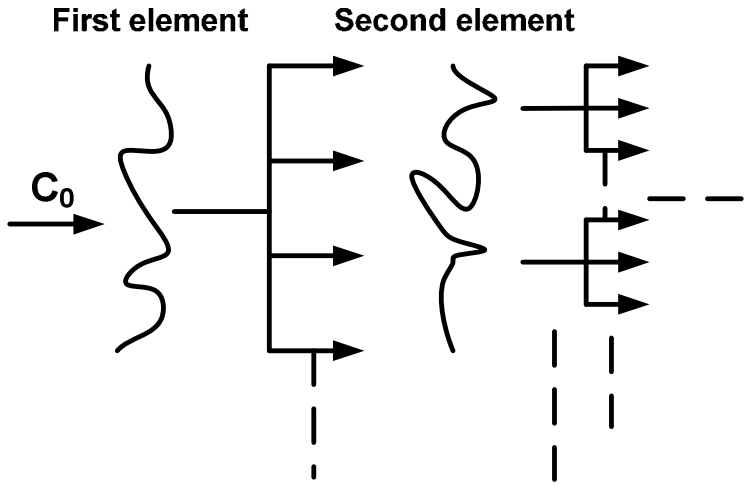

Fig. 1.11 Schematic diagram of the cluster model

1.4 The RTD Simulation Using Three Dimension Numerical Simulation

The complexity of the flow in twin-screw extruders, as well as the large number of parameters and interrelated variables that affect the flow, make this process difficult to understand, control, and optimize. The 1-D reactor flow model methods consider an oversimplification of the flow conditions. The main advantage of 1-D reactor model is that it makes the computation and simulation simple, rapid and easy, and can be applied for the process control. However, phenomena described by the flow model are different from the realistic conditions in the extruders. That is to say, the parameters of the model are lack of physical significance. Meanwhile, when a process is calculated, the parameters of the flow model have to be adjusted to satisfy

the operating conditions. The parameters included the number and the type of reactors. Therefore, it cannot be used as predictive tools to describe the real flow and mixing behavior in detail, and are inefficient to solve scale-in and scale-up problems.

The other calculation method is based on computational fluid dynamics (CFD). The flow fields are obtained by solving classical continuum mechanics equations including mass, momentum, energy balances equations. The method can analyze the influence of local geometry, kinematics and boundary conditions on RTD. Because the calculation reflects the real flow and mixing behaviors in extruders, which can be used not only to calculate certain screw configurations such as conveying elements. Kneading discs and special mixing elements, but also to optimize, scale-in and scale-up it and to predict the change of flow fields when changing processing conditions or screw configuration.

Methods used to analyze RTD and distributive and dispersive mixing start by determining the velocity field. Once the velocity field is obtained, a number of different approaches are used to characterize the mixing performance and efficiency. Pinto and Tadmor[60] derived the RTD and cumulative RTD functions for screw extruders based on the "parallel plate" model and investigated the influence of operating conditions on RTD. They concluded that the minimum residence time is equal to the 3/4 of mean residence time. Bigg and Middleman[9] expanded the study of Pinto and Tadmor[60] to non-Newtonian fluid. A model for the 2-D flow field of power-law fluids is developed and used to calculate the RTD. Experiments were carried out to validate the model theory. Joo et al.[61] used a quasi-three-dimensional finite element method to calculate velocity field, then proposed a new method to accurately determine the RTD, cumulative RTD taking into account the three-dimensional circulatory flow. The results showed that the previous method based on a simplified two-dimensional velocity field has a tendency to underestimate the RTD due to the neglect of the three-dimensional circulatory flow.

Recently, three-dimensional (3-D) numerical simulations for Newtonian and non-Newtonian fluids have been performed. Bravo et al.[62] investigated the flow behavior, particle trajectories and RTD in kneading discs of intermeshing co-rotating twin-screw extruders. It was predicted that particle movement history can be used to evaluate mixing performance of different kneading discs, and the geometry configuration and clearance of kneading discs has important influence on backflow and relative mixing performance. Ishikawa et al.[63] investigated the 3-D flow of

non-Newtonian fluid in fully filled kneading discs with different tip clearance of a twin-screw extruder. Large tip clearance narrowed the RTD because of the decrease of backflow. Lawal et al.[64] studied the mixing mechanisms in single screw and co-rotating twin-screw extruders based on 3-D numerical simulation. The RTD and numerical tracer analysis were combined to analyze the mixing performance of different screw elements. Meanwhile, Commercial software packages such as Fluent, Polyflow, Fidap and CFX can be used to perform such calculations. Zhu et al.[51] used Fluent code to calculate the reactive extrusion process, and investigated the influence of residence time and RTD on conversion rate. Cheng and Manas-Zloczower[65] simulated 3-D isothermal flow patterns in conveying element using the FIDAP software based on the finite element method. Distributive mixing was studied by particle tracking and quantified in terms of length, area stretch and strain distributions. Ficarella et al.[66, 67] used the code POLYFLOW to simulate the extrusion process. The simulation code is based on a finite element velocity-pressure formulation. They concluded that residence time depend on the screw speed and production temperature.

1.5 Investigations of Distributive Mixing

During polymer processing, dispersive and distributive mixing occur simultaneously. Both types of mixing are required to obtain good properties in the final product. Fig. 1.12 is a schematic representation of a mixing system[68]. It is possible to regard distributive mixing operation as a transformation from one state to the next. Distributive mixing of polymer melts can be characterized by tracking the spatial distribution of minor phase within the major phase as shown in Fig. 1.12, and by the generation of interfacial area (Fig. 1.13)[69, 70]. The two methods are much more difficult to measure by experiment approach. Numerical simulation is an effective approach to solve the problems.

Danckwerts[71] proposed scale of segregation and the intensity of segregation concepts to characterize the quality of distributive mixing. At time *t*, consider a set of *J* pairs material points separated by a distance *r*: for the *j*th pair, let $c_j^{'}$ and $c_j^{''}$ represent the concentrations at both points respectively, let $\overline{c}$ denote the average concentration of all points. The σ_c is defined as:

$$\sigma_c^2 = \frac{\sum_{i=1}^{2J}(c_i - \overline{c})^2}{2J-1} \tag{1.7}$$

The coefficient of correlation, R(r), measures the degree of correlation between the concentrations at two points separated by distance r which represent the probability of the J pairs materials points will have the same concentrations and is defined as:

$$R(r,t) = \frac{\sum_{j=1}^{J}(c_j^{'} - \overline{c})(c_j^{''} - \overline{c})}{J\sigma_c^2} \tag{1.8}$$

The coefficient of correlation ranges from 1 to -1, denoting, respectively, perfect positive (the J pairs materials points have the same concentration) and perfect negative (the J pairs materials points have the opposite concentration, in other words, one point is pure minor, the other is pure major) correlations. The scale of segregation is the integral of the coefficient of correlation from distance zero, where R(0) = 1, to distance ξ at which there is no correlation R(ξ) = 0.

$$S(t) = \int_0^{\xi} R(r,t)dr \tag{1.9}$$

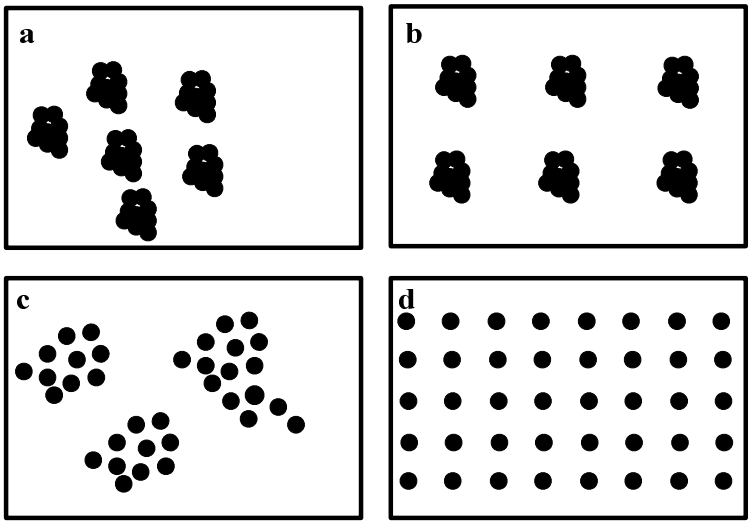

Fig. 1.12 Schematic plan of dispersive and distributive mixing during extrusion

a) bad dispersive, bad distributive； b) bad dispersive, good distributive

c) good dispersive, bad distributive; d) good dispersive, good distributive

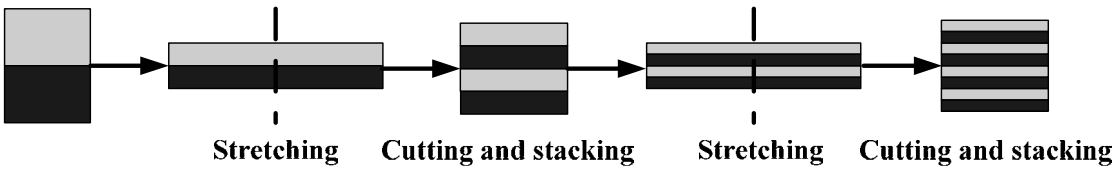

（a）

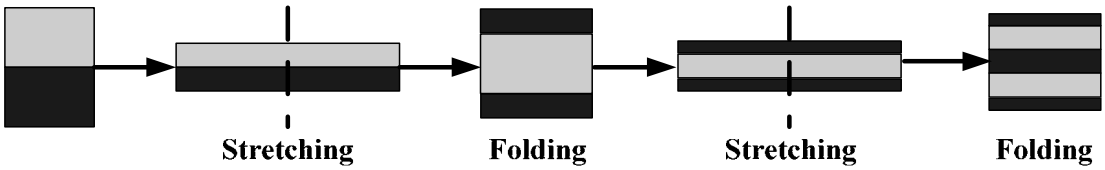

（b）

Fig. 1.13 The area change of distributive mixing: (a) a stretching-cutting-stacking sequence which yields 2^{n+1}layers after n operations, in this case, n = 2; (b) a stretching-folding transformation yielding $1+2^n$ layers, in this case, n=2.

However, the scale of segregation method has been considered as too complex and was rarely used in practice. Manas-Zloczower's research group[65, 72-75] presented the pairwise correlation function to characterize the degree of distributive mixing. The schematic diagram for the pairwise correlation function calculation is depicted in Fig. 1.14. The black spots represent the minor phase particles. The position of a particle is described by vector r'. The quantification of the distributive mixing can be carried out by tracing the spatial position change of particles. The distance r variation between pairs of particles is an efficient way to quantify the distributive mixing process. The pairwise correlation function is defined as:

$$f(r) = \frac{2}{N(N-1)} \sum_i \delta(\mathrm{r}_i' + \mathrm{r})\delta(\mathrm{r}_i') \qquad (1.10)$$

where N is the number of particles, which can provide N(N-1)/2 pairs of particles. $\delta(\mathrm{r})$ = 1 if a particle is present and 0 if absent in the shell of radius $r \pm \Delta r/2$ around the point located at r'. The f(r) can be interpreted as the probability of finding a neighbor particle that is at a displacement ranging from $r - \Delta r/2$ to $r + \Delta r/2$.

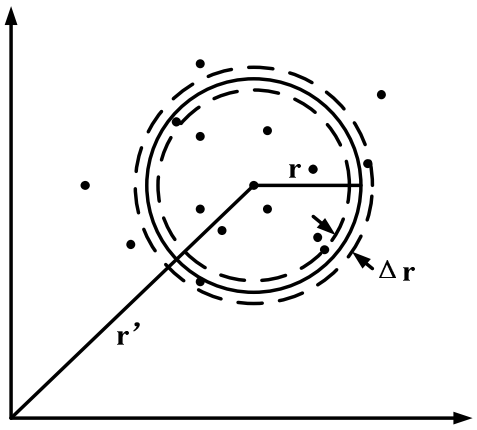

Fig. 1.14 Schematic diagram for the pairwise correlation function calculation

The f(r) depends on the exact value of Δr, it is customary to the results in terms of probability density function which is related to the f(r) through the following equation:

$$f(r) = \int_{r-\Delta r/2}^{r+\Delta r/2} c(r)dr \approx c(r)\Delta r \tag{1.11}$$

where c(r) is the coefficient of the probability density function of the correlation function f(r). The area under the curve of c(r) is a constant, independent of the distribution c(r). Therefore, the following equation is obtained:

$$\int_{r=0}^{r=\infty} c(r)dr \approx \sum_{r=0}^{r=r_{\max}} c(r)\Delta r = 1 \tag{1.12}$$

where r_{max} is the largest dimension of the system. It should be pointed out that the c(r) depends on the exact geometry of the mixing equipment, so c(r) cannot be used to compare the distributive mixing performance of different mixing devices. The difference between an actual distribution and its corresponding ideal distribution is given to measure the distributive mixing performance of different mixing equipments, which is quantified by a parameter ε, defined as[72]:

$$\varepsilon = \frac{\int_0^{\infty} \left[c(r) - c(r)_{ideal}\right]^2 dr}{\int_0^{\infty} \left[c(r)_{ideal}\right]^2 dr} \tag{1.13}$$

where $c(r)_{ideal}$ is the corresponding coefficient for the ideal system which is a measure of the absolute difference between actual simulations and ideal system.

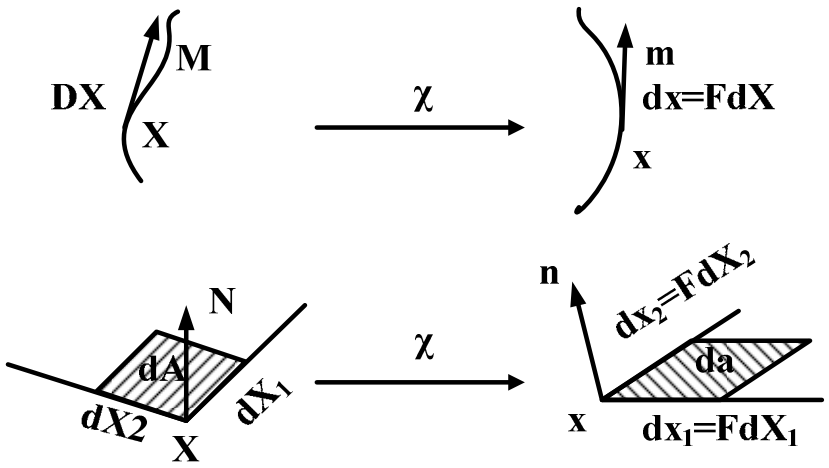

Fig. 1.15 Deformation of infinitesimal elements: line and surface

Ottino et al.[76] developed a kinematic approach to model distributive mixing that used a lamellar model to track the amount of deformation experienced by fluid elements (line, surface and volume). The kinematic model is based on two levels of knowledge: i) the whole motion that produces mixing is known; and (ii) external macroscopic parameters are known, e.g., power input to produce mechanical stirring. The deformation process of fluid element including line and surface is illustrated in Fig. 1.15. Consider in a flow domain an infinitesimal area dA with a unit normal N that deforms into an area da with a unit normal n. The area stretch η is defined as:

$$\eta = da/dA \tag{1.14}$$

The material time rate of area stretch per unit of present area stretch is given by:

$$\frac{\dot{\eta}}{\eta} = \frac{d(\ln \eta)}{dt} = D : nn \tag{1.15}$$

where D is rate of deformation tensor, $\dot{\eta}$ is the derivative of area stretch. A good mixing quality is usually related to high η through time and space. An evaluation of instantaneous mixing efficiency is given by a ratio

$$e_\eta = \frac{\dot{\eta}/\eta}{(D:D)^{1/2}} = \frac{d(\ln \eta)/dt}{(D:D)^{1/2}} \tag{1.16}$$

The instantaneous mixing efficiency are included in the interval [-1, 1] according to the Cauchy-Schwarz inequality $-(D:D)^{1/2} \le \dot{\eta}/\eta \le (D:D)^{1/2}$. A positive (negative) value e_η indicates that the element of area stretches (shrinks). The e_η is a local measure along the path of a material point. It is interesting to calculate the time-averaged efficiency which is defined as:

$$< e_\eta >= \frac{1}{t}\int_0^t e_\eta dt \qquad (1.17)$$

Several characteristic features of the time-averaged efficiency can be identified According to the time history of the stretching efficiency (Fig. 1.16)[77-79]. In flow without reorientation, the efficiency $< e_\eta >$ decays as t^{-1}. In flows with partial reorientation, there is some periodic restoration, but where on the average the efficiency also decays as t^{-1}. In flow with strong reorientation, the time average of the efficiency tends to a constant value.

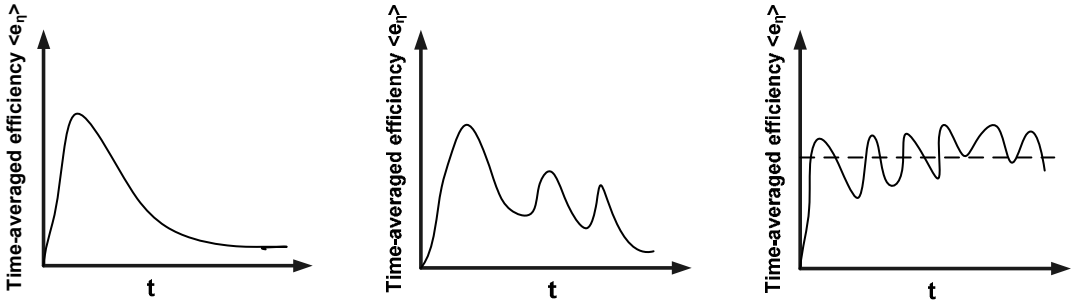

(a) (b) (c)

Fig. 1.16 Typical behavior of mixing efficiency; (a) flow with decaying efficiency; (b) flow with partial restoration; and (c) flow with strong reorientation.

Avalosse and Crochet[80, 81] calculated the complex mixing flows and mixing parameters to evaluate the mixing equality based on the Ottino's kinematic theory. They compared the mixing quality of single cam and co- or counterrotating cam devices, and validated the simulation result with experimental data. Avalosse and Crochet[81] also used the kinematic theory to analyze the mixing performance of a Kenics mixer. They found the rheological properties of clays have little influence on the quality of the mixture. Prakash and Kokino[82, 83] used Laser-Doppler Anemometry (LDA) to measure the velocity field in Brabender Farinogragh. Then the velocity gradient and mixing parameters were calculated to investigate the flow behavior and mixing performance of Brabender batch mixer. Connelly and Kokini[84, 85] simulated the flow of generalized Newtonian fluid in a twin sigma blade using finite element method. The resulting velocity fields are used to calculate the kinematic mixing parameters. The distributive mixing of different positions were analyzed to find the "dead zone" of mixing.

1.6 Scope of This Thesis

1.6.1 Incentive for This Work

This work aimed at developing a new instrument to measure in real time the global and partial RTD which characterized the axial mixing and transport abilities of different screw elements based on analysis of the transient flow pattern and systematic evaluation of mixing theory in TSE. That made the assessment of the local RTD along the extruder possible. The motivation for this research was the lack of experimental data on partial and local axial mixing in extruders because of the difficulty in directly measuring partial and local RTD. The research was divided into the following three objectives: i) developing a new set-up to measure in real time the RTD in screw extruders, ii) derivation of deconvolution method and application of the method to the calculation of local RTD during extrusion process, and iii) foundation of the relationships among the RTD, RRD, RVD and dimensionless RTD by a key process parameter Q/N, defined as a ratio of throughput (Q) over screw speed (N). For the first objective, we developed a new instrument to measure in real time the RTD in screw extruders based on the tracer fluorescent characteristic. The device had to be evaluated. It was done in terms of the determination of tracer concentration of the tracer in the masterbatch, the reproducibility, the linearity between the amplitude of the response signal and the amount of the tracer. To accomplish the second objective, the deconvolution method is derived and applied for calculating the local RTD of different screw elements. Finally, it was confirmed theoretically and experimentally that specific throughput Q/N, was indeed a key process parameter for controlling the dimensionless time distribution, RRD and RVD. Investigated factors included the operating conditions and screw configurations.

The other objective of this thesis is to analyze the flow mechanisms and distributive mixing in the kneading disc domain of co-rotating twin screw extruders by the 3-D finite element method. Simulated RTD results are compared with experimental ones obtained by an in-line measuring instrument. Distributive mixing of polymer melts is characterized by generation of interfacial area, which is much more difficult to experimentally measure. The numerical simulation based on computational fluid dynamics (CFD) is a key tool to solve this difficulty. The

distributive mixing parameters such as the area stretch ratio of material surface η, instantaneous mixing efficiency e_η and time-averaged mixing efficiency $\langle e_\eta \rangle$ are calculated using the interface tracking techniques. These parameters are then used to compare the distributive mixing performance and efficiency of different kneading discs.

1.6.2 Dissertation Outline

In chapter 2, an in-line RTD measuring system using to measure global and partial RTD is described. The deconvolution method is derived and applied to calculation of local RTD in extruders. Chapter 3 studies the overall, partial and local residence time distributions (RTD); overall, partial and local residence revolution distributions (RRD) and overall, partial and local residence volume distributions (RVD) in a co-rotating twin screw extruder and established the relationships among them. Chapter 4 develops an approach to model the flow and evaluate the distributive mixing performance and mixing efficiency of block discs using finite element method (FEM), and presents the experimental validation of RTD calculated from numerical simulations by comparing them with the experimental RTD data in Chapters 2 and 3. Finally, Chapter 5 gives an overview of the work done and summarizes the main conclusions. Chapter 5 also includes a section with recommendation for the future work.

1.7 References

[1]. Hu, G. H. Reactive Polymer Processing: Fundamentals of Reactive Extrusion. In *Encyclopaedia of Materials: Science and Technology*, Buschow, K. H. J., Cahn, R. W., Flemings, M. C., Ilschner, B., Kramer, E. J., Mahajan, S., Eds.; Elsevier Science: Amsterdam, The Netherlands, 2001; pp 8045-8057.

[2]. Todd, D. B. Mixing of Highly Viscous Fluids, Polymers, and Pastes. In *Handbook of Industrial Mixing: Science and Practice*, Paul, E. L., Atiemo-Obengm, V. A., Kresta, S. M., Eds.; John Wiley & Sons, Inc.: Hoboken, 2004; pp 987-1025.

[3]. Sakai, T. Intermeshing twin-screw extruder. In *Mixing and Compounding of Polymer: Theory and Practice*, Manas-Zloczower, I., Tadmor, Z., Eds.; Hanser

Publishers: Munich, 1994; pp 707-733.

[4]. Janssen, L. P. B. M. *Reactive extrusion systems;* Marcel Dekker: NEW YORK, 2004.

[5]. White, J. L.; Keum, J.; Jung, H.; Ban, K.; Bumm, S. Corotating twin-screw extrusion reactive extrusion-devolatilization model and software. *Polymer - Plastics Technology and Engineering* **2006,** *45* (4), 539-548.

[6]. Brouwer, T.; Todd, D. B.; Janssen, L. P. B. M. Flow characteristics of screws and special mixing enhancers in a co-rotating twin screw extruder. *International Polymer Processing* **2002,** *17* (1), 26-32.

[7]. Nauman, E. B. Residence Time Distributions. In *Handbook of Industrial Mixing: Science and Practice*, Paul, E. L., Atiemo-Obengm, V. A., Kresta, S. M., Eds.; John Wiley & Sons, Inc.: Hoboken, 2004; pp 1-17.

[8]. Shon, K.; Chang, D.; White, J. L. A comparative study of residence time distributions in a kneader, continuous mixer, and modular intermeshing co-rotating and counter-rotating twin screw extruders. *International Polymer Processing* **1999,** *14* (1), 44-50.

[9]. Bigg, D.; Middleman, S. Mixing in a screw extruder. A model for residence time distribution and strain. *Industrial and Engineering Chemistry Fundamentals* **1974,** *13* (1), 66-74.

[10]. Todd, D. B. Residence time distribution in twin-screw extruders. *Polymer Engineering and Science* **1975,** *15* (6), 437-443.

[11]. Weiss, R. A.; Stamato, H. Development of an ionomer tracer for extruder residence time distribution experiments. *Polymer Engineering and Science* **1989,** *29* (2), 134-139.

[12]. Kao, S. V.; Allison, G. R. Residence time distribution in a twin screw extruder. *Polymer Engineering and Science* **1984,** *24* (9), 645-651.

[13]. Cassagnau, P.; Mijangos, C.; Michel, A. An ultraviolet method for the determination of the residence time distribution in a twin screw extruder. *Polymer Engineering and Science* **1991,** *31* (11), 772-778.

[14]. Oberlehner, L.; Caussagnau, P.; Michel, A. Local residence time distribution in a twin screw extruder. *Chemical Engineering Science* **1994,** *49* (23), 3897-3907.

[15]. Sun, Y. J.; Hu, G. H.; Lambla, M. Free radical grafting of glycidyl methacrylate onto polypropylene in a co-rotating twin screw extruder. *Journal*

of Applied Polymer Science **1995,** *57* (9), 1043-1054.

[16]. Hu, G. H.; Sun, Y. J.; Lambla, M. Effects of processing parameters on the in situ compatibilization of polypropylene and poly(butylene terephthalate) blends by one-step reactive extrusion. *Journal of Applied Polymer Science* **1996,** *61* (6), 1039-1047.

[17]. Hoppe, S.; Detrez, C.; Pla, F. Modeling of a cokneader for the manufacturing of composite materials having absorbent properties at ultra-high-frequency waves. Part 1: modeling of flow from residence time distribution investigation. *Polymer Engineering and Science* **2002,** *42* (4), 771-780.

[18]. Janssen, L. P. B. M.; Hollander, R. W.; Spoor, M. W.; Smith, J. M. Residence time distributions in a plasticating twin screw extruder. *AIChE Journal* **1979,** *25* (2), 345-351.

[19]. Tzoganakis, C.; Tang, Y.; Vlachopoulos, J.; Hamielec, A. E. Measurements of residence time distribution for the peroxide degradation of polypropylene in a single-screw plasticating extruder. *Journal of Applied Polymer Science* **1989,** *37* (3), 681-693.

[20]. Kemblowski, Z.; Sek, J. Residence time distribution in a real single screw extruder. *Polymer Engineering and Science* **1981,** *21* (18), 1194-1202.

[21]. Rauwendaal, C. J. Analysis and experimental evaluation of twin screw extruders. *Polymer Engineering and Science* **1981,** *21* (16), 1092-1100.

[22]. Carneiro, O. S.; Caldeira, G.; Covas, J. A. Flow patterns in twin-screw extruders. *Journal of Materials Processing Technology* **1999,** *92-93*, 309-315.

[23]. Hu, G. H.; Kadri, I.; Picot, C. On-line measurement of the residence time distribution in screw extruders. *Polymer Engineering and Science* **1999,** *39* (5), 930-939.

[24]. Wolf, D.; White, D. H. Experimental study of the residence time distribution in plasticating screw extruders. *AIChE Journal* **1976,** *22* (1), 122-131.

[25]. Thompson, M.; Puaux, J. P.; Hrymak, A. N.; Hamielec, A. E. Modeling the residence time distribution of a non-intermeshing twin screw extruder. *International Polymer Processing* **1995,** *X* (2), 111-115.

[26]. Kiani, A.; Burkhardt, U.; Heidemeyer, P.; Franzheim, O.; Rische, T.; Stephan, M.; Baetz, H.; Pallas, R.; Sahoub, M.; Zeuner, A. New online technique for morphology analysis and residence time measurement in a twin screw extruder. Indianapolis, America, 1996; pp 427-434.

[27]. Kiani, A.; Heidemeyer, P.; Pallas, R. Study of flow and RTD in a ZSK twin screw extruder. Toronto, America, 1997; pp 94-99.

[28]. Gendron, R.; Daigneault, L.; Tatibouet, J.; Dumoulin, M. Residence time distribution in extruders determined by in-line ultrasonic measurements. *Advances in Polymer Technology* **1996,** *15* (2), 111-125.

[29]. Chalamet, Y.; Taha, M. In-line residence time distribution of dicarboxylic acid oligomers/dioxazoline chain extension by reactive extrusion. *Polymer Engineering and Science* **1999,** *39* (2), 347-355.

[30]. Lee, S. M.; Park, J. C.; Lee, S. M.; Ahn, Y. J.; Lee, J. W. In-line measurement of residence time distribution in twin-screw extruder using non-destructive ultrasound. *Korea-Australia Rheology Journal* **2005,** *17* (2), 87-95.

[31]. Choudhury, G. S.; Gautam, A. On-line measurement of residence time distribution in a food extruder. *Journal of Food Science* **1998,** *63* (3), 529-534.

[32]. Unlu, E.; Faller, J. F. Geometric mean vs. arithmetic mean in extrusion residence time studies. *Polymer Engineering and Science* **2001,** *41* (5), 743-751.

[33]. Unlu, E.; Faller, J. F. RTD in twin-screw food extrusion. *Journal of Food Engineering* **2002,** *53* (2), 115-131.

[34]. Van Den Einde, R. M.; Kroon, P.; Van Der Goot, A. J.; Boom, R. M. Local mixing effects of screw elements during extrusion. *Polymer Engineering and Science* **2005,** *45* (3), 271-278.

[35]. Wetzel, M. D.; Shih, C. K.; Sundararaj, U. Determination of residence time distribution during twin screw extrusion of model fluids. Toronto, America, 1997; pp 3707-3712.

[36]. Gao, J.; Walsh, G. C.; Bigio, D.; Briber, R. M.; Wetzel, M. D. Mean residence time analysis for twin screw extruders. *Polymer Engineering and Science* **2000,** *40* (1), 227-237.

[37]. Gao, J.; Walsh, G. C.; Bigio, D.; Briber, R. M.; Wetzel, M. D. Residence-time distribution model for twin-screw extruders. *AIChE Journal* **1999,** *45* (12), 2541-2549.

[38]. Elkouss, P.; Bigio, D. I.; Wetzel, M. D.; Raghavan, S. R. Influence of polymer viscoelasticity on the residence distributions of extruders. *AIChE Journal* **2006,** *52* (4), 1451-1459.

[39]. Chen, T.; Patterson, W. I.; Dealy, J. M. On-line measurement of residence time

distribution in a twin-screw extruder. *International Polymer Processing* **1995,** *10* (1), 3-9.

[40]. Melo, T. J. A.; Canevarolo, S. V. An optical device to measure in-line residence time distribution curves during extrusion. *Polymer Engineering and Science* **2002,** *42* (1), 170-181.

[41]. Melo, T. J. A.; Canevarolo, S. V. In-line optical detection in the transient state of extrusion polymer blending and reactive processing. *Polymer Engineering and Science* **2005,** *45* (1), 11-19.

[42]. Bur, A. J.; Shibata, J.; Trout, T. K.; Wang, F. W.; Thomas, C. L. Monitoring the quality of mix of polymer melts with particulate fillers using fluorescence spectroscopy. *Polymer Engineering and Science* **1989,** *29* (24), 1759-1765.

[43]. Hu, G. H.; Kadri, I. Preparation of macromolecular tracers and their use for studying the residence time distribution of polymeric systems. *Polymer Engineering and Science* **1999,** *39* (2), 299-311.

[44]. Poulesquen, A.; Vergnes, B.; Cassagnau, P.; Michel, A.; Carneiro, O. S.; Covas, J. A. A study of residence time distribution in co-rotating twin-screw extruders. Part II: Experimental validation. *Polymer Engineering and Science* **2003,** *43* (12), 1849-1862.

[45]. Cassagnau, P.; Melis, F.; Bounor-Legare, V. UV fluorescence monitoring of the mixing of molten polymers in a batch mixer. *Polymer Engineering and Science* **2003,** *43* (4), 923-932.

[46]. Cassagnau, P.; Courmont, M.; Melis, F.; Puaux, J. P. Study of mixing of liquid/polymer in twin screw extruder by residence time distribution. *Polymer Engineering and Science* **2005,** *45* (7), 926-934.

[47]. Carneiro, O. S.; Covas, J. A.; Ferreira, J. A.; Cerqueira, M. F. On-line monitoring of the residence time distribution along a kneading block of a twin-screw extruder. *Polymer Testing* **2004,** *23,* (8), 925-937.

[48]. Puaux, J. P.; Bozga, G.; Ainser, A. Residence time distribution in a corotating twin-screw extruder. *Chemical Engineering Science* **2000,** *55* (9), 1641-1651.

[49]. Razaviaghjeh, M. K.; Nazockdast, H.; Assempour, H. Determination of the residence time distribution in twin screw extruders via free radical modification of PE. *International Polymer Processing* **2004,** *19* (4), 335-341.

[50]. Gilmor, C.; Balke, S. T.; Calidonio, F.; Rom-Roginski, A. In-line color monitoring of polymers during extrusion using a charge coupled device

spectrometer: color changeovers and residence time distributions. *Polymer Engineering and Science* **2004,** *43* (2), 356-368.

[51]. Zhu, L. J.; Narh, K. A.; Hyun, K. S. Evaluation of numerical simulation methods in reactive extrusion. *Advances in Polymer Technology* **2005,** *24* (3), 183-193.

[52]. Vergnes, B.; Berzin, F. Modeling of reactive system in twin-screw extrusion: challenges and applications. *Comptes Rendus Chimie* **2006,** *9* (11-12), 1409-1418.

[53]. Chen, L.; Pan, Z.; Hu, G. H. Residence time distribution in screw extruders. *AIChE Journal* **1993,** *39* (3), 1455-1464.

[54]. Chen, L.; Hu, G. H.; Lindt, J. T. Residence time distribution in non-intermeshing counter-rotating twin-screw extruders. *Polymer Engineering and Science* **1995,** *35* (7), 598-603.

[55]. Poulesquen, A.; Vergnes, B. A study of residence time distribution in co-rotating twin-screw extruders. Part I: Theoretical modeling. *Polymer Engineering and Science* **2003,** *43* (12), 1841-1848.

[56]. Kim, P. J.; White, J. L. Flow visualization and residence time distributions in a modular co-rotating twin screw extruder. *International Polymer Processing* **1994,** *IX* (2), 108-118.

[57]. De Graaf, R. A.; Rohde, M.; Janssen, L. P. B. M. A novel model predicting the residence-time distribution during reactive extrusion. *Chemical Engineering Science* **1997,** *52* (23), 4345-4356.

[58]. Mehranpour, M.; Nazokdast, H.; Dabir, B. Estimation of residence time distribution in two elements of a Ko-Kneader. *International Polymer Processing* **2002,** *17* (1), 22-25.

[59]. Mehranpour, M.; Nazokdast, H.; Dabir, B. Prediction of residence time distribution for different screw configurations of a Ko-kneader by using a cluster model. *International Polymer Processing* **2004,** *19* (1), 13-15.

[60]. Pinto, G.; Tadmor, Z. Mixing and residence time distribution in melt screw extruders. *Polymer Engineering and Science* **1970,** *10* (5), 279-288.

[61]. Joo, J. W.; Kwon, T. H. Analysis of residence time distribution in the extrusion process including the effect of 3-d circulatory flow. *Polymer Engineering and Science* **1993,** *33* (15), 959-970.

[62]. Bravo, V. L.; Hrymak, A. N.; Wright, J. D. Study of particle trajectories,

residence times and flow behavior in kneading discs of intermeshing co-rotating twin-screw extruders. *Polymer Engineering and Science* **2004,** *44* (4), 779-793.

[63]. Ishikawa, T.; Nagano, F.; Kajiwara, T.; Funatsu, K. Tip-clearance effect on mixing performance of twin screw extruders. *International Polymer Processing* **2006,** *21* (4), 354-360.

[64]. Lawal, A.; Kalyon, D. M.; Li, Z. H. Computational study of chaotic mixing in co-rotating two-tipped kneading paddles: Two-dimensional approach. *Polymer Engineering and Science* **1993,** *33* (3), 140-148.

[65]. Cheng, H.; Manas-Zloczower, I. Study of mixing efficiency in kneading discs of co-rotating twin-screw extruders. *Polymer Engineering and Science* **1997,** *37* (6), 1082-1090.

[66]. Ficarella, A.; Milanese, M.; Laforgia, D. Numerical study of the extrusion process in cereals production: Part I. Fluid-dynamic analysis of the extrusion system. *Journal of Food Engineering* **2006,** *73* (2), 103-111.

[67]. Ficarella, A.; Milanese, M.; Laforgia, D. Numerical study of the extrusion process in cereals production: Part II. Analysis of variance. *Journal of Food Engineering* **2006,** *72* (2), 179-188.

[68]. Gale, M. Compounding with single-screw extruders. *Advances in Polymer Technology* **1997,** *16* (4), 251-262.

[69]. Tadmor, Z.; Gogos, C. G. *Principles of polymer processing (the second edition);* John Wiley & Sons, Inc.: New Jersey, 2006.

[70]. Kruijt, P. G. M. Analysis and optimization of laminar mixing: design, development and application of the mapping method. Doctor Technische Universiteit Eindhoven, 2000.

[71]. Danckwerts, P. V. The definition and measurement of some characteristics of mixtures. *Applied Scientific Research* **1952,** *3*, 279-296.

[72]. Yang, H.-H.; Manas-Zloczower, I. 3D flow analysis of a Banbury mixer. In *Theoritical and Applied Rheology*, Moldenaers, P., Keuning, P., Eds.; Elsevier Science Publisher B. V.: 1992; pp 408-410.

[73]. Yang, H.-H.; Manas-Zloczower, I. 3D flow field analysis of a banbury mixer. In *Theoretical and Applied Rehology*, Moldenaers, P., Keunings, R., Eds.; Elservier Science Publishers B.V.: 1992; pp 408-410.

[74]. Yang, H.-H.; Manas-Zloczower, I. Analysis of mixing performance in a VIC

mixer. *International Polymer Processing* **1994,** *9* (3), 291-302.

[75]. Yang, H.-H.; Manas-Zloczower, I. Flow field analysis of the kneading disc region in a co-rotating twin screw extruder. *Polymer Engineering and Science* **1992,** *32* (19), 1411-1417.

[76]. Ottino, J. M. *The kinematics of mixing: Stretching, chaos and transport.;* Cambridge University Press: Cambridge, 1989.

[77]. Ottino, J. M.; Ranz, W. E.; Macosko, C. W. A framework for description of mechanical mixing of fluids. *AIChE Journal* **1981,** *27* (4), 565-577.

[78]. Ottino, J. M.; Ranz, W. E.; Macosko, C. W. Lamellar model for analysis of liquid-liquid mixing. *Chemical Engineering Science* **1979,** *34* (6), 877-890.

[79]. Chella, R.; Ottino, J. M. Fluid mechanics of mixing in a single-screw extruder. *Industrial and Engineering Chemistry Fundamentals* **1985,** *24* (2), 170-180.

[80]. Avalosse, T.; Crochet, M. J. Finite-element simulation of mixing: 1. two-dimensional flow in periodic geometry. *AIChE Journal* **1997,** *43* (3), 577-587.

[81]. Avalosse, T.; Crochet, M. J. Finite-element simulation of mixing: 2. three-dimensional flow through a kenics mixer. *AIChE Journal* **1997,** *43* (3), 588-597.

[82]. Prakash, S.; Kokini, J. L. Determination of mixing efficiency in a model food mixer. *Advances in Polymer Technology* **1999,** *18* (3), 209-224.

[83]. Prakash, S.; Kokini, J. L. Estimation and prediction of shear rate distribution as a model mixer. *Journal of Food Engineering* **2000,** *44* (3), 135-148.

[84]. Connelly, R. K.; Kokini, J. K. Mixing simulation of a viscous Newtonian liquid in a twin sigma blade mixer. *AIChE Journal* **2006,** *52* (10), 3383-3393.

[85]. Connelly, R. K.; Kokini, J. L. Examination of the mixing ability of single and twin screw mixers using 2D finite element method simulation with particle tracking. *Journal of Food Engineering* **2007,** *79* (3), 956-969.

CHAPTER 2 Assessing Local Residence Time Distributions in Screw Extruders through a New In-line Measurement Instrument

ABSTRACT

This worked aimed at developing a new instrument to measure in real time the residence time distribution (RTD) in screw extruders. The instrument followed the same principle as the one reported in the literature but possessed several important advantages. For example, the detection system had two probes that allowed to simultaneously measure RTDs at any two different locations of an extruder, thus providing the possibility of calculating the local RTD between them by a deconvolution method based on a statistical theory for the RTD. Its performance was evaluated on a co-rotating twin screw extruder using anthracene as tracer and polystyrene as flowing material. The effects of various process parameters such as feed rate and screw speed on the RTDs were investigated. The emphasis was placed, however, on effect of the staggering angle of kneading discs on local RTDs both in the kneading zone itself and its neighboring upstream and downstream screw zones. This work is in support of an ongoing project on the simulation of flow in co-rotating twin screw extruders.

2.1 Introduction

Extrusion of polymers in a screw extruder is composed of a series of thermal, physical and eventually chemical histories/changes occurring in a simultaneous and/or consecutive manner inside the extruder. The time a flow element spends in the extruder can be a measure of the extent of these histories/changes. Thus the residence time distribution (RTD) provides an aspect of the heating and shearing histories in the screw channel and is helpful for understanding the effects of extrusion parameters and screw geometry.

Typically the RTD is measured when the extrusion process has reached a steady state. A tracer is injected to the flow stream (usually at the hopper) as a pulse, the time interval being so short that the input can be considered as a Dirac function. The relationship between the variation of the tracer concentration and time at a chosen test point is the RTD density function, E(t), between the tracer injection point and a test point. E(t) can be determined using the following equation[1]:

$$E(t) = \frac{c(t)}{\int_0^\infty c dt} = \frac{c(t)}{\sum_{i=1}^{\infty} c(t)\Delta t} \tag{2.1}$$

where c is the tracer concentration at time t. Another function closely related to E(t) is the cumulative residence time distribution function F(t):

$$F(t) = \int_0^t E(t)dt = \sum_0^t E(t)\Delta t = \frac{\sum_0^t c\Delta t}{\sum_0^\infty c\Delta t} \tag{2.2}$$

The first moment of E(t) is the mean residence time, $\bar{t}$, and is defined as:

$$\bar{t} = \int_0^\infty tE(t) = \frac{\int_0^\infty tcdt}{\int_0^\infty cdt} = \frac{\sum_0^\infty tc\Delta t}{\sum_0^\infty c\Delta t} \tag{2.3}$$

The second moment of E(t), σ_t^2, called the variance, is a measure of the spread of the RTD about the mean residence time and is defined as:

$$\sigma_t^2 = \int_0^\infty (t-\bar{t})^2 E(t)dt = \sum_0^\infty (t-\bar{t})^2 E(t)\Delta t \tag{2.4}$$

The RTD can be measured off-line, on-line or in-line. Off-line methods are relatively simple in device. However, measurements are done in a discrete manner. Thus, they are often very time-consuming and generally cannot be performed automatically. Moreover, the resulting data points may not be numerous enough and/or may lack accuracy. By contrast, in-line measurements continuously analyze the flow material in real time and have no need to collect samples like off-line methods do. Thus, they have many advantages over off-line ones. On-line methods slightly differ from in-line ones in that samples are collected through a bypass and then analyzed. Thus the flow stream is more or less perturbed. However, both sample collection and analysis are done in a continuous manner.

Recent studies developed on-line and in-line methods for the RTD measurement that used different tracers and detection devices. Detection principles are based on properties such as radioactivity (MnO_2, La_2O_3, etc.)[2], ultrasound reflectivity (filling, carbon black, etc.)[3], optical reflectivity (TiO_2)[4], electrically conductivity (KNO_3, $NaNO_3$, KCl, etc.)[5], light transmission (carbon black)[6], and fluorescence emission (anthracene)[7]. Hu et al.[8, 9] developed an in-line RTD measuring device based on fluorescence emission and applied it to twin-screw extruders. However, the device as it was reported in ref. [9] could measure the RTD at a single test point, the die exit only because the optical probe was made of poly(methyl methacrylate). This work aimed at developing a new device based on the principle of ref. [9]. The new in-line RTD measurement device possessed many advantages over the one of ref. [9]. For example, it was capable of simultaneously measuring the RTDs at two test points instead of one. Moreover, two test points could, in principle, be located anywhere along the extruder. This provided a possibility to study local RTDs, which are very important for screw design, diagnosis, optimization and scale-up of compounding, reactive extrusion and reactive blending processes[10-15].

Like ref. [9], in this work we also chose to use a co-rotating twin screw extruder to assess the performance and explore the potential of the new in-line RTD measurement device. There are usually three main types of screw elements for such an extruder. One type is full-flight right-handed screw elements and is often used for conveying materials from the feed section toward the die exit. Another one is full-flight left-handed screw elements and is often used for creating a material hold-up. The third type is mixing

elements, commonly called kneading discs. The latter play an important role in dispersive and distributive mixing. The mixing performance of different kneading discs remains difficult to assess and can be quantified, to a certain degree, by the RTD (delay time, mean residence time and variance).

In this work, the performance of the new device was first evaluated in terms of the reproducibility and the appropriate tracer concentration range. It was then used to study the effects of various operating conditions such as feed rate and screw speed on the RTD with emphasis on the effect of the staggering angle of different kneading discs on local RTDs.

2.2 Experimental

2.2.1 Extruder and Screw Configurations

Experiments were carried out on a co-rotating twin screw extruder with a diameter of 35 mm and a length-to-diameter ratio of 48. Fig. 2.1 shows the locations of the RTD probes and three screw configurations used in the study. The latter differed only in the kneading zone in terms of the geometry of the kneading discs (Fig. 2.1b). The kneading zone was composed of four identical kneading discs whose geometry was either of the type 30/7/32, 45/5/32 or 90/5/32 (Fig. 2.1c). The head of the extruder was equipped with a strip die, which was 30 mm in length and 1.2 mm in height.

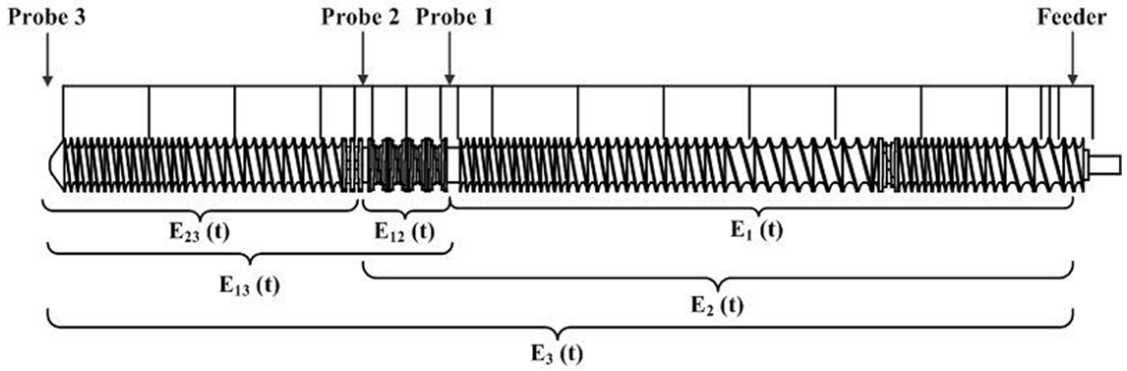

(a)

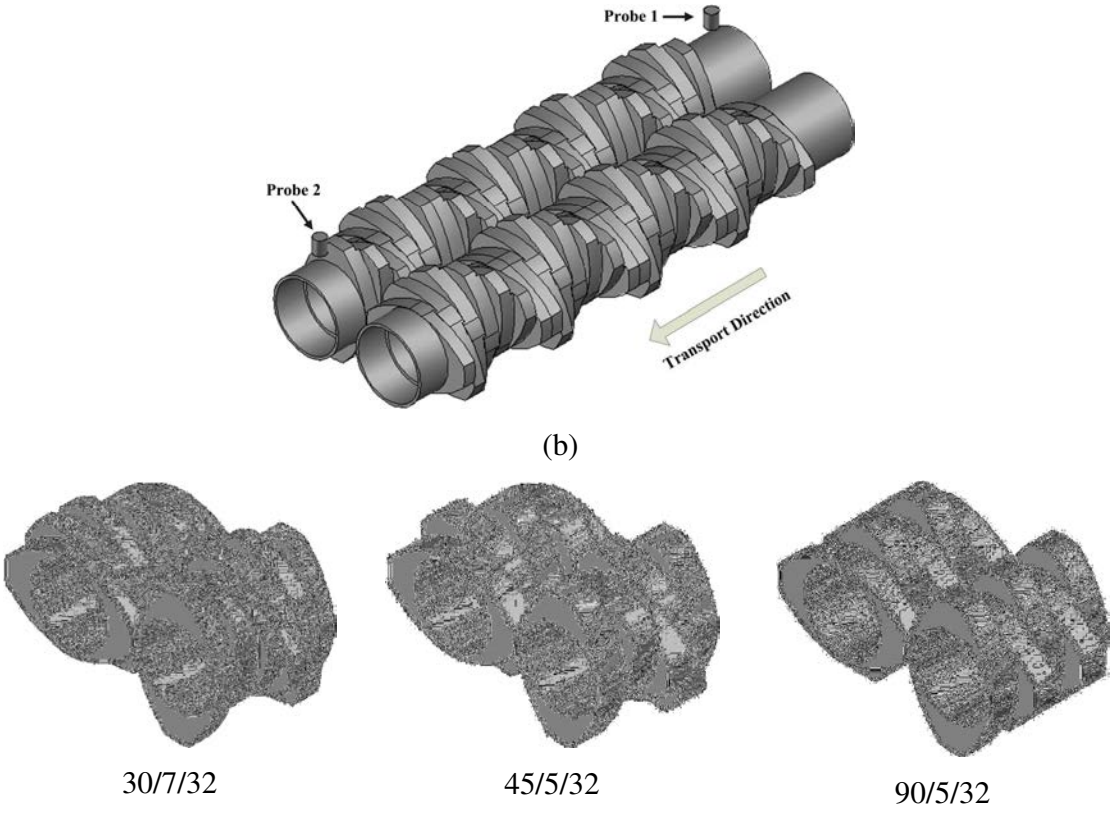

Fig. 2.1. (a) Three locations (three test points) where the RTD probes were placed; (b) details of the screw profile of the kneading zone between probes 1 and 2; (c) details of the three different types of kneading discs used for the kneading zone. A kneading block x/y/z is one which has a length of z mm and y discs. The latter are assembled x degrees one with respect to the other. The set barrel temperature was 220 °C throughout.

There were three RTD test points, as marked by probes 1, 2 and 3, respectively. Probes 1 and 2 were placed at the front and the rear ends of the kneading zone, respectively. They measured the partial RTD density functions $E_1(t)$ and $E_2(t)$, respectively. Probe 3 was placed in the die and measured the overall RTD density function of the extruder between the feeder and the die, $E_3(t)$. The local RTDs, $E_{12}(t)$, $E_{23}(t)$ and $E_{13}(t)$, corresponding to the three local zones of the extruder, can be obtained by the deconvolution of experimental RTDs $E_1(t)$, $E_2(t)$ and $E_3(t)$, as will be further discussed later.

2.2.2 Materials

Polystyrene (PS) was used as the flow material. It was supplied by YANGZI - BASF, China. Fig. 2.2 shows the variation of its viscosity as a function of shear rate at 220 °C. The tracer was in the form of masterbatch containing the PS and anthracene. The concentration of anthracne in the masterbatch was 1, 3, 5 or 10 % by mass, respectively. Those masterbatches were prepared by blending the PS with anthracene in a Haake batch mixer and then extruded into pellets whose dimensions were similar to those of the PS. Table 2.1 shows the various experiments carried out in this work and their operating conditions.

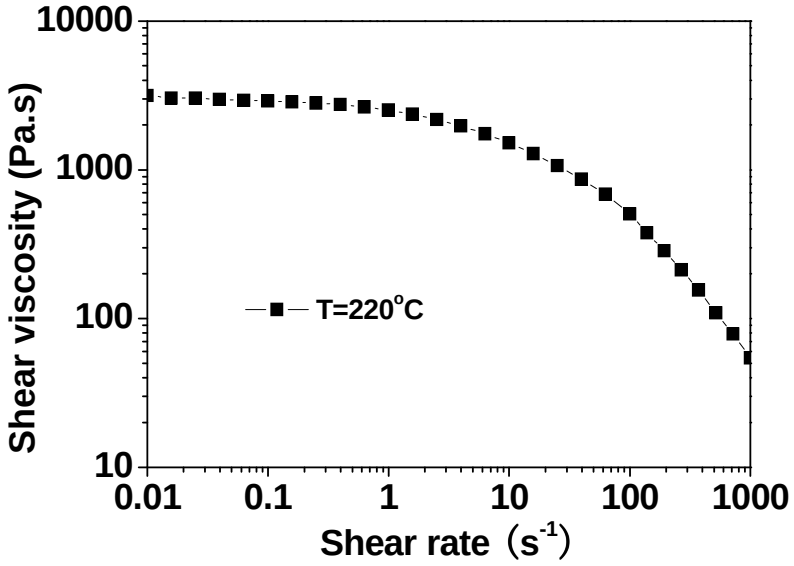

Fig. 2.2 Variation of the viscosity of the polystyrene used in this work as a function of shear rate at 220 °C.

Table 2.1 Experiments carried out in this work and their operating conditions (processing temperature: 220°C).

Experiment No.	1	2	3	4	5	6	7	8	9
Screw Speed N（rpm）	60	90	120	150	120	120	90	150	150
Mass feed rate Q（kg/h）	10.7	10.7	10.7	10.7	14.3	15.5	8	17.8	13.4

2.2.3 Instrumentation

The new in-line RTD measuring system developed in this work was mainly composed of the following three parts: fluorescent light generation, fluorescent light detection and signal processing (see Fig. 2.3). The fluorescent light source was an ultraviolet high-pressure mercury lamp (125W) and was split into two beams. Each of them successively passed through a coupler and a bifurcated optical fiber before it irradiated the tracer containing polymer flow stream in the extruder. The light with a specific wavelength emitted from the provocative tracer was subsequently transmitted to a fluorescent detector (a photomultiplier) through the bifurcated optical fiber probe and was then amplified through an amplifier. Finally the amplified optical signals coming from the two fluorescent detectors reached the signal processing unit. The latter converted them to two analog ones. They were then collected by the computer system and were displayed in real time on the screen. The sensitivity of the measuring system could be regulated by a knob with respect to different amounts of tracer. Signals were collected once every second.

It should be noted that the above in-line RTD measuring instrument followed exactly the same basic principle as the one developed by Hu et al.[9, 16]. However, there were a few important differences/improvements. First, a reference detector was added to the system to improve the resistance of the latter to both external and internal disturbances. As a result, baseline noises were reduced and the quality of the signals enhanced. Second, it had two light paths or two optical probes instead of one in [9]. Thus it allowed to

simultaneously measure the RTDs at two different locations. Assessment of local RTDs then became possible. Third, the material used for the optical fiber was silica instead of poly(methyl methacrylate) used in [9]. Silica withstood much higher temperatures than poly(methyl methacrylate). Therefore, the probe could be installed anywhere along the extruder. Finally, the design of the probe was very different from that of the probe in [9], as show in Fig. 2.4. Its front end was a quartz window. The latter allowed to prevent the probe from polymer deposition. Moreover, part of the probe body was a ribbed radiator capable of rapidly dissipating heat, which was very important for improving the robustness of the probe because temperatures to which it was subjected could be very high (150 to 300 °C). As for the light filter, it served to ensure that only the desired monochromatic light could pass through.

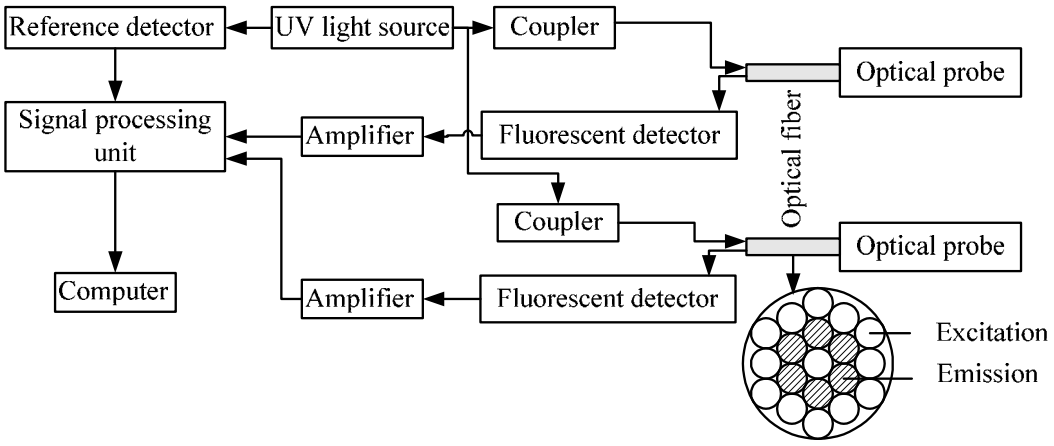

Fig. 2.3 Diagram of the in-line RTD measuring system involving three main parts: a fluorescent light generating source, fluorescent light detection and signal processing.

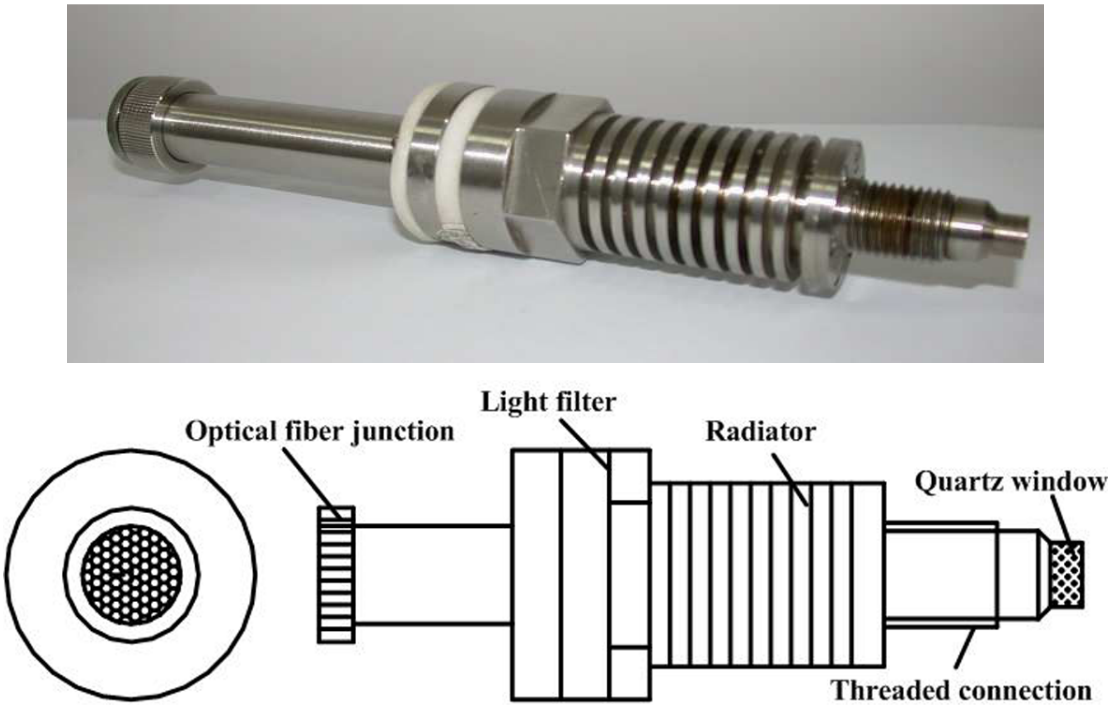

Fig. 2.4. A picture and a schematic diagram of optical probe.

2.3 Results and Discussion

2.3.1 Performance of the New In-Line RTD Measuring Instrument

The new in-line RTD measuring instrument was very different from the one reported in the literature [9], as outlined in the experimental section. Therefore its performance had to be evaluated first. It was done in terms of the reproducibility, on the one hand; and the linearity between the amplitude of the response single and the amount of the tracer, on the other hand. The former was verified by doing repeated experiments. Fig. 2.5 shows the raw analog signals collected from probes 1 and 2 for three repeated experiments. The relative voltage vs. time curves were very smooth and the reproducibility was very good for each of the two probes. However, it is noted that the baselines were not at zero. Nevertheless, they were all virtually at the same and small value.

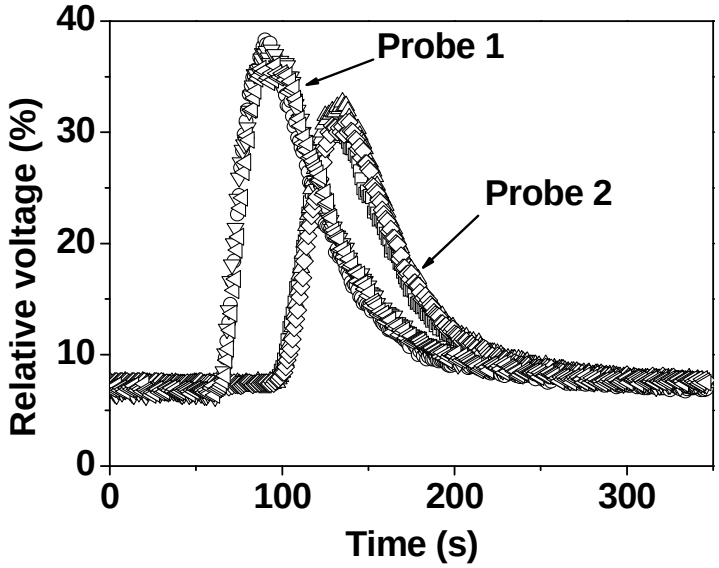

Fig. 2.5 Raw analogue signal (relative voltage) vs. time curves for three repeated experiments carried out under the following conditions: screw configuration 3; screw speed = 90 rpm, feed rate = 8 kg/h; tracer = masterbatch containing 5% anthracene by mass; amount of the tracer = three pellets.

Fig. 2.6 shows the effect of the concentration of the tracer (anthracene) in the masterbatch on the raw analogue signal (relative voltage) vs. time detected by probe 3. As the concentration of the tracer in the masterbatch increased, the relative voltage vs. time curve was shifted upward, as expected. The curves in Fig. 2.6a should all fall on two single and separate master curves if they are normalized with respect to the areas under them and if the relative voltage is linearly proportional to the concentration of the tracer in the masterbatch. That was basically the case, as shown in Fig. 2.6b. However, the baselines were more scattered when the concentration of the tracer in the masterbatch was lower, say, 1 or 3%. Based on those results, the masterbatch containing 5% anthracene was chosen for subsequent RTD experiments.

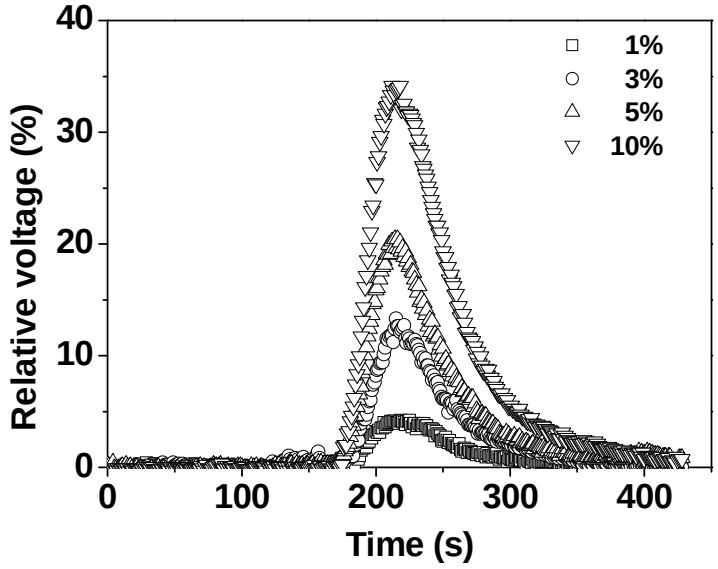

（a）

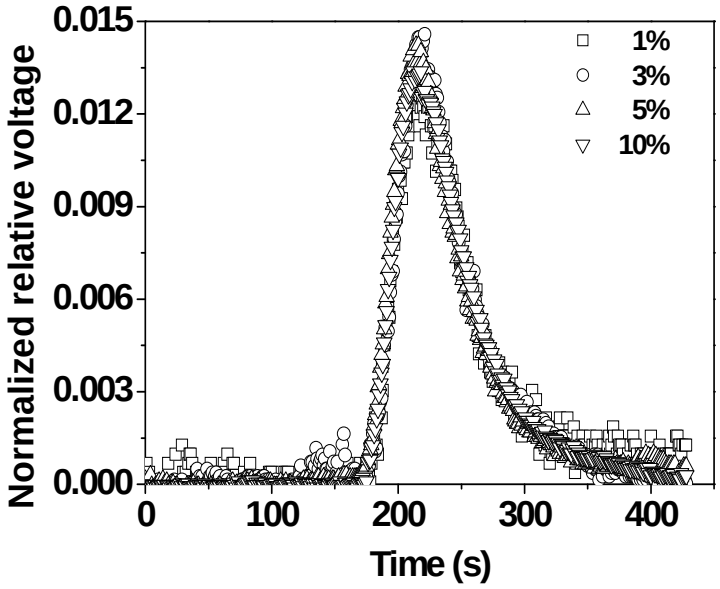

（b）

Fig. 2.6 (a) Effect of the concentration of the tracer (anthracene) in the masterbatch on the raw analog signal at probe 3; (b) Normalized relative voltage vs. time curves based on Fig. 2.6a. Screw configuration 1; screw speed = 60 rpm; feed rate = 10.7 kg/h; amount of the tracer masterbatch = 0.1 g (4 pellets); concentration of the tracer in the masterbatch varying from 1 to 10% by mass. The baselines of the raw analogue signal were scaled to zero.

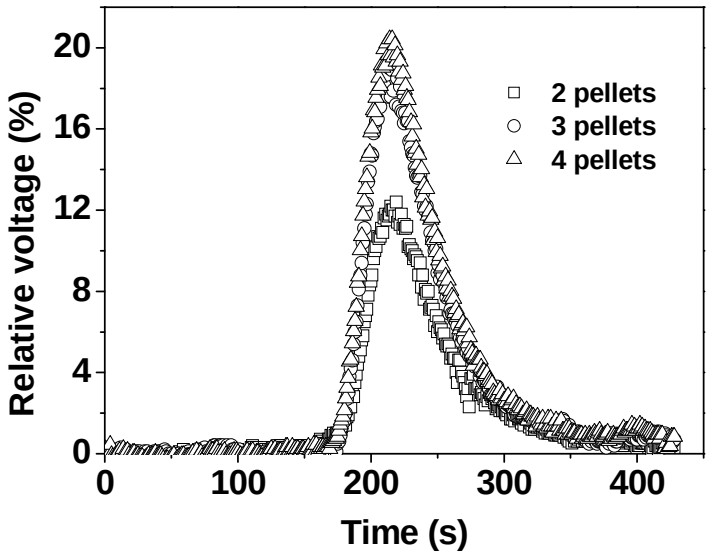

(a)

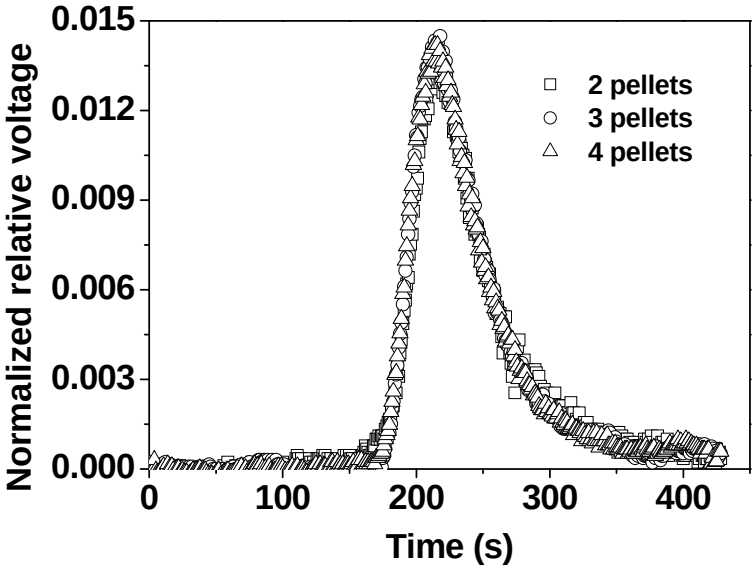

(b)

Fig. 2.7 (a) Effect of the amount of the masterbatch (number of pellets) on the raw analog signal at probe 3; (b) Normalized relative voltage vs. time curves based on Fig. 2.7a. Screw configuration 1; screw speed = 60 rpm; feed rate = 10.7 kg/h. The baselines of the raw analog signal were scaled to zero.

Fig. 2.7a shows the effect of the amount of the masterbach (number of pellets) on the relative voltage measured at probe 3. Again as expected, the relative voltage vs. time

curve was shifted upward when the amount of the masterbatch increased. Fig. 2.7b shows the normalized relative voltage vs. time for the results in Fig. 2.7a. A single master curve was obtained. Based on the results obtained with the different amounts of tracer, 3 pellets of the masterbatch containing 5% anthracene were used for subsequent experiments. Since under those conditions the relative voltage was linearly proportional to the tracer concentration, a normalized relative voltage vs. time curve obtained under those conditions could be taken as the RTD density function E(t).

2.3.2 Effects of Screw Speed and Feed Rate on RTD

A twin-screw extruder often works under starved conditions. Therefore, screw speed (N) and feed rate (Q) are two independent operating parameters. In this work, their effects on the RTD were studied with screw configuration 3. Fig. 2.8 shows that at a given feed rate, increasing screw speed shifted the RTD curve towards the shorter time domain, whatever the probe location. However, their width seemed to be only slightly affected. This implies that under the specified conditions, increasing screw speed did not improve much the quality of the axial mixing. Rather it simply conveyed the material toward the die exit in a more rapid manner. Fig. 2.9 shows that at a given screw speed, increasing feed rate shifted the RTD curve towards the shorter time domain, whatever the probe location. This is similar to the effect of increasing screw speed. However, the RTD curves significantly narrowed, which was different from increasing screw speed. This infers that increasing feed rate tended to decrease the quality of the axial mixing.

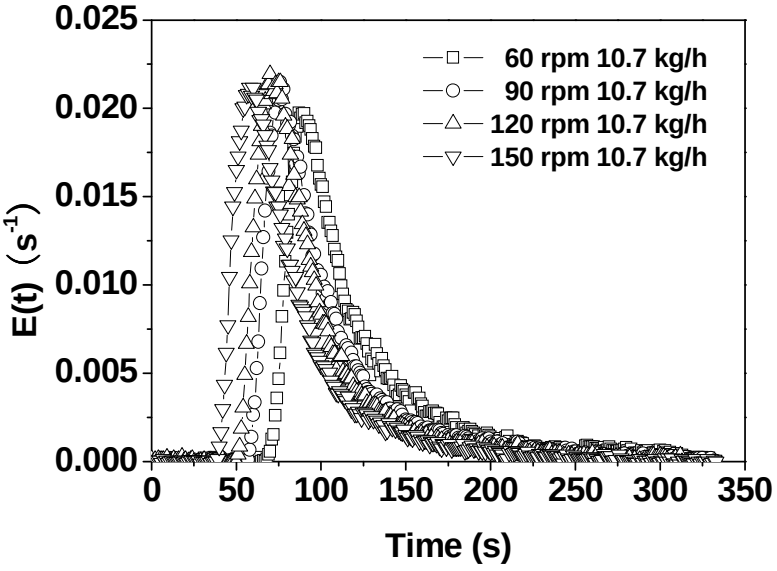

(a)

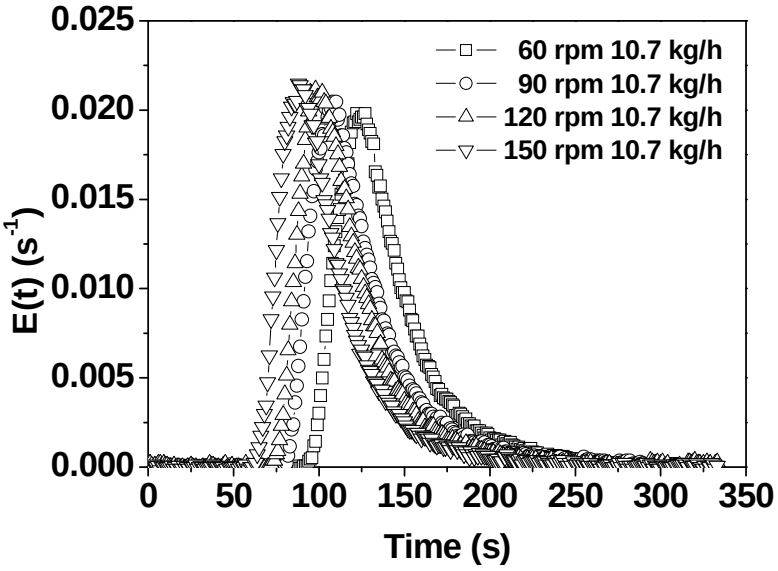

(b)

Fig. 2.8 Effect of screw speed on the RTD. (a) screw configuration 3 and probe 1; (b) screw configuration 3 and probe 2.

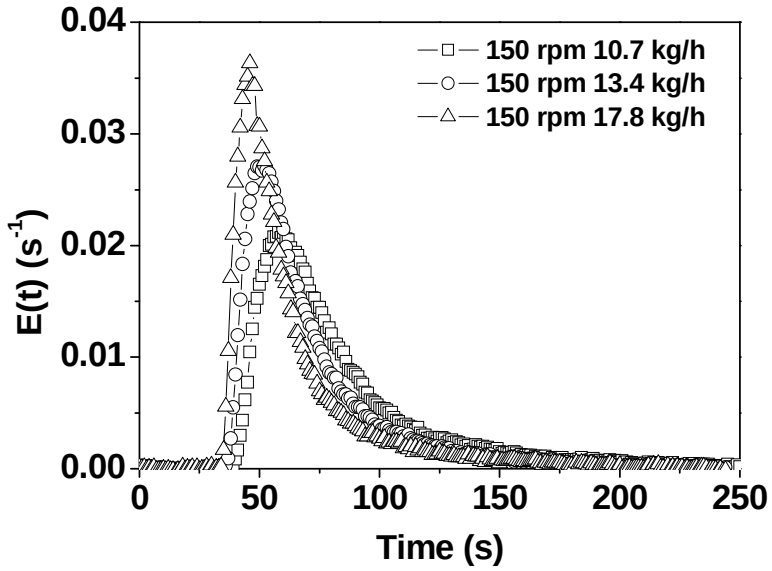

（a）

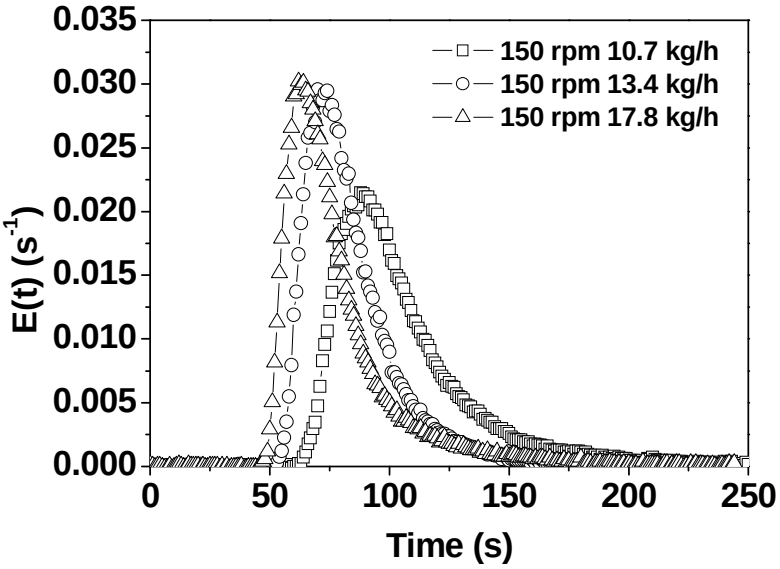

(b)

Fig. 2.9 Effect of feed rate on the RTD. (a) screw configuration 3 and probe 1; (b) screw configuration 3 and probe 2.

The above finding that increasing screw speed or feed rate shifted the RTD curve to the shorter time domain is in agreement with all the works reported in the literature[6, 9, 10, 17, 18]. As for the finding that the shape of the RTD curve was more affected by feed rate than screw speed is in line with some works reported in the literature[17, 18] and is in

contradiction to some others[6, 9, 10]. Understanding the exact reasons for the contradiction is of very practical significance because it will help conduct (reactive) extrusion processes under optimal conditions. However, thus far they remain unclear and would likely be related to differences that existed among those works in terms of the type, the size and the screw profile of the extruder, the material and the operating conditions. A rational model capable of taking into account all relevant parameters is thus needed, which is out of the scope of this paper and will be dealt with in a forthcoming one.

2.3.3 Assessment of the Local RTD in the Kneading Disc Zone

An important aim of this work to develop a new in-line RTD measurement device was to assess the local RTD of a kneading zone, on the one hand; and the effect of the geometry of the latter on its RTD, on the other hand. For those purposes, two probes were placed at the two ends of a kneading zone, respectively, as shown in Fig. 2.1. The flow and mixing conditions were expected to be such that they met those under such the statistical theory for the RTD would apply. Detailed discussion on the validity and applicability of that theory can be found elsewhere[19-21]. That theory stipulates that for a closed system composed of two statistically independent elements, A and B, the overall RTD density function E(t) is related to those of the two elements $E_A(t)$ and $E_B(t)$ by the following equation:

$$E(t) = \int_0^t E_A(t) \cdot E_B(t-\tau) d\tau \qquad (5)$$

This equation shows that knowing any two of the three RTD density functions allows to calculate the third one either by convolution or deconvolution. Assessment of the local RTDs calls upon deconvolution. Details on the deconvolution procedure are given in Appendix A.

Fig. 2.10 shows the effects of the staggering angle of the kneading discs on the partial and overall RTDs, $E_1(t)$, $E_2(t)$ and $E_3(t)$, measured by probes 1, 2 and 3, respectively. While all those RTD curves were very similar for the 30° and 45° kneading discs, they were significantly different from those obtained with the 90°. The width of the partial RTD curves with the 90° kneading discs was larger, indicating that the 90° kneading discs had a better axial mixing capacity than the 30° or 45° ones, as intuition or

some modeling works might suggest. It is also seen from Fig. 2.10a that the RTD of the screw zone located upstream with regard to the kneading zone between the feeder and probe 1, $E_1(t)$, could eventually be affected by the screw configuration of the kneading zone itself. Otherwise $E_1(t)$ should have always been the same, irrespective of the type of the kneading discs used for the kneading zone. Nevertheless, under the conditions of this work, the effect was relatively small.

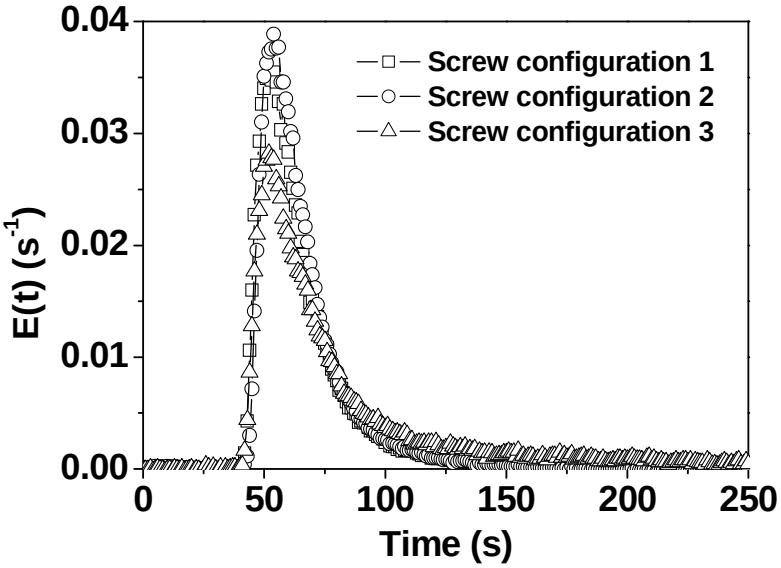

（a）

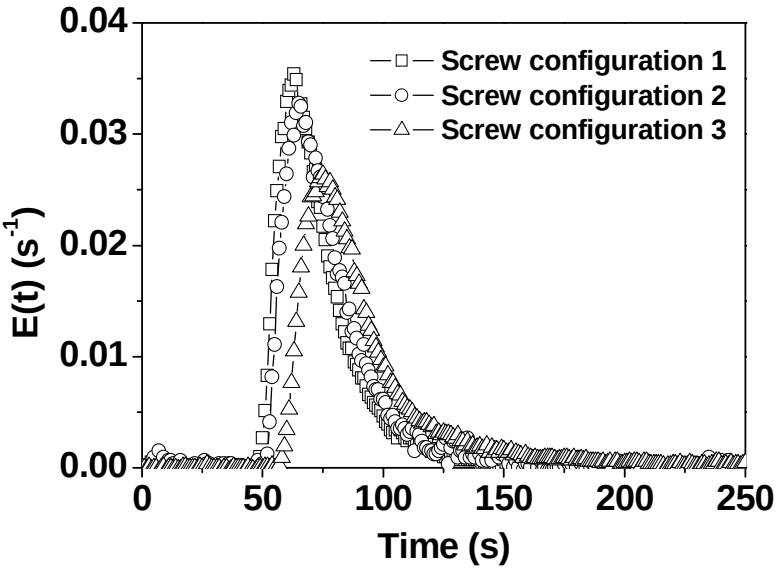

（b）

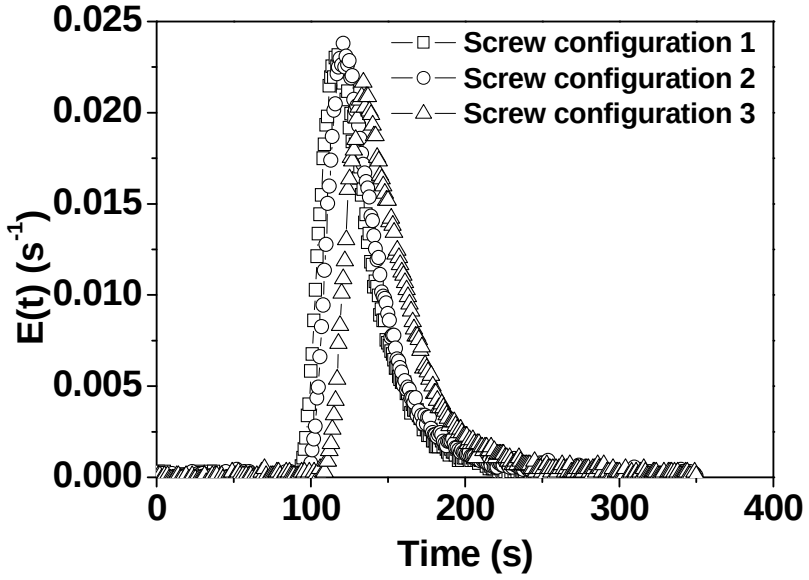

（c）

Fig. 2.10 Effect of the staggering angle of the kneading discs on the partial RTDs. (a) probe 1 (b) probe 2 (c) probe 3. Screw speed = 120 rpm; feed rate = 15.5 kg/h.

Fig. 2.11 shows the local RTDs in the kneading zone between probes 1 and 2, $E_{12}(t)$, for the three screw configurations that differed only in the staggering angle of the kneading discs used for the kneading zone (Fig. 2.1c). They were obtained by deconvolution using the RTD curves in Fig. 2.10 and following the procedure outlined in Appendix A. The effect of the staggering angle of the kneading discs can now be appreciated in a clearer manner. Both the mean residence time and the axial mixing quality characterized quantitatively by the width of the $E_{12}(t)$ curve followed the order: $30° < 45° << 90°$.

Fig. 2.12 shows the local RTDs in the last part of the extruder between probes 2 and 3, $E_{23}(t)$. The width of the $E_{23}(t)$ was slightly different among the three screw configurations, implying that the mixing performance of the screw zone between probes 2 and 3 was almost unaffected by the screw configuration of the upstream kneading zone. However, obvious differences existed among the three screw configurations in terms of the delay time and mean residence time. The above results imply that the screw profile of the kneading zone affected more the downstream velocity than the flow pattern.

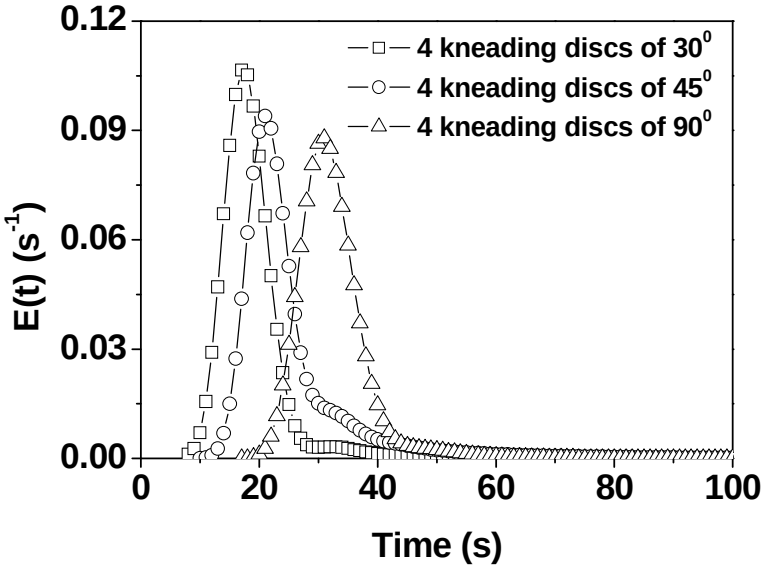

Fig. 2.11 Effect of the staggering angle on the RTD over the kneading zone between probes 1 and 2. See Fig. 2.10 for the screw configurations and the operating conditions.

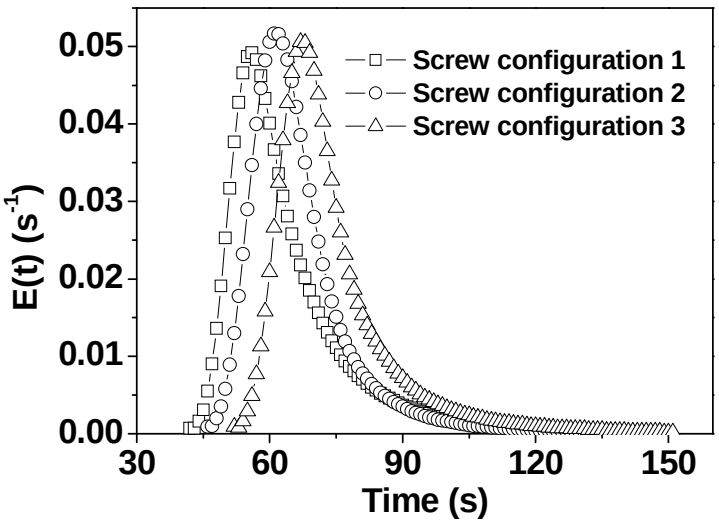

Fig. 2.12 Effect of the staggering angle on the RTD between probes 2 and 3. See Fig. 2.10 for the operating conditions.

Fig. 2.13 shows the local RTDs between probes 1 and 3, $E_{13}(t)$, for the three screw configurations (Fig. 2.1c). They were obtained by the deconvolution of the experimental data collected at probe 3 and probe 1 (see the discrete points). They are compared with those obtained by the convolution of $E_{12}(t)$ and $E_{23}(t)$ (see the solid curves). The $E_{13}(t)$ curves obtained by the deconvolution of the experimentally measured $E_3(t)$ and $E_1(t)$

agreed well with those obtained by the convolution of the $E_{12}(t)$ and $E_{23}(t)$, showing that both the deconvolution and convolution methods worked well.

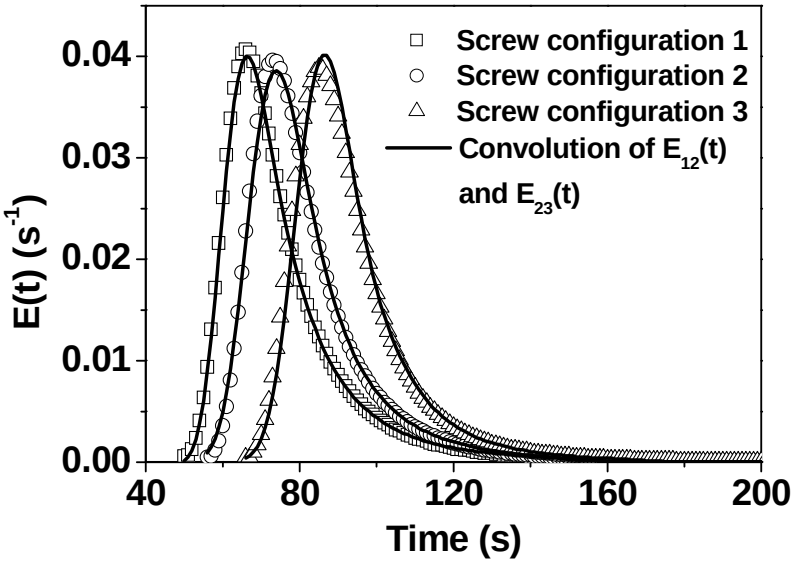

Fig. 2.13 Effect of the staggering angle on the RTD between probes 1 and 3. The deconvolution result of E3(t) and E1(t) are agree with convolution results of E12(t) and E23(t) corresponding to Fig. 2.12 and Fig. 2.13 well. See Fig. 2.10 for the operating conditions.

2.4 Conclusions

The main objective of the work reported here was to develop a new in-line residence time distribution (RTD) measuring instrument to assess local RTDs in a screw extruder. The basic principle of that instrument was the same as the one in the literature [9]. The new instrument possessed several important improvements/advantages over the one in ref. [9]. For example, it had a reference detector that allowed to improve the resistance of the latter to both external and internal disturbances. As a result, baseline noises were reduced and the quality of the signals enhanced. It possessed two light paths/two optical probes instead of one in [9]. Thus it allowed to simultaneously measure the RTDs at two different locations. Assessment of local RTDs then became possible. The material used for the optical fibers was silica instead of poly(methyl methacrylate) used in [9]. Therefore, the probes could be installed anywhere along the extruder. Also the design of the optical probes was different, making them much more robust. The new device indeed

showed good reproducibility and reliability when it was tested on a co-rotating twin screw extruder using anthracene as tracer and polystyrene as flowing material.

Increasing screw speed or feed rate shifted the overall, partial and local RTDs toward the shorter time domain, as expected. On the other hand, increasing screw speed did not affect much the spread of the RTD whereas increasing feed rate decreased its spread, implying that the former did not improve much the axial mixing and the latter decreased it.

The local RTD of a kneading zone depended very much on the geometry (staggering angle) of the kneading discs and provided a mean to quantifying, to some extent, the mixing performance of various types of kneading elements. The mean residence time and the width of the RTD in a kneading zone composed of kneading discs followed the order: $30° < 45° << 90°$, indicating that kneading discs with a staggering angle of 90° had the best axial mixing performance.

The geometry (staggering angle) of the kneading discs in a kneading zone could have an effect on the flow of its neighboring and partly filled upstream and downstream. Under the conditions studied in this work, its effect on the flow of its neighboring and partly filled upstream was small. On the other hand, its effect on the flow of its neighboring and partly filled downstream zone was significant in terms of axial velocity and not much so in terms of flow pattern.

2.5 Appendix A

Deconvolution of Eq. 5 is an ill-defined numerical problem, particularly when it comes to deconvoluting experimental data which are always more or less scattered. To get rid of numerical difficulties, we first fit experimental data using an appropriate mathematical function. Gao et al. [17]chose to use the following equation to fit their RTD curves:

$$E(t) = \frac{d^3}{2}(t - t_d)^2 e^{-d(t-t_d)} \qquad (2.5)$$

where d is the RTD shape factor and t_d is the delay time. They used this equation to fit each of twelve operating conditions for two different screw geometries with d and t_d as

adjustable parameters. Poulesquen et al. [22]used the following expression to fit their RTD curves:

$$E(t) = a \cdot t^{-c-1} \cdot b^{c+1} \exp[(b^c t^{-c} - 1) \cdot (\frac{-c-1}{c})] \tag{2.6}$$

where a, b and c are adjustable parameters, determined to fit the measured data using a least square optimization method. We found that both Gao's and Poulesquen's equations fit our RTD data well. The latter did a slightly better job, likely because it had one more adjustable parameter. We finally chose to use Poulesquen's equation to fit our data for subsequent deconvolution purposes.

After the experimental data are fitted, the $E_1(t)$, $E_{12}(t)$ and $E_2(t)$ can be expressed by vectors $u = (u_0, u_1, u_2, \cdots, u_m)$, $v = (v_0, v_1, v_2, \cdots, v_n)$ and $w = (w_0, w_1, w_2, \cdots w_{m+n-1})$, respectively. The length of vector w is m+n-1 as a result of the convolution of vectors u and v. According to the numerical solution of the convolution, the following equation set can be derived:

$$\begin{cases} w_0 = u_0 v_0 \\ w_1 = u_0 v_1 + u_1 v_0 \\ w_2 = u_0 v_2 + u_1 v_1 + u_2 v_0 \\ \cdots \\ w_n = u_0 v_n + u_1 v_{n-1} + \ldots + u_n v_0 \\ \cdots \\ w_{m+n-1} = u_m v_n \end{cases} \tag{2.7}$$

Eq. (2.7) can also be written in a matrix form as follows:

$$\begin{bmatrix} u_0 & 0 & 0 & \cdots & 0 & 0 & \cdots & 0 & 0 \\ u_1 & u_0 & 0 & \cdots & 0 & 0 & \cdots & 0 & 0 \\ u_2 & u_1 & u_0 & \cdots & 0 & 0 & \cdots & 0 & 0 \\ \vdots & \vdots & \vdots & & \vdots & \vdots & & \vdots & \vdots \\ u_n & u_{n-1} & u_{n-2} & \cdots & u_0 & 0 & \cdots & 0 & 0 \\ 0 & u_n & u_{n-1} & \cdots & u_1 & u_0 & \cdots & 0 & 0 \\ \vdots & \vdots & \vdots & & \vdots & \vdots & & \vdots & \vdots \\ 0 & 0 & 0 & \cdots & u_m & u_{m-1} & \cdots & u_1 & u_0 \end{bmatrix} \begin{bmatrix} v_0 \\ v_1 \\ v_2 \\ \vdots \\ v_n \\ 0 \\ \vdots \\ 0 \end{bmatrix} = \begin{bmatrix} w_0 \\ w_1 \\ w_2 \\ \vdots \\ w_n \\ w_{n+1} \\ \vdots \\ w_{m+n-1} \end{bmatrix} \tag{2.8}$$

Since vectors u and w are known, the unknown vector v, i.e. $E_{12}(t)$, can be calculated. However, it should be noted that Eq. A3 is an over-determined one. Its solution can be

found by a classical least square minimization method.

Since the statistical theory for the RTD assumes that the partial and local RTDs are statistically independent, the unknown delay time for $E_{12}(t)$ can be determined from the difference between the delay time of $E_2(t)$ and that of $E_1(t)$. $E_{23}(t)$ and $E_{13}(t)$ can be obtained by the same procedure.

2.6 References

[1]. Nauman, E. B.; Buffham, B. A. *Mixing in continuous flow system;* John Wiley & Sons, Inc.: New York, USA, 1983.

[2]. Kiani, A.; Heidemeyer, P.; Pallas, R. Study of flow and RTD in a ZSK twin screw extruder. Toronto, America, 1997; pp 94-99.

[3]. Sun, Z.; Jen, C. K.; Shih, C. K.; Denelsbeck, D. A. Application of ultrasound in the determination of fundamental extrusion performance: residence time distribution measurement. *Polymer Engineering and Science* **2003,** *43* (1), 102-111.

[4]. Wetzel, M. D.; Shih, C. K.; Sundararaj, U. Determination of residence time distribution during twin screw extrusion of model fluids. Toronto, America, 1997; pp 3707-3712.

[5]. Unlu, E.; Faller, J. F. Geometric mean vs. arithmetic mean in extrusion residence time studies. *Polymer Engineering and Science* **2001,** *41* (5), 743-751.

[6]. Chen, T.; Patterson, W. I.; Dealy, J. M. On-line measurement of residence time distribution in a twin-screw extruder. *International Polymer Processing* **1995,** *10* (1), 3-9.

[7]. Carneiro, O. S.; Covas, J. A.; Ferreira, J. A.; Cerqueira, M. F. On-line monitoring of the residence time distribution along a kneading block of a twin-screw extruder. *Polymer Testing* **2004,** *23,* (8), 925-937.

[8]. Hu, G. H.; Kadri, I. Preparation of macromolecular tracers and their use for studying the residence time distribution of polymeric systems. *Polymer Engineering and Science* **1999,** *39* (2), 299-311.

[9]. Hu, G. H.; Kadri, I.; Picot, C. On-line measurement of the residence time distribution in screw extruders. *Polymer Engineering and Science* **1999,** *39* (5), 930-939.

[10]. Sun, Y. J.; Hu, G. H.; Lambla, M.; Kotlar, H. K. In situ compatibilization of polypropylene and poly(butylene terephthalate) polymer blends by one-step reactive extrusion. *Polymer* **1996,** *37* (18), 4119-4127.

[11]. Cartier, H.; Hu, G. H. Morphology development of in situ compatibilized semicrystalline polymer blends in a co-rotating twin-screw extruder. *Polymer*

Engineering and Science **1999,** *39* (6), 996-1013.

[12]. Cartier, H.; Hu, G. H. Plastification or melting: A critical process for free radical grafting in screw extruders. *Polymer Engineering and Science* **1998,** *38* (1), 177-185.

[13]. Hu, G. H.; Cartier, H. Free radical grafting of glycidyl methacrylate onto PP in a co-rotating twin screw extruder: Influence of feeding mode. *International Polymer Processing* **1998,** *13* (2), 111-117.

[14]. Hu, G. H. Reactive Polymer Processing: Fundamentals of Reactive Extrusion. In *Encyclopaedia of Materials: Science and Technology*, Buschow, K. H. J., Cahn, R. W., Flemings, M. C., Ilschner, B., Kramer, E. J., Mahajan, S., Eds.; Elsevier Science: Amsterdam, The Netherlands, 2001; pp 8045-8057.

[15]. Baker, W.; Scott, C.; Hu, G. H. *Reactive Polymer Blending;* Hanser: Muinich, Germany, 2001.

[16]. Xu, Z. B.; Feng, L. F.; Hu, G. H.; Wang, L. G.; Zhang, X. M.; Li, B. G. An apparatus for in-line measurement of the residence time distribution of thermomechanically complex systems. *Recent Progress in Process Engineering* **2005,** *92*, 7-16.

[17]. Gao, J.; Walsh, G. C.; Bigio, D.; Briber, R. M.; Wetzel, M. D. Residence-time distribution model for twin-screw extruders. *AIChE Journal* **1999,** *45* (12), 2541-2549.

[18]. Razaviaghjeh, M. K.; Nazockdast, H.; Assempour, H. Determination of the residence time distribution in twin screw extruders via free radical modification of PE. *International Polymer Processing* **2004,** *19* (4), 335-341.

[19]. Chen, L.; Hu, G. H. Applications of a statistical theory in residence time distributions. *AIChE Journal* **1993,** *39* (9), 1558-1562.

[20]. Chen, L.; Pan, Z.; Hu, G. H. Residence time distribution in screw extruders. *AIChE Journal* **1993,** *39* (3), 1455-1464.

[21]. Chen, L.; Hu, G. H.; Lindt, J. T. Residence time distribution in non-intermeshing counter-rotating twin-screw extruders. *Polymer Engineering and Science* **1995,** *35* (7), 598-603.

[22]. Poulesquen, A.; Vergnes, B.; Cassagnau, P.; Michel, A.; Carneiro, O. S.; Covas, J. A. A study of residence time distribution in co-rotating twin-screw extruders. Part II: Experimental validation. *Polymer Engineering and Science* **2003,** *43* (12), 1849-1862.

CHAPTER 3 Local Residence Time, Residence Revolution and Residence Volume Distributions in Twin-Screw Extruders

ABSTRACT

(a) This work was aimed at studying the overall, partial and local residence time distributions (RTD); overall, partial and local residence revolution distributions (RRD) and overall, partial and local residence volume distributions (RVD) in a co-rotating twin screw extruder, on the one hand; and establishing the relationships among them, on the other hand. Emphasis was placed on the effects of the type and geometry of mixing elements (a gear block and various types of kneading elements differing in staggering angle) and process parameters on the RTD, RRD and RVD. The overall and partial RTD were directly measured in-line during the extrusion process and the local ones were calculated by deconvolution based on a statistical theory. The local RTD allowed comparing the mixing performance of mixing elements. Also it was confirmed both experimentally and theoretically that specific throughput, defined as a ratio of throughput (*Q*) over screw speed (*N*), controlled all the above three types of residence distributions, be they local, partial or overall. The RRD and RVD do not provide more information on an extrusion process than the corresponding RTD. Rather they are different ways of representing the same phenomena.

3.1 Introduction

Twin-screw extruders are one of the most important types of equipment for both food and polymer processing. In the field of polymers, they are mainly used as mixers/reactors for blending, compounding and reactive processing[1]. During an extrusion process, each material element may undergo a different temporal, thermal and/or mechanical history. As a result, its final properties may be different from those of the other material elements[2-5]. The residence time of a material element is the time it spends in the extruder. Since all material elements do not necessarily spend the same elapse of time in the extruder, the residence times have a distribution, called residence time distribution (RTD). The latter provides information not only about the spread of the residence time but also the flow pattern and mixing quality in the extruder. Experimentally the RTD density function, ***E(t)***, can be obtained by injecting an inert tracer as a pulse to the extruder and measuring its concentration at a chosen location. The amount of the tracer used should be low enough so as not to disturb the flow field. E(t) can then be calculated according to Eq. (3.1)[6]:

$$E(t) = \frac{c(t)}{\int_0^\infty c(t)dt} = \frac{c(t)}{\sum_{i=0}^{\infty} c(t)\Delta t} \tag{3.1}$$

where c is the tracer concentration at time t. The mean residence time is defined as

$$\bar{t} = \int_0^\infty tE(t)dt = \frac{\int_0^\infty tc(t)dt}{\int_0^\infty c(t)dt} = \frac{\sum_{i=0}^{\infty} tc(t)\Delta t}{\sum_{i=0}^{\infty} c(t)\Delta t} \tag{3.2}$$

Besides the above distribution in the residence time which is characterized by ***E(t)***, there are also distributions in residence revolution and residence volume, called residence revolution distribution (RRD) and residence volume distribution (RVD), respectively[7]. The RRD and RVD are obtained when the time coordinate of the RTD is converted to the number of accumulated screw revolutions (n) and the volume of the extrudate (v), respectively. They are given by Eqs. (3.3) and (3.4), respectively:

$$F(n) = \frac{c(\frac{n}{N})}{\int_0^\infty c(\frac{n}{N})dn} \tag{3.3}$$

$$G(v) = \frac{c(\frac{v}{Q})}{\int_0^\infty c(\frac{v}{Q})dv} \tag{3.4}$$

where N and Q are the screw speed (revolutions per min or rpm) and material volume throughput (liter/min), respectively. The integration variables of $F(n)$ and $G(v)$ are the cumulative screw revolutions (n) and cumulative extrudate volume (v), respectively. Their relationships with time are the following:

$$t = n / N = v / Q \tag{3.5}$$

According to reference [7], the RVD was a direct measure of the tracer distribution along the screw length, thus a measure of the degree of the axial mixing. On the other hand, the RRD may shed light on the transport behavior of the material in the extruder.

Most previous studies[7-9] dealt with the overall RTD, RRD and RVD, i.e., those of the entire extruder from the hopper to the die exit. Wetzel et al.[10] proposed a method to deconvolute the RTD curves of a model fluid by a pre-determined mathematical function. Canevarolo et al.[11] used a direct method to determine the RTD curves of individual elements. However, those studies were limited to the RTD. Potente et al.[12, 13] investigated the local RTD and RVD using a method similar to the one proposed by Wetzel et al.[10]. However, the extruder used was a model twin-screw extruder.

Screw configuration has a pronounced effect on the RTD. Xie et al.[14] analyzed the effects of different screw configurations on the broadness of mixing and compared their subtle differences. Elkouss et al.[15] illustrated a linear relationship between the mean number of screw revolution and the inverse of specific throughput. Specific throughput is defined as the ratio between throughput and screw speed. The linear relationship could differentiate screws composed of different elements. Oberlehner et al.[16] used an off-line method to study the RTD of different types of screw elements such as right- and left-handed ones and mixing ones.

Based on the above mentioned state of the art, this work was aimed at: (1)

systematically investigating, at the same time, the overall, partial and local RTD, RRD and RVD in an industrially relevant co-rotating twin-screw extruder with emphasis on the local ones; (2) developing and validating relationships among the above three types of residence distributions; (3) comparing the local RTD, RRD and RVD among different screw elements. This work was made possible by a newly developed in-line measuring instrument[17, 18].

3.2 Experimental

Experiments were carried out on a co-rotating twin screw extruder with a diameter of 35 mm. Fig. 3.1 shows the locations of RTD probes and four different screw configurations used in the study. The head of the extruder was equipped with a strip die (L = 30 mm; H = 1.2 mm).

Three probes, 1, 2 and 3, were installed along the extruder length. Details about the characteristics and working principles of those probes can be found elsewhere[17, 18]. There were four identical kneading blocks or gear blocks between probes 1 and 2, called the test zone. Three types of kneading blocks (30/7/32, 60/4/32 and 90/5/32) and one type of gear block were chosen to study the effect of the screw configuration on the overall, partial and local RTD. Four screw configurations were used in this work. They differed only in the screw configuration of the test zone. Screw configurations 1, 2 and 3 corresponded to the cases where the test zone was composed of four 30/7/32, 60/4/32 and 90/5/32 kneading blocks, respectively. In screw configuration 4, the test zone was composed of 4 gear blocks. Probe 3 allowed measuring the overall RTD of the extruder between the feeder and the die exit, denoted as $E_3(t)$. Probe 2 measured the partial RTD of the extruder between the feeder and the rear test point of the test zone, denoted as $E_2(t)$. Similarly probe 1 measured the partial RTD of the extruder between the feeder and the front test point of the test zone, denoted as $E_1(t)$. The local RTD density function between probes 1 and 2 will be denoted as $E_{12}(t)$. The screw elements beneath probes 1 and 2 were cylinders. The cylinders ensured full fill of the screw elements beneath probes 1 and 2 and a constant depth between the probes and the screw element surfaces.

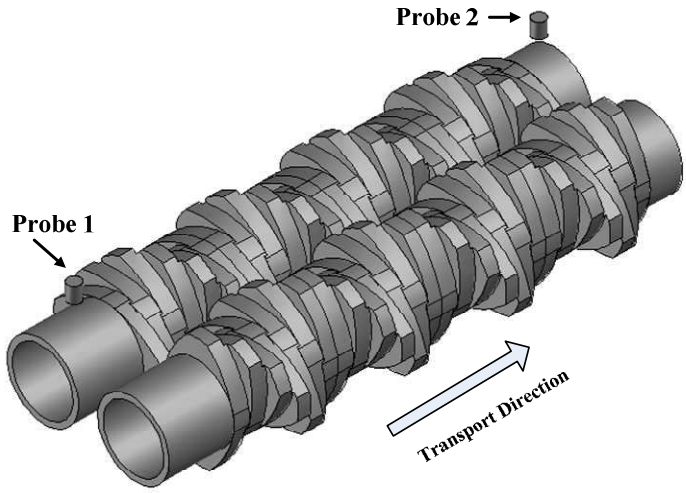

(a)

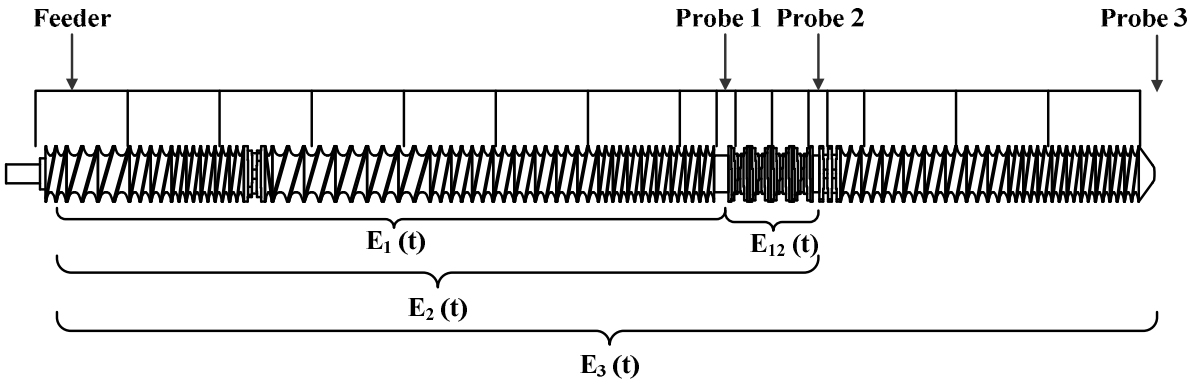

(b)

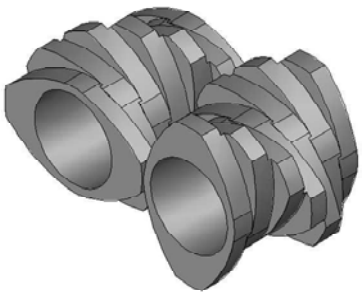

30/7/32

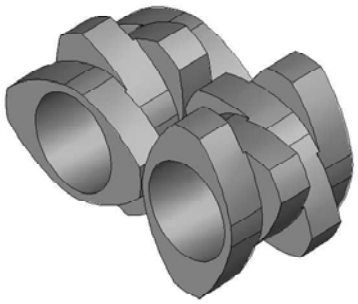

60/4/32

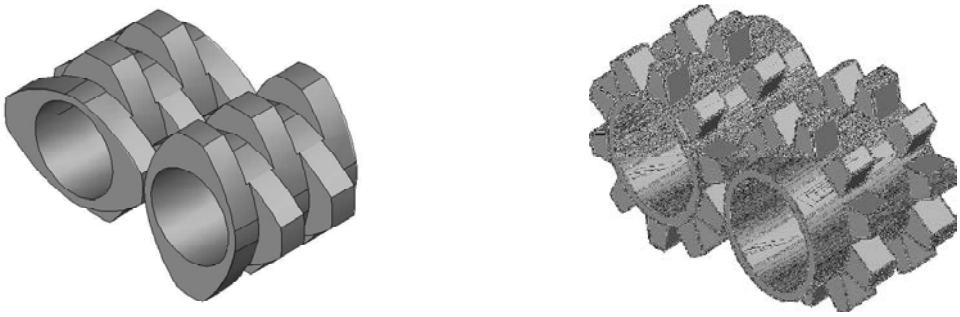

90/5/32 Gear block

(c)

Fig. 3.1 (a) Details of the screw profile of the test zone between probes 1 and 2; (b) locations (test points) of three RTD probes; (c) Detailed geometries of the three different types of kneading blocks and one type of gear blocks used for the test zone. A kneading block x/y/z had a length of z mm and y disc. The latter were assembled x degrees one with respect to the adjacent one. A gear block had two rows of gears along its length of 32 mm. There were 10 gears per row.

Polystyrene (PS) was used as the flow material. Its number and mass average molar masses were 1.23×10^5 and 2.76×10^5 g/mole, respectively. The tracer was in the form of masterbatch composed of the PS and anthracene. The concentration of anthracne in the masterbatch was 5% by mass. Those masterbatches were prepared by blending the PS with anthracene in a Haake batch mixer and then extruded into pellets similar to the PS. More details can be found elsewhere[17, 18]. Table 3.1 shows the experiments carried out in this work and their operating conditions. The volume throughput was calculated by dividing the mass throughput by the melt density of the PS, 970 kg/m^3.

Table 3.1 Experiments carried out in this work and their operating conditions. The barrel temperature was set at 220 °C throughout the screw length.

Experimental No.	1	2	3	4	5	6	7	8	9
Screw speed N (rpm)	60	90	120	150	120	120	150	150	90
Mass throughput (kg/h)	10.7	10.7	10.7	10.7	14.3	15.5	13.4	17.8	8.0
Volume throughput Q ($\times 10^{-3}$ liter/min)	183.8	183.8	183.8	183.8	245.7	266.3	230.2	305.8	137.5
Specific throughput Q/N ($\times 10^{-3}$ liter/rev.)	3.06	2.04	1.53	1.23	2.04	2.22	1.53	2.04	1.53

3.3 Results and Discussion

3.3.1 Partial RTD, RRD and RVD

A twin screw extrusion process often works under starved conditions (portions of the extruder are completely filled and others are partially filled). In order to better understand the process, it would be useful to search for a process parameter whose variation would not change the intensity of mixing but the RTD, or vice versa. Early studies[19-24] showed that specific throughput (*Q/N*) could be one. Fig. 3.2 and Fig. 3.3 show the RTDs of screw configuration 1 measured at probes 1 and 2 for two different specific throughputs. An increase in screw speed with a corresponding increase in throughput shifted the RTD curve to the shorter time domain, as expected. Moreover the RTD curve became narrower. Besides those classical two observations, there was not any obvious correlation or relationship among the RTD curves obtained at different screw speeds and throughputs at a given *Q/N*. However, when they were normalized with regard to their respective mean residence times, then they all superimposed on single master curves, respectively. Those are shown in Fig. 3.4 and Fig. 3.5 in which the $E(t)$ versus t curves are converted to $E(\tau)$ versus τ curves. $E(\tau)$ is the dimensionless residence time distribution density function and τ is the dimensionless residence time ($\tau = t/\bar{t}$)[23, 24]. This confirms the results of the literature that the dimensionless RTD density function $E(\tau)$ versus τ curve was unique when *Q/N* and screw configuration were fixed, irrespective of Q and N.

When the RTD curves in Fig. 3.2 and Fig. 3.3 were converted to the screw revolution and extrudate volume coordinates using (3.3) and (3.4), respectively, two pairs of master curves were obtained. They are shown in Fig. 3.6 and Fig. 3.7, Fig. 3.8 and Fig. 3.9, respectively. This indicates that the RRD and RVD were also unique when *Q/N* and screw configuration were fixed, irrespective of Q and N.

The key question is then what are the inherent factors that led to the master curves of the $E(\tau)$ versus τ, RRD versus n and RVD versus v shown in Figs. 3.4-3.9, respectively? What are the relationships among the $E(\tau)$ versus τ, RRD versus n and RVD versus v? Actually all of them are derived from the E(t) versus t and their respective abscissas are as follows:

$$\tau = t/\bar{t} \tag{3.6}$$

$$n = tN \tag{3.7}$$

$$v = tQ \tag{3.8}$$

According to Eq. (3.5), one has the following equality:

$$\tau = \frac{t}{\bar{t}} = \frac{n}{\bar{t}N} = \frac{v}{\bar{t}Q} \tag{3.9}$$

Considering Eq. (3.9) and the fact that when *Q/N* is fixed, *E(τ)* versus *τ*, RRD versus *n* and RVD versus *v* are master curves and are independent of Q and N, one arrives at the following relationships for a given *Q/N*:

$$N\bar{t} = k_1 = \text{constant1} \tag{3.10}$$

$$Q\bar{t} = k_2 = \text{constant2} \tag{3.11}$$

where k_1 and k_2 are constants and $k_2/k_1 = Q/N$. In other words, when *Q/N* is fixed, $N\bar{t}$ and $Q\bar{t}$ should be constants, whatever the values of *Q* and *N*. This will be discussed later.

The mean residence time can be determined by:

$$\bar{t} = \frac{V \times f}{Q} \tag{3.12}$$

where *V* is the free volume in the extruder barrel and *f* is the mean degree of fill. When Eq. (3.12) is introduced to Eqs. (3.10) and (3.11), respectively, the following equation is obtained:

$$f = \frac{k_1}{V} \times \frac{Q}{N} = \frac{k_2}{V} = \text{constant3} \tag{3.13}$$

Eq. (3.13) indicates that when *Q/N* is fixed, the mean degree of fill is fixed, regardless of *Q* and *N*. Mudalamane et al.[25] proposed the following equation to describe the relationship between the complete fill length, *FL*, and *Q/N*:

$$FL = K_{sc}\left(\frac{Q/N}{K_{pump} - Q/N}\right) \tag{3.14}$$

where K_{sc} is a constant that only depends on screw geometry and K_{pump} is a function of screw design. This equation shows that for given screw geometry and screw design, once *Q/N* is fixed the complete fill length is fixed.

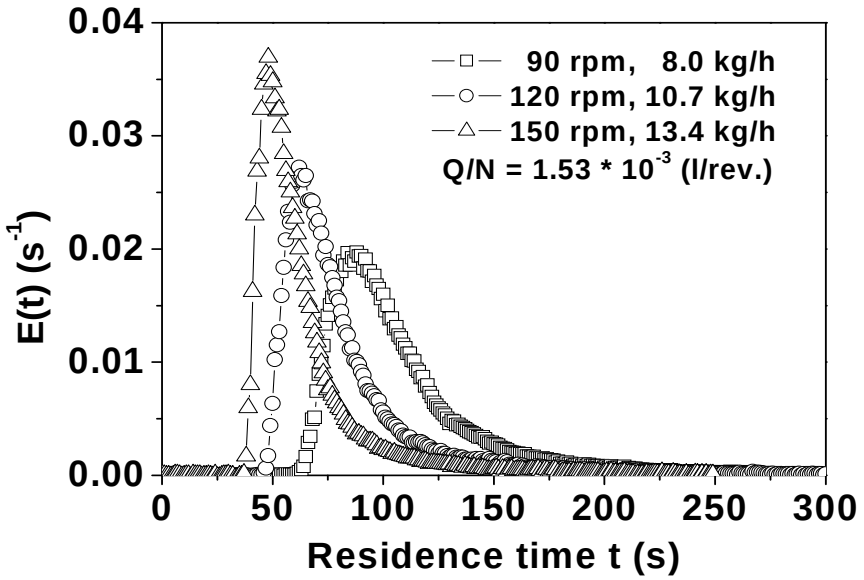

(a)

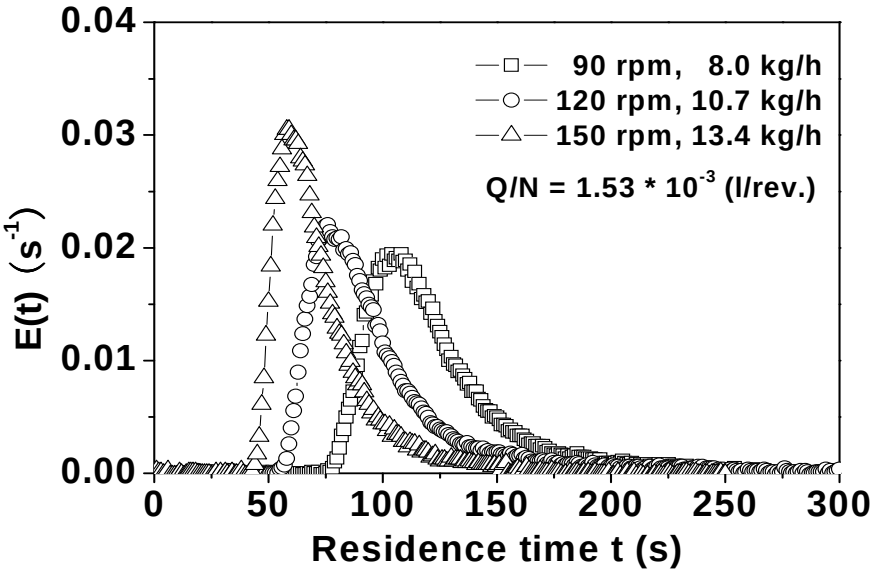

(b)

Fig. 3.2 Effect of increasing screw speed and throughput on the RTD for a *Q/N* of 1.53 ×10^{-3} liter/revolution. (a) Probe 1; (b) probe 2. Screw configuration 1.

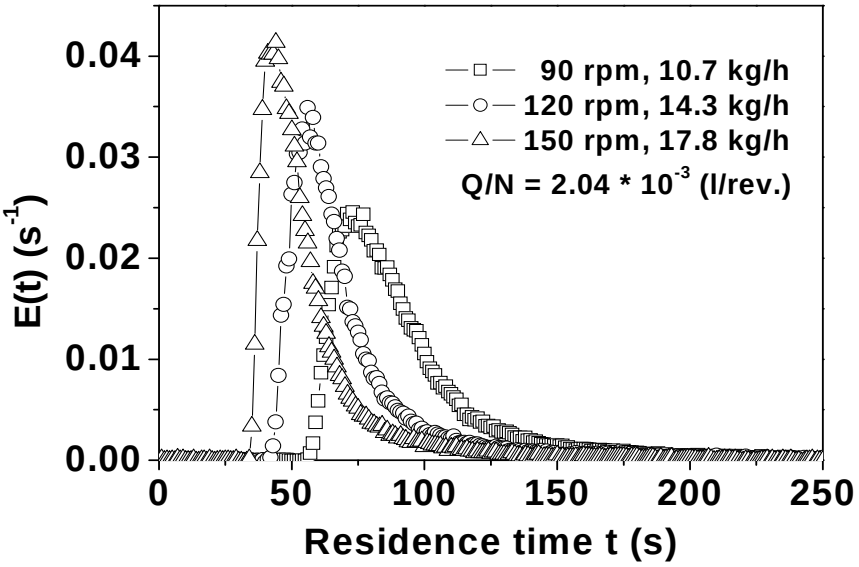

(a)

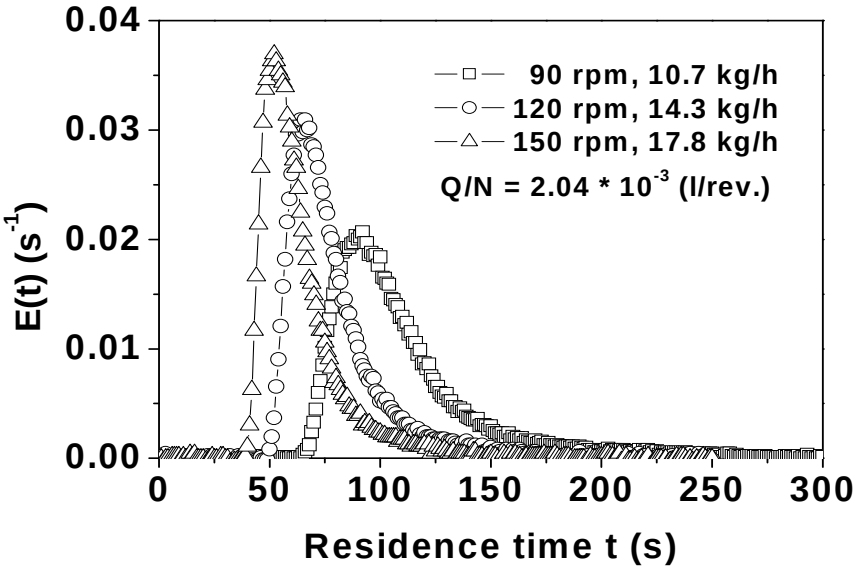

(b)

Fig. 3.3 Effect of increasing screw speed and throughput on the RTD for a *Q/N* of 2.04 × 10^{-3} liter/revolution. (a) Probe 1; (b) probe 2. Screw configuration 1.

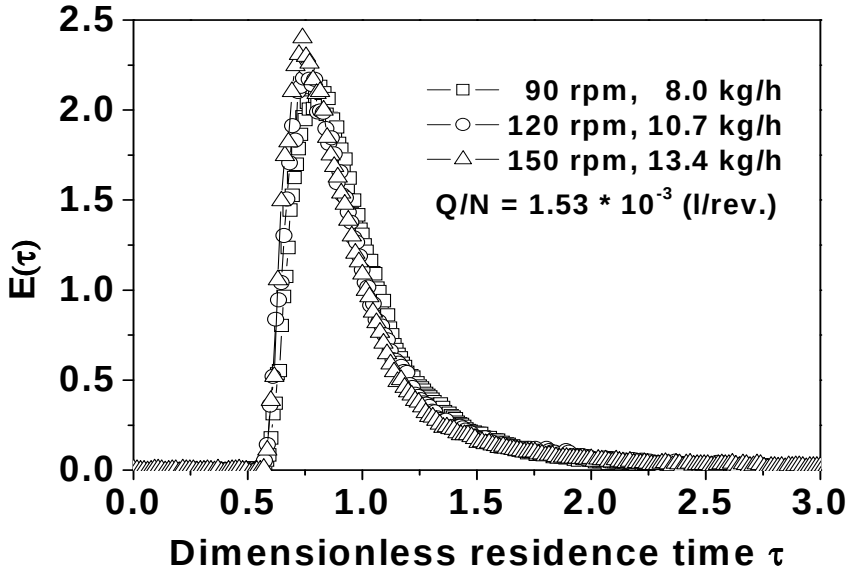

(a)

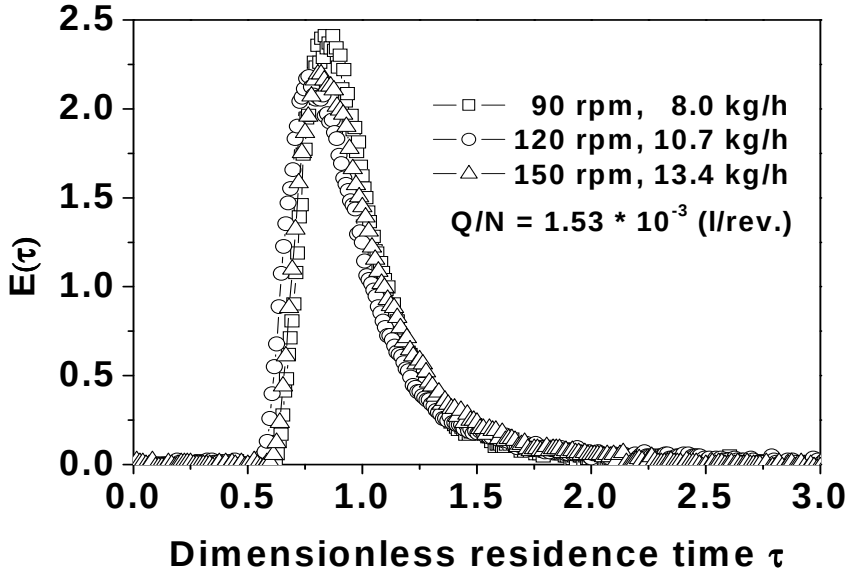

(b)

Fig. 3.4 Dimensionless residence time distribution density function *E(τ)* versus *τ* curves corresponding to the *E(t)* versus *t* curves in Fig. 3.2. (a) Probe 1; (b) probe 2. Screw configuration 1, *Q/N* = 1.53 × 10^{-3} liter/revolution. Note that all the *E(τ)* versus *τ* curves fall on a single curve.

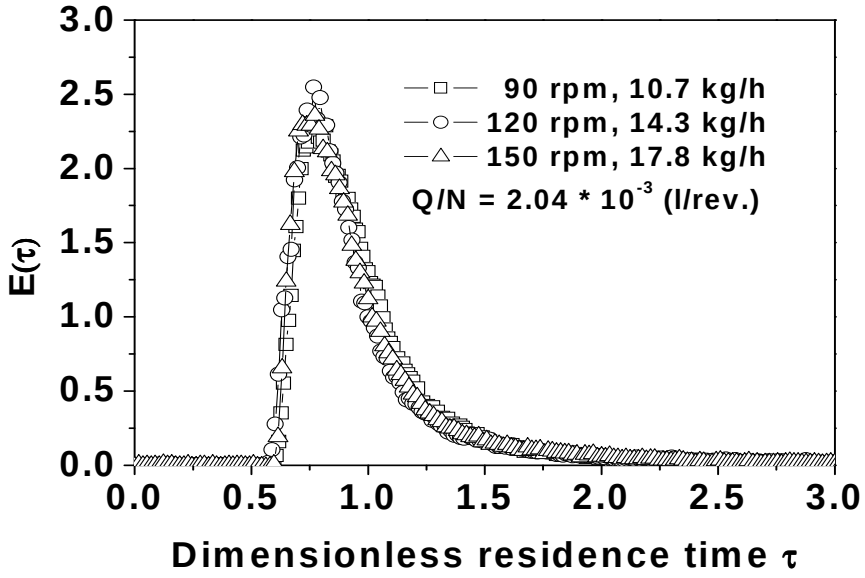

(a)

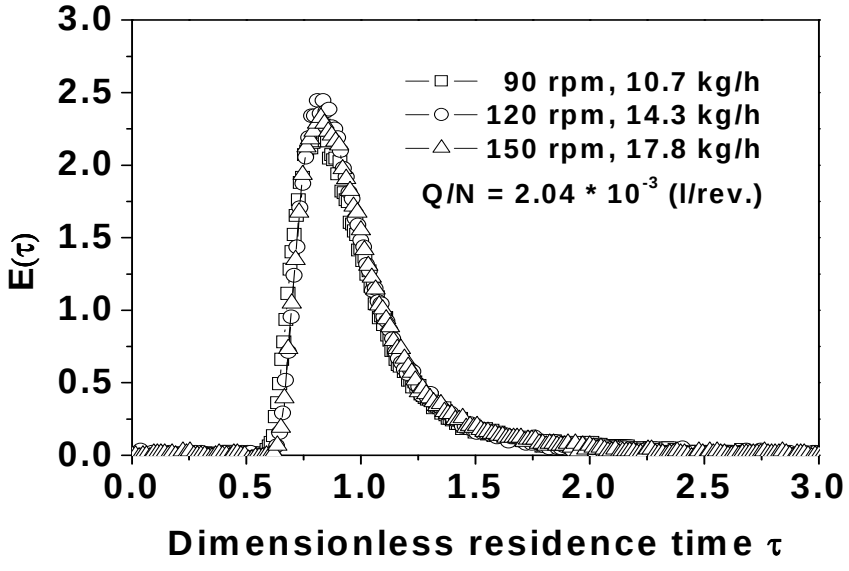

(b)

Fig. 3.5 Dimensionless residence time distribution density function *E(τ)* versus *τ* curves corresponding to the *E(t)* versus *t* curves in Fig. 3.3. (a) Probe 1; (b) probe 2. Screw configuration 1, *Q/N* = 2.04 × 10^{-3} liter/revolution. Note that all the *E(τ)* versus *τ* curves fall on a single curve.

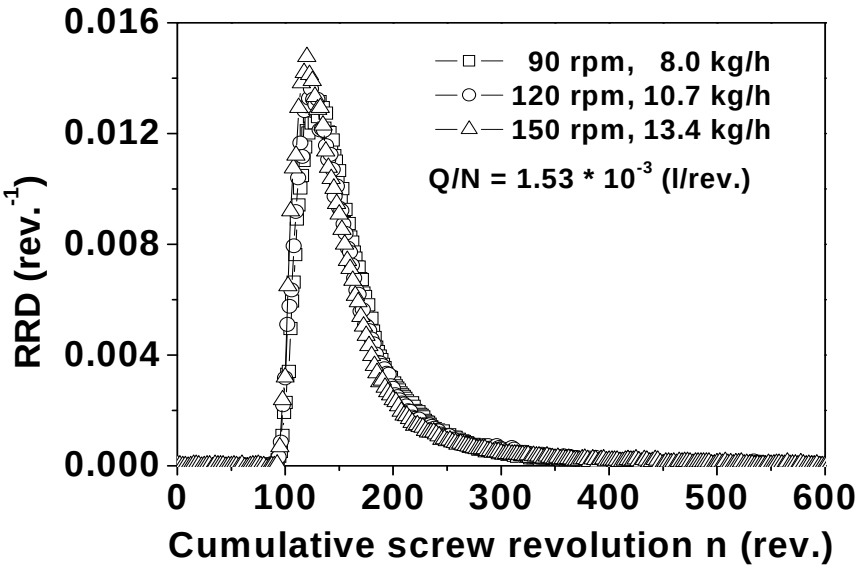

(a)

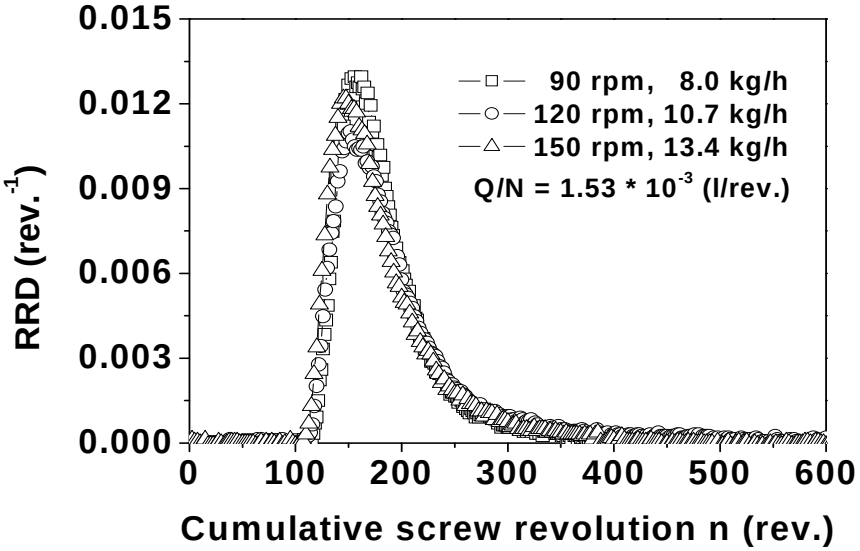

(b)

Fig. 3.6 RRD corresponding to probes 1 and 2, respectively. (a) Probe 1; (b) probe 2; screw configuration 1; $Q/N = 1.53 \times 10^{-3}$ liter/revolution. Note that all the RRD curves overlap.

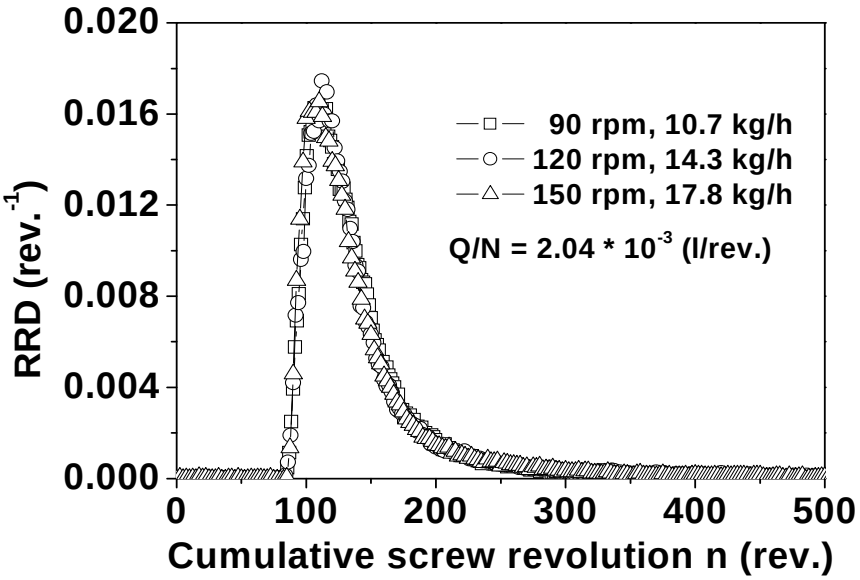

(a)

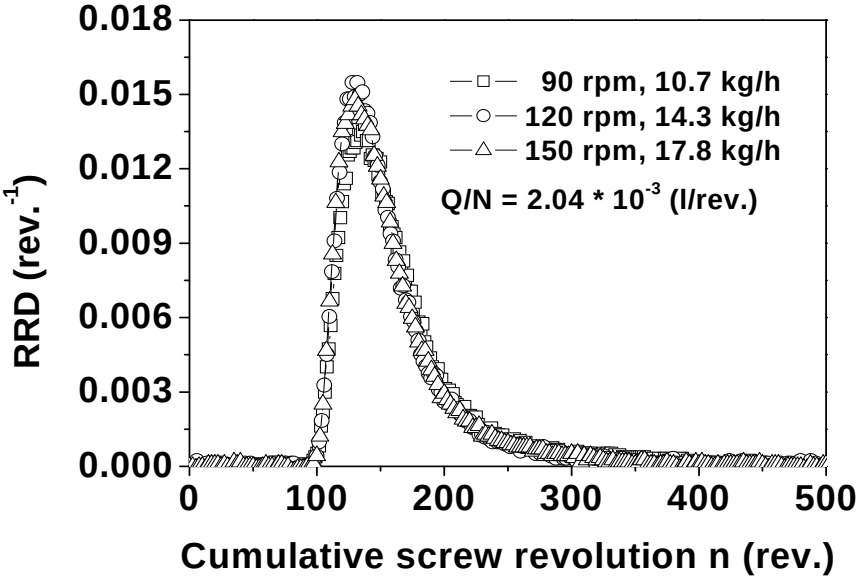

(b)

Fig. 3.7 RRD corresponding to probes 1 and 2, respectively. (a) Probe 1; (b) probe 2; screw configuration 1; $Q/N = 2.04 \times 10^{-3}$ liter/revolution. Note that all the RRD curves overlap.

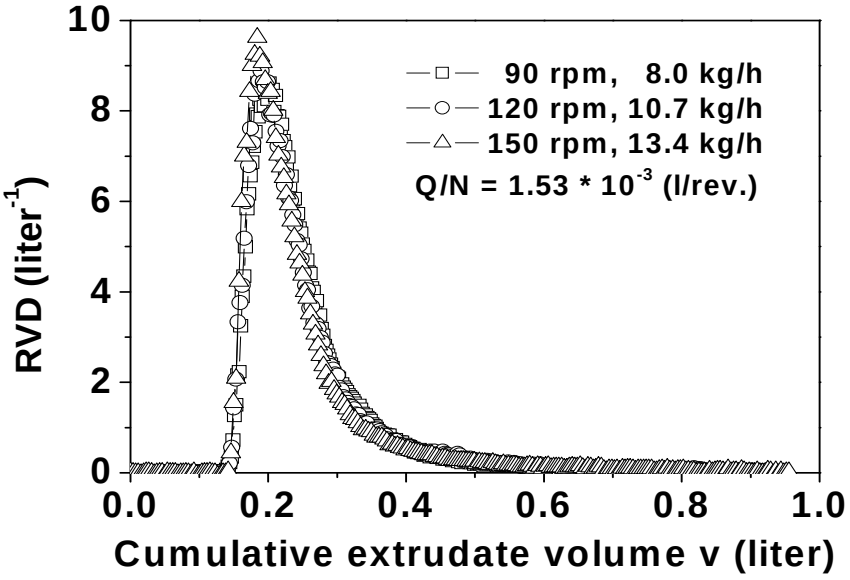

(a)

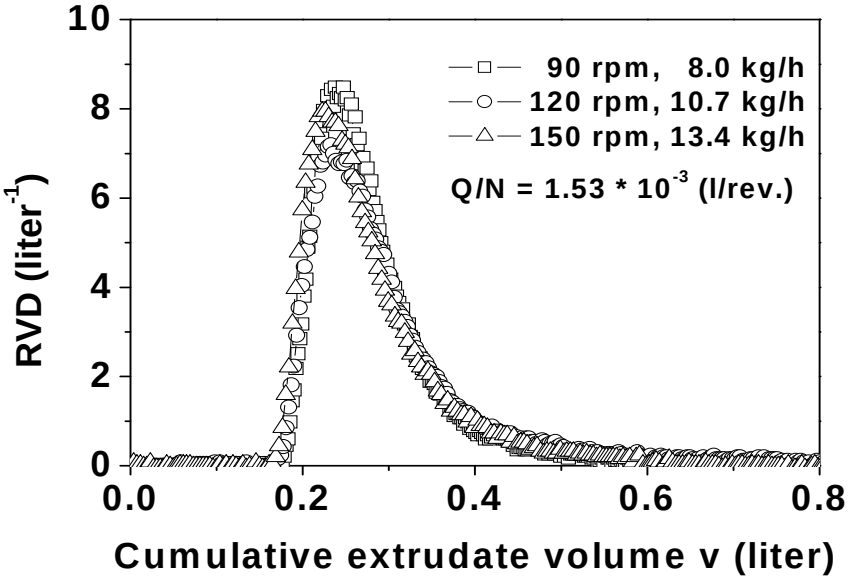

(b)

Fig. 3.8 RVD corresponding to probes 1 and 2, respectively. (a) Probe 1; (b) probe 2; screw configuration 1; $Q/N = 1.53 \times 10^{-3}$ liter/revolution. Note that all the RVD curves overlap.

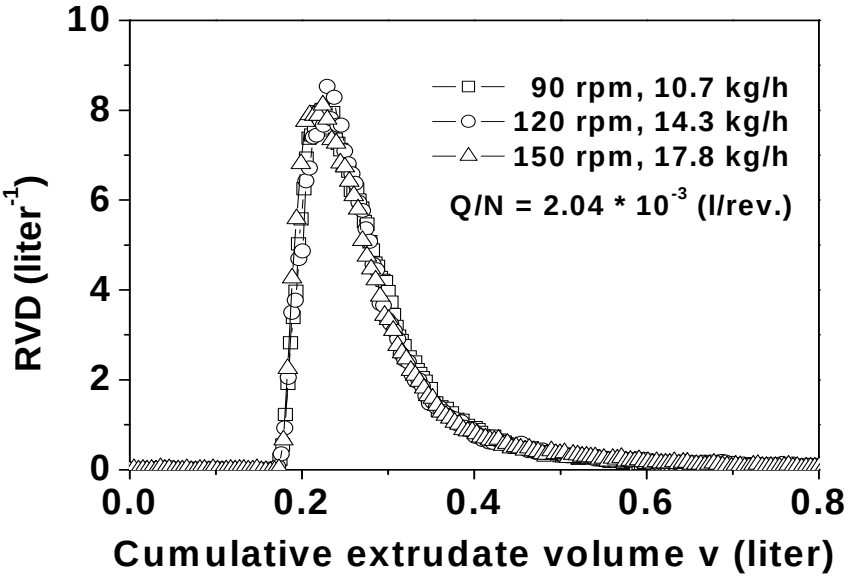

(a)

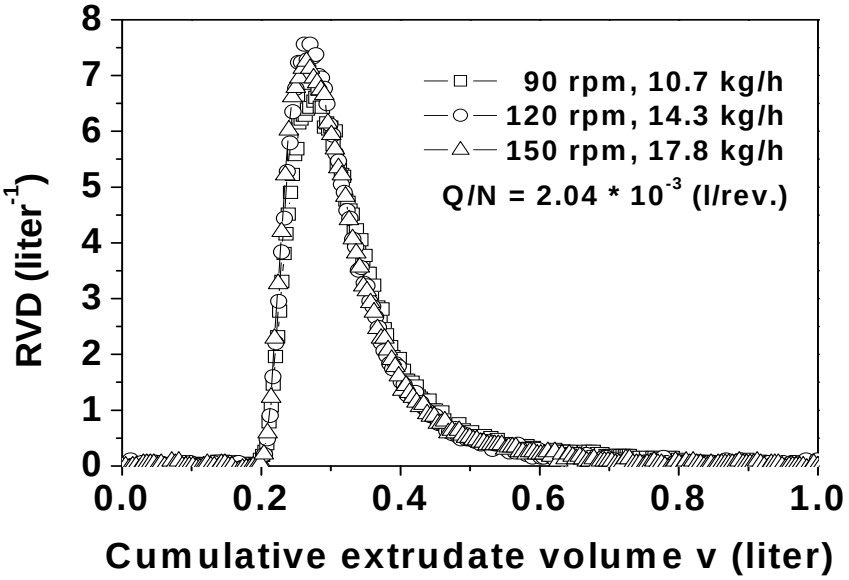

(b)

Fig. 3.9 RVD corresponding to probes 1 and 2, respectively. (a) Probe 1; (b) probe 2; screw configuration 1; $Q/N = 2.04 \times 10^{-3}$ liter/revolution. Note that all the RVD curves overlap.

According to Eqs. (3.10) and (3.11), for given screw profile and Q/N, the value of $\bar{t}N$ and that of $\bar{t}Q$ should be constant, respectively, regardless of N or Q. This is

confirmed by the data shown in Table 3.2 corresponding to the values of $\bar{t}Q$ obtained at probes 1 and 2 for the four different screw configurations in Fig. 3.1 and for a *Q/N* of 2.04×10^{-3} liter/revolution with three pairs of *Q* and *N* values. When *Q/N*, screw configuration and probe location are fixed, the values of $\bar{t}Q$ for all the three different values of *Q* are indeed the same within the experimental and numerical calculation errors. For example, the value of $\bar{t}Q$ was between 0.42 and 0.44 for the 4 gear block configuration and probe 2, regardless of the values of *Q* and *N*.

Table 3.2 Values of $\bar{t}Q$ corresponding to a given *Q/N* for four screw configurations in Fig. 3.1 at probes 1 and 2.

	4 x 30° kneading blocks			4 x 60° kneading blocks			4 x 90° kneading blocks			4 x gear blocks		
Probe	$\bar{t}_1Q_1$ (liter)	$\bar{t}_2Q_2$ (liter)	$\bar{t}_3Q_3$ (liter)	$\bar{t}_1Q_1$ (liter)	$\bar{t}_2Q_2$ (liter)	$\bar{t}_3Q_3$ (liter)	$\bar{t}_1Q_1$ (liter)	$\bar{t}_2Q_2$ (liter)	$\bar{t}_3Q_3$ (liter)	$\bar{t}_1Q_1$ (liter)	$\bar{t}_2Q_2$ (liter)	$\bar{t}_3Q_3$ (liter)
Probe 1	0.29	0.30	0.29	0.30	0.31	0.31	0.32	0.34	0.32	0.31	0.29	0.33
Probe 2	0.34	0.37	0.32	0.35	0.37	0.36	0.39	0.40	0.40	0.42	0.44	0.42

Note: *Q/N* = 2.04×10^{-3} liter/revolution with mass throughputs of Q_1, Q_2 and Q_3 being 10.7, 14.3 and 17.8 kg/h and the corresponding screw speeds, N_1, N_2 and N_3 being 90, 120 and 150 rpm, respectively. $\bar{t}_1$, $\bar{t}_2$ and $\bar{t}_3$ were the mean residence times of the three pairs of *Q* and *N*, respectively.

3.3.2 Local RTD, RRD and RVD

The flow and mixing conditions at the two boundaries of the test zone of this work were expected to be such that the statistical theory for the RTD would apply. Detailed discussions on the validity of that theory can be found elsewhere[26-28]. That theory stipulates that for a closed system composed of two statistically independent elements, A and B, the overall RTD density function *E(t)* is related to those of the two elements, $E_A(t)$ and $E_B(t)$, by the following equation:

$$E(t) = \int_0^t E_A(t) \cdot E_B(t-\tau) d\tau \qquad (3.15)$$

This equation shows that knowing any two of the three RTD density functions

allows calculating the third one either by convolution or deconvolution. However, it should be pointed that when it comes to deconvoluting experimental data, numerical difficulties often rise because of data scattering. To get rid of numerical difficulties, we first fit the experimental data with an appropriate mathematical function. We used the following expression to fit our RTD curves[29]:

$$E(t) = a \cdot t^{-c-1} \cdot b^{c+1} \exp[(b^c t^{-c} - 1) \cdot (\frac{-c-1}{c})] \qquad (3.16)$$

where a, b and c are adjustable parameters. They were obtained by fitting the experimental data using a least squared optimization method. Then the fitted curve was normalized, assuring that $\int_0^\infty E(t)dt = 1$.

The local RTD curves in the test zone between probes 1 and 2, $E_{12}(t)$, were obtained by the deconvolution of the experimental data of $E_1(t)$ and $E_2(t)$. The method used for the deconvolution can be found elsewhere [17].

Fig. 3.10 shows the effects of screw speed and throughput on $E_{12}(t)$ for screw configuration 1. Increasing screw speed with throughput being held constant shifted the local RTD curve to the short time domain. However, its shape did not change much (Fig. 3.10a). Increasing throughput with screw speed being held constant also shifted the RTD curve to the short time domain. Moreover, its width became shaper. Therefore, the shape of the RTD was much more affected by throughput than screw speed.

Fig. 3.11 shows the local RTD, RRD and RVD curves between probes 1 and 2 for given values of Q/N. Again they all fall on a single curve. This indicates that for a given screw profile, Q/N not only controls the overall and partial RTD, RRD and RVD, but also local ones. Moreover, local RRD and RVD do not provide more information on a given screw zone than the corresponding local RTD.

Fig. 3.12 shows the effect of screw configuration on the local RTD, RRD and RVD curves of the test zone between probes 1 and 2. They were obtained by deconvolution of the data obtained by probes 1 and 2 using Eq. (3.15) It is seen that both the mean residence time and the axial mixing quality characterized by the width of the RTD, followed the order: 30° < 60° << 90° < gear block.

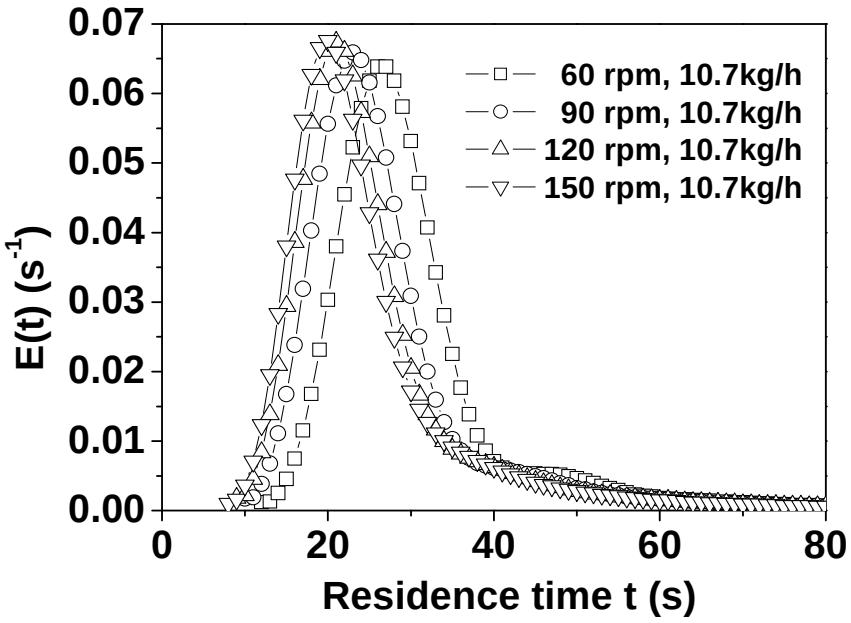

(a)

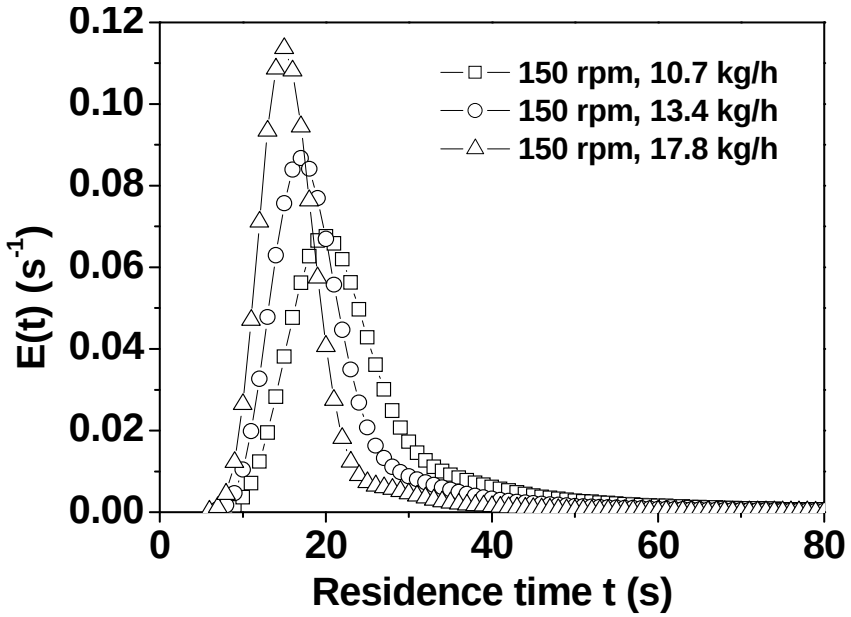

(b)

Fig. 3.10 Effects of the screw speed (a) and throughput (b) on the local RTD of the test zone of screw configuration 1.

The RRD and RVD curves followed the same trend as the RTD, as expected. When the operating conditions were fixed, an increase in the staggering angle of the kneading block from 30 to 90° shifted the local RRD and RVD to higher screw revolution and the

larger extrudate volume domains, respectively. The shift with the gear blocks was the most significant, indicating that conveying a given amount of tracer from probe 1 to probe 2 needed more screw revolutions or more extrudate volume when the gear blocks were used.

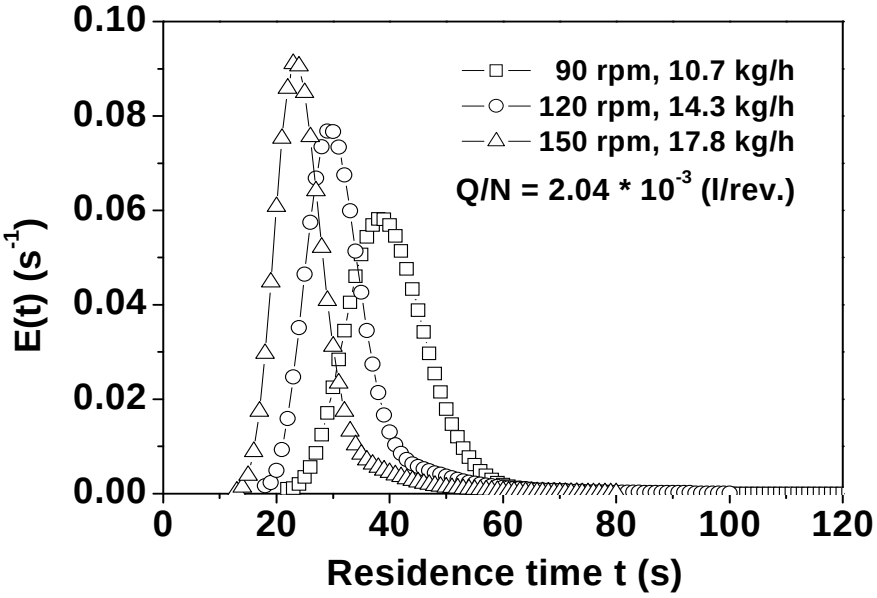

(a)

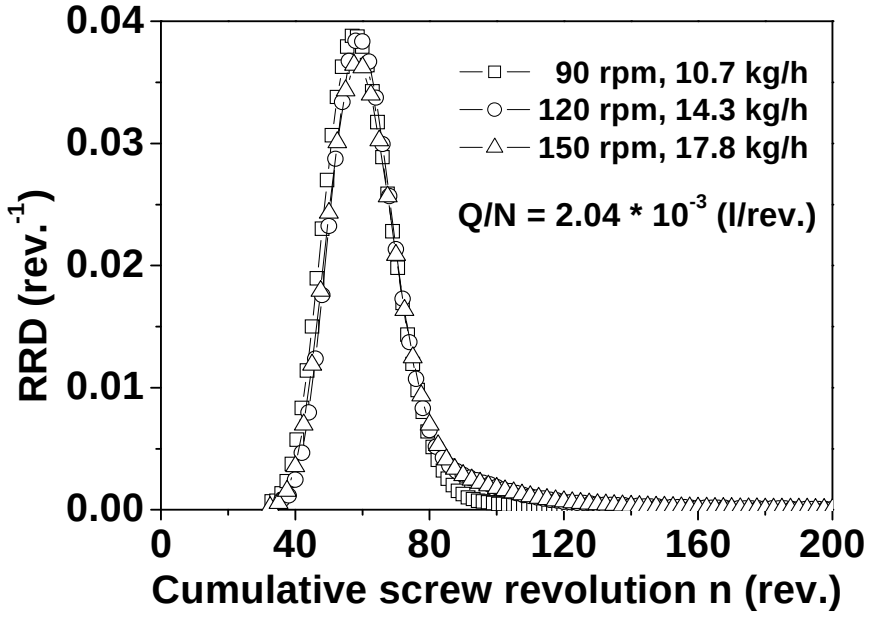

(b)

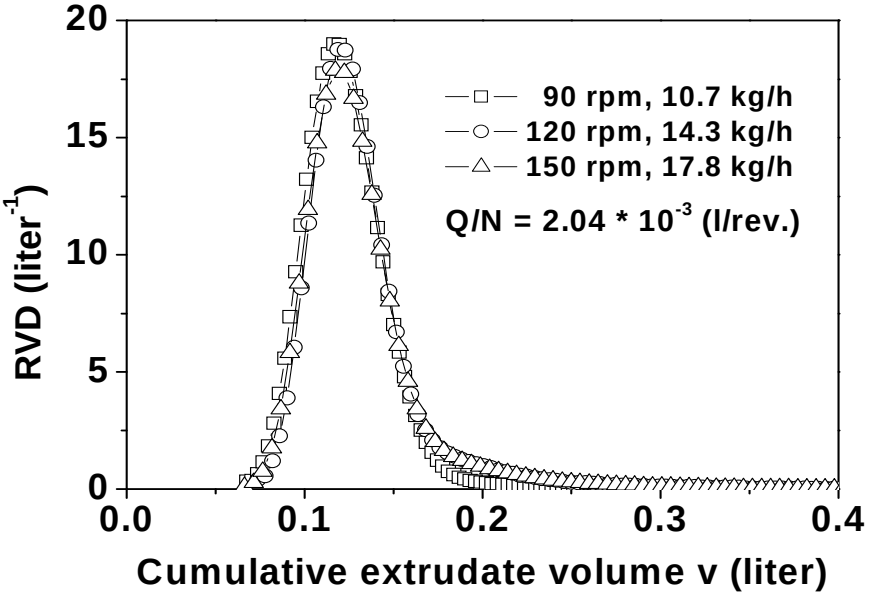

(c)

Fig. 3.11 Local RTD (a), RRD (b) and RVD (c) curves between probes 1 and 2 for screw configuration 3 at a given *Q/N* (2.04×10^{-3} liter/revolution). They are obtained by deconvolution. Note that all the local RTD, RRD and RVD curves fall on single master curves, respectively.

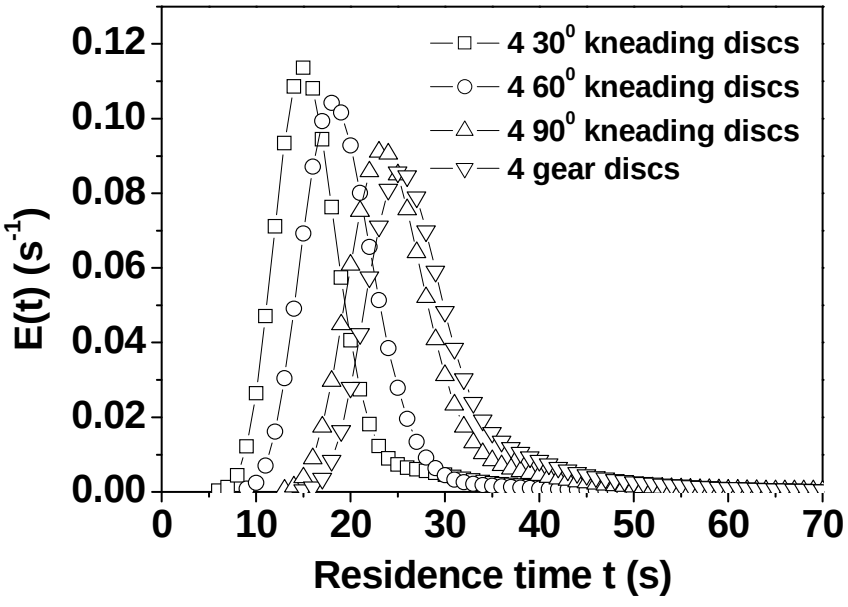

(a)

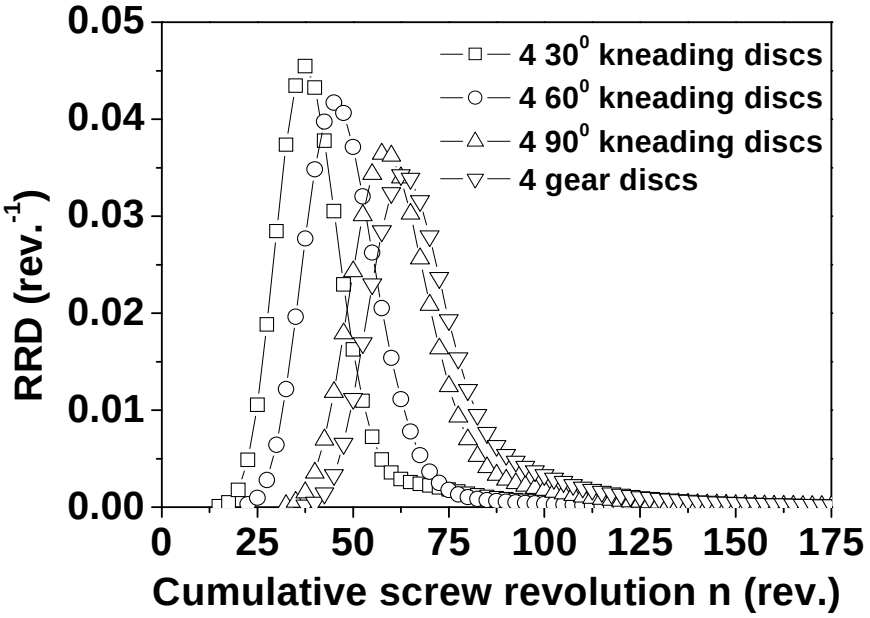

(b)

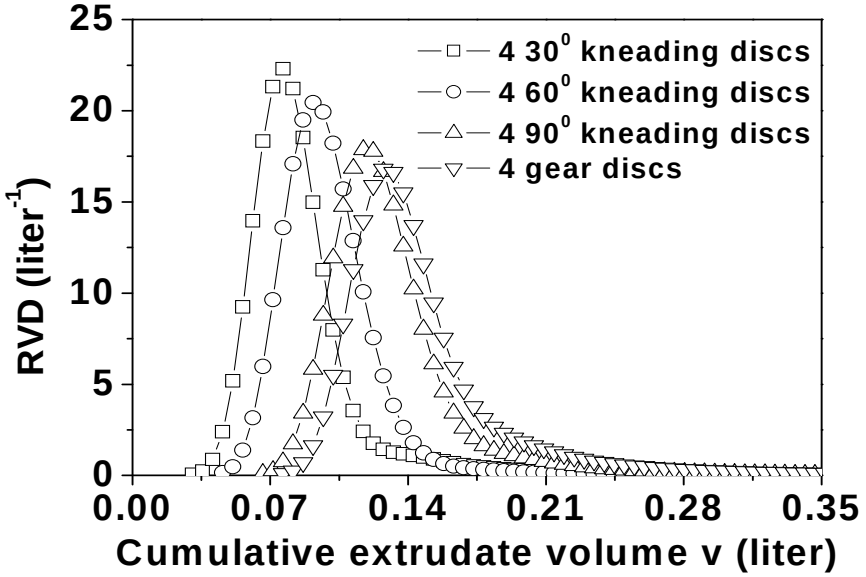

(c)

Fig. 3.12 Effect of screw configuration on the local RRD and RVD for screw speed: 150 rpm, feed rate: 17.8 kg/h. (a) RTD, (b) RRD and (c) RVD.

3.4 Conclusions

The overall and partial RTD were measured directly during the extrusion process

using a new in-line RTD measurement instrument that was developed in a previous study. The local RTD were calculated by deconvolution based on a statistical theory. We studied the overall, partial and local residence time distributions (RTD); overall, partial and local residence revolution distributions (RRD) and overall, partial and local residence volume distributions (RVD) in a co-rotating twin screw extruder and established the relationships among them. It was confirmed theoretically and experimentally that specific throughput Q/N, defined as a ratio of throughput (Q) over screw speed (N), was indeed a key process parameter for controlling all the above three types of residence distributions. For a given value of Q/N, the overall, partial and local RTD were different when Q and N varied. However the corresponding dimensionless RTD as well as the RRD and RVD all fell on single master curves, respectively. This is because the mean degree of fill and complete fill length were the same for a given value of Q/N. This indicates that the RRD and RVD, be they overall, partial or local, do not provide more information on an extrusion process than the corresponding RTD. Rather they offer different ways of representing the same phenomena.

Comparison of the local RTD for a local zone composed of 4 identical gear blocks or 4 identical kneading blocks with a staggering angle of 30, 60 or 90° led to the conclusion that the delay time, the mean residence time and mixing performance followed the order: 30° < 60° << 90°< gear blocks.

3.5 References

[1]. Baker, W.; Scott, C.; Hu, G. H. *Reactive Polymer Blending;* Hanser: Muinich, Germany, 2001.

[2]. Puaux, J. P.; Bozga, G.; Ainser, A. Residence time distribution in a corotating twin-screw extruder. *Chemical Engineering Science* **2000,** *55* (9), 1641-1651.

[3]. Melo, T. J. A.; Canevarolo, S. V. In-line optical detection in the transient state of extrusion polymer blending and reactive processing. *Polymer Engineering and Science* **2005,** *45* (1), 11-19.

[4]. Lee, S. M.; Park, J. C.; Lee, S. M.; Ahn, Y. J.; Lee, J. W. In-line measurement of residence time distribution in twin-screw extruder using non-destructive ultrasound. *Korea-Australia Rheology Journal* **2005,** *17* (2), 87-95.

[5]. Pinheiro, L. A.; Chinelatto, M. A.; Canevarolo, S. V. The role of chain scission and chain branching in high density polyethylene during thermo-mechanical degradation. *Polymer Degradation and Stability* **2004,** *86* (3), 445-453.

[6]. Nauman, E. B.; Buffham, B. A. *Mixing in continuous flow system;* John Wiley & Sons, Inc.: New York, USA, 1983.

[7]. Gao, J.; Walsh, G. C.; Bigio, D.; Briber, R. M.; Wetzel, M. D. Residence-time distribution model for twin-screw extruders. *AIChE Journal* **1999,** *45* (12), 2541-2549.

[8]. Elkouss, P.; Bigio, D. I.; Wetzel, M. D.; Raghavan, S. R. Influence of polymer viscoelasticity on the residence distributions of extruders. *AIChE Journal* **2006,** *52* (4), 1451-1459.

[9]. Gao, J.; Walsh, G. C.; Bigio, D.; Briber, R. M.; Wetzel, M. D. Mean residence time analysis for twin screw extruders. *Polymer Engineering and Science* **2000,** *40* (1), 227-237.

[10]. Wetzel, M. D.; Shih, C. K.; Sundararaj, U. Determination of residence time distribution during twin screw extrusion of model fluids. Toronto, America, 1997; pp 3707-3712.

[11]. Canevarolo, S. V.; Melo, T. J. A.; Covas, J. A.; Carneiro, O. S. Direct method for

deconvoluting two residence time distribution curves. *International Polymer Processing* **2001,** *16* (4), 334-340.

[12]. Potente, H.; Kretschmer, K.; Preu, Th.; Flecke, J. Investigation of the local residence time distribution in special mixing elements for co-rotating twin screw extruders. *SPE ANTEC Tech. Papers* **2002,** *48*, 273-277.

[13]. Potente, H.; Kretschmer, K.; Hofmann, J.; Senge, M.; Mours, M.; Scheel, G.; Winkelmann, Th. Process behavior of special mixing elements in twin-screw extruders. *International Polymer Processing* **2001,** *16* (4), 341-350.

[14]. Xie, Y.; Tomayko, D.; Bigio, D. I.; Batch, G. On the effect of operating parameters and screw configuration on residence time distribution. *Journal of Reinforced Plastics and Composites* **1998,** *17* (15), 1338-1349.

[15]. Elkouss, P.; Bigio, D.; Walsh, G. C.; Andersen, P. Mean residence time characterization in co-rotating twin screw extruder: screw configuration comparison. *SPE ANTEC Tech. Papers* **2000,** *46*, 29-33.

[16]. Oberlehner, L.; Caussagnau, P.; Michel, A. Local residence time distribution in a twin screw extruder. *Chemical Engineering Science* **1994,** *49* (23), 3897-3907.

[17]. Zhang, X. M.; Xu, Z. B.; Feng, L. F.; Song, X. B.; Hu, G. H. Assessing local residence time distributions in screw extruders through a new in-line measurement instrument. *Polymer Engineering and Science* **2006,** *46* (4), 510-519.

[18]. Xu, Z. B.; Feng, L. F.; Hu, G. H.; Wang, L. G.; Zhang, X. M.; Li, B. G. An apparatus for in-line measurement of the residence time distribution of thermomechanically complex systems. *Recent Progress in Process Engineering* **2005,** *92*, 7-16.

[19]. Elkouss, P.; Bigio, D.; Wetzel, M. D. Deconvolution of residence time distribution signals to individually describe zones for better modeling. *SPE ANTEC* **2003,** 344-348.

[20]. Gasner, G. E.; Bigio, D.; Marks, C.; Magnus, F.; Kiehl, C. A new approach to analyzing residence time and mixing in a co-rotating twin screw extruder. *Polymer Engineering and Science* **1999,** *39* (2), 286-298.

[21]. Sun, Y. J.; Hu, G. H.; Lambla, M. Free radical grafting of glycidyl methacrylate

onto polypropylene in a co-rotating twin screw extruder. *Journal of Applied Polymer Science* **1995,** *57* (9), 1043-1054.

[22]. Hu, G. H.; Sun, Y. J.; Lambla, M. Effects of processing parameters on the in situ compatibilization of polypropylene and poly(butylene terephthalate) blends by one-step reactive extrusion. *Journal of Applied Polymer Science* **1996,** *61* (6), 1039-1047.

[23]. Hu, G. H.; Kadri, I. Preparation of macromolecular tracers and their use for studying the residence time distribution of polymeric systems. *Polymer Engineering and Science* **1999,** *39* (2), 299-311.

[24]. Hu, G. H.; Kadri, I.; Picot, C. On-line measurement of the residence time distribution in screw extruders. *Polymer Engineering and Science* **1999,** *39* (5), 930-939.

[25]. Mudalamane, R.; Bigio, D. Experimental characterization of fill length behavior in extruders. *Polymer Engineering and Science* **2004,** *44* (3), 557-563.

[26]. Chen, L.; Hu, G. H. Applications of a statistical theory in residence time distributions. *AIChE Journal* **1993,** *39* (9), 1558-1562.

[27]. Chen, L.; Pan, Z.; Hu, G. H. Residence time distribution in screw extruders. *AIChE Journal* **1993,** *39* (3), 1455-1464.

[28]. Chen, L.; Hu, G. H.; Lindt, J. T. Residence time distribution in non-intermeshing counter-rotating twin-screw extruders. *Polymer Engineering and Science* **1995,** *35* (7), 598-603.

[29]. Poulesquen, A.; Vergnes, B.; Cassagnau, P.; Michel, A.; Carneiro, O. S.; Covas, J. A. A study of residence time distribution in co-rotating twin-screw extruders. Part II: Experimental validation. *Polymer Engineering and Science* **2003,** *43* (12), 1849-1862.

CHAPTER 4 Numerical Simulation and Experimental Validation of Mixing Performance of Kneading Discs in a Twin Screw Extruder

ABSTRACT

This work aims at simulating by particles tracking local residence time distributions (RTD) of a co-rotating twin-screw extruder using computational fluid dynamics (CFD). Simulated results follow reasonably well the trend of experimental results obtained by an in-line measuring instrument for different screw configurations and feed rates. In order to analyze the distributive mixing performance and overall efficiency of different types of kneading discs, mixing parameters such as area stretch ratio, instantaneous efficiency and time-average efficiency are calculated. Among kneading discs with stagger angles 45°, 60° and 90°, the 90/10/64 with disc gaps is most efficient in terms of distributive mixing. The effects of the disc width and disc gap on the local RTD and distributive mixing are also discussed. This provides a numerical tool to assessing point-by-point information on the local RTD, flow and mixing along the screw extruder.

4.1 Introduction

4.1.1 Simulation and Experimental Validation

Co-rotating intermeshing twin-screw extruders have attracted considerable attention during the last twenty years, mainly in the field of food and polymer processing[1]. Among different modules of a co-rotating twin-screw extruder, kneading discs are the dominant ones in mixing efficiency. It remains empirical when it comes to designing kneading discs and optimizing extrusion conditions for a specific application due to the very large number of geometrical, rheological and operating parameters that may influence the flow. The simplified 1-D model is currently the important method used in predicting the temperature, pressure profile and residence time distribution in extrusion processing[2, 3]. However, 1-D models only provide the average values of different parameters along the extruder which is insufficient for description of flow pattern and mixing[4, 5]. In recent years, much attention has been paid to full 3-D simulation of the flow field in different regions of a co-rotating twin-screw extruder. Manas-Zloczower et al. investigated the distributive mixing, dispersive mixing and flow field of different regions in co-rotating twin-screw extruders including mixing and conveying elements[6-8]. Bravo et al. presented a 3-D flow field analysis for kneading discs[9, 10]. Ishikawa et al. performed non-isothermal simulation in kneading discs, rotors, conveying element, and screw mixing elements (SME)[11-13]. Lawal et al. discussed mixing mechanisms in co-rotating twin screw extruders[14].

It is not easy to solve for the flow patterns in complex geometry such as kneading discs. Time dependent boundaries as kneading discs rotate make numerical simulations more difficult. Avalosse et al. introduced a so-called mesh superposition technique (MST) to model intermeshing twin-screw extruders without calling upon remeshing[15]. They used the Polyflow software (Fluent Inc.) based on the MST to analyze mixing efficiency and flow field in a kneading block section of a twin-screw extruder[16-18]. Connelly and Kokini used Polyflow to discuss the effects of shear thinning and viscoelasticily fluid on mixing in a 2D mixer[19, 20] They simulated the flow of a viscous Newtonian fluid in a twin sigma blade mixer using Polyflow code with MST and analyzed the distributive mixing and mixing efficiency of the mixer[21].

However, those studies were limited to batch mixers. Breuer et al. simulated the flow pattern in a miniature mixer and compared the performance of the APAM (Albert polymer asymmetric minimixer) to that of the MiniMAX molder[22]. Ficarella et al. investigated the fluid-dynamic behavior of an extrusion cooking process for cereals in a co-rotating twin-screw extruder using Polyflow code[23, 24].

Experimental validation of simulated results is another big challenge. There have been studies on numerical simulations of pressure, temperature and velocity profiles and their comparison with experiments[9, 11, 25]. Potente et al. used a 2.5 D finite element method to analyze the minimal residence time in conveying elements and compared the minimal residence time with experimental data[26]. The modeling was based on the plain unwinding of the intermeshing twin screws. Huneault et al. measured the RTD in co-rotating twin-screw extruders and used the RTD to determine the effect of operating conditions on the degree of fill[27]. They compared the experimental data of the degree of fill with the calculated ones. However, to the best of the authors' knowledge, numerical simulations and experimental validations of the local RTD in mixing sections of a twin-screw extruder are still rare due to experimental difficulties, and yet they are crucial.

4.1.2 Kinematic Model of Distributive Mixing

For a viscous fluid, the distributive mixing mechanism is the stretching and reorientation of fluid elements[28]. Ottino et al. developed a lamellar model to quantify the capacity of a flow to deform matter and to generate interface between two components in a mixture, which gives a kinematic approach to modeling distributive mixing by tracking the amount of deformation experienced by a fluid element[28-32]. In the initial fluid domain, when an infinitesimal material area |dA| with normal direction $\hat{N}$ is transformed into an area |da| with normal direction $\hat{n}$ at time t, the area stretch ratio of material surface η is defined as[29]:

$$\eta = \frac{|da|}{|dA|} \tag{4.1}$$

A good distributive mixing quality requires a high value of η over space and time. An instantaneous stretching efficiency e_η based on stretching of material surfaces is defined as [30]:

$$e_\eta = \frac{\dot{\eta}/\eta}{(D:D)^{1/2}} = \frac{d(\log\eta)/dt}{(D:D)^{1/2}} = \frac{-D:\hat{m}\hat{m}}{(D:D)^{1/2}} \tag{4.2}$$

where $\dot{\eta}$ is a material time derivative of η, D is a rate of deformation tensor and $\hat{m}$ is a local normal unit vector of current surface. e_η characterizes the fraction of the dissipated energy used for stretching the area and falls in the range [-1, 1]. A positive (negative) value indicates that the dissipated energy is used for stretching (shrinking) the surface. A time-averaged efficiency $<e_\eta>$ is defined as[29]:

$$< e_\eta >= \frac{1}{t}\int_0^t e_\eta dt \tag{4.3}$$

The above mixing parameters can be calculated when the velocity field is known. The logarithm of the area stretch ratio logη can compare the distributive mixing performance of different mixers. Distributive mixing efficiency can be characterized by time-average efficiency $<e_\eta>$. Some researchers defined a distribution function F_α associated with the field α. The quantity $F_\alpha(\alpha_p, t)$ is given as[33, 34]:

$$F_\alpha(\alpha_p, t) = p \tag{4.4}$$

where α_p is a critical value, which indicates that p % of marker particles have a value of α lower than or equal to α_p at time t. The field α may be η, e_η or $<e_\eta>$.

This work aims at analyzing the mixing of a generalized Newtonian fluid in kneading discs using numerical simulation and experiments. The velocity field in kneading zones is simulated using a commercial CFD code: POLYFLOW 3.10.0®. The local RTD of the same domains is then calculated based on the velocity field. Simulated results are compared with experimental ones obtained by an in-line measuring instrument[35, 36]. The distributive mixing parameters such as the area stretch ratio of material surface η, instantaneous stretching efficiency e_η and time-averaged efficiency $<e_\eta>$ are calculated using the interface tracking techniques. These parameters are then used to compare the distributive mixing performance and efficiency of different types of kneading discs.

4.2 Numerical Simulation

4.2.1 Geometry of Kneading Discs

Fig. 4.1 shows the geometry of eight different kneading discs (KD) simulated in this work. They all have the same axial length, i.e., 64 mm, and differ in stagger angle, disc width and/or disc gap. Table 4.1 gives the description of kneading discs KD1 to KD8 and flow channel in Fig. 4.1. The first three kneading discs KD1 to KD3 are used for experimentally validating the simulated results. KD4 to KD6 have the same disc width and gap, but differ in stagger angle. They are chosen to analyze the effect of the stagger angle on the local RTD and distributive mixing parameters. The effects of the disc width and gap on the axial and distributive mixing are studied by KD6, KD7 and KD8. The KD7 and KD8 do not have disc gap between the two discs. The flow channel includes three parts: inlet section, kneading section and outlet section. The kneading section accommodates a kneading disc. Sufficiently long inlet and outlet sections are added to the computational domains where fully developed flows are assumed[37]. Fig. 4.2 shows the disc gaps of a kneading disc.

Table 4.1 The description of kneading discs KD1 to KD8 and flow channel in Fig. 4.1.

	The description of kneading discs
KD1	Two pairs of intermeshing 45/5/32 kneading discs
KD2	Two pairs of intermeshing 60/4/32 kneading discs
KD3	Two pairs of intermeshing 90/5/32 kneading discs
KD4	One pair of intermeshing 45/10/64 kneading discs
KD5	One pair of intermeshing 60/10/64 kneading discs
KD6	One pair of intermeshing 90/10/64 kneading discs
KD7	One pair of intermeshing 90/10/64 kneading discs
KD8	One pair of intermeshing 90/5/64 kneading discs
Flow channel	Inlet section (2 mm)+ kneading section (64 mm) + outlet section (4 mm)

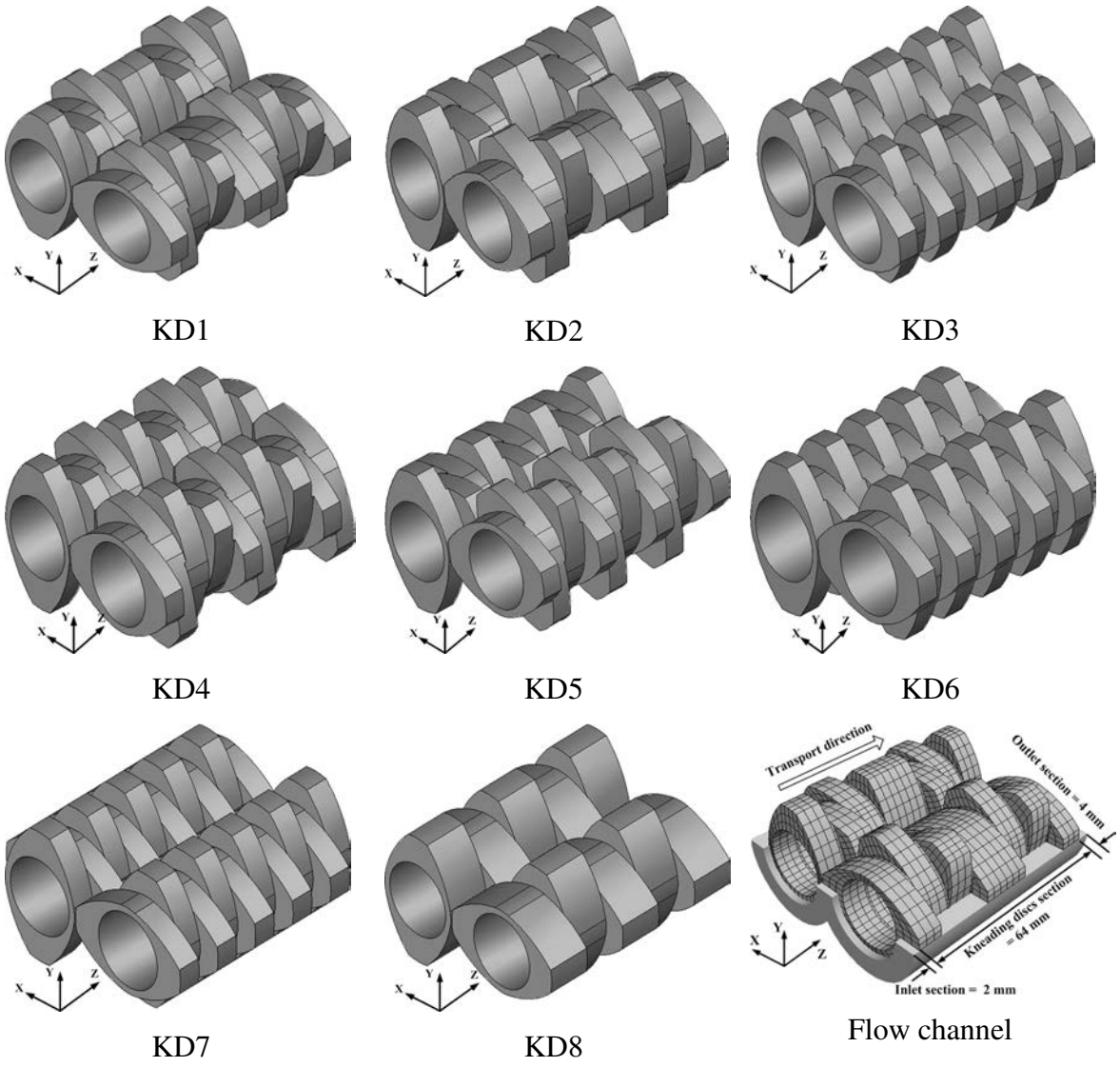

Fig. 4.1 Geometry of the kneading discs and flow channel for simulation. A kneading disc x/y/z is one that has y discs and a total a length of z mm.

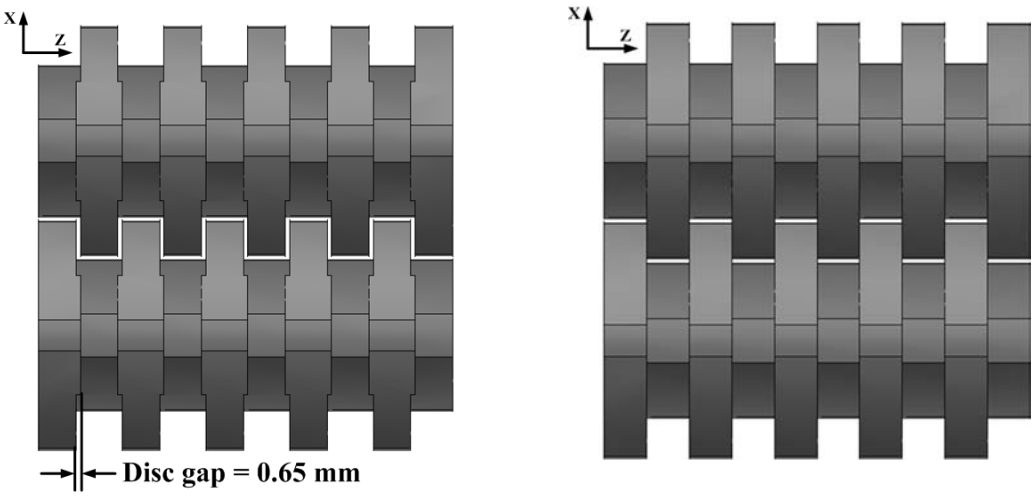

(a) (b)

Fig. 4.2 Top view of (a) KD6 with gaps and (b) KD7 without gap

Meshing is carried out using the commercial preprocessor software GAMBIT (Fluent Inc.). The meshes of each kneading disc are chosen after a preliminary mesh-discretization study. A convergence analysis compares the velocity and pressure solutions of different mesh numbers along the axial direction. The number of meshes is increased till the solutions are insensitive to it. Table 4.2 gives the number of 3D elements for KD1 to KD8 and the flow channel.

Table 4.2 The number of 3D elements for KD1 to KD8 and the flow channel.

	The number of 3D elements
KD1	8,960
KD2	8,122
KD3	8,512
KD4	9,880
KD5	10,100
KD6	9,976
KD7	9,260
KD8	9,260
Flow channel	21,000

4.2.2 Numerical Simulation and Material Parameters

Polyflow software incorporates a so-called mesh superposition technology (MST) to simulate transient flows with internal moving parts[37]. The MST generates finite

element meshes for the flow domain and each screw element, respectively. They are then superimposed. Since the position of each screw element is updated at each time step, the flow domain can be calculated by the weak formulation of the Navier-Stokes equations and the screw element domain can be constrained by the screw speed.

The flow is assumed to be a time-dependent, isothermal, incompressible and generalized Newtonian fluid with no body forces. The governing equations are the momentum and continuity equations and can be written as:

$$\Delta \cdot \tau - \Delta P = 0 \tag{4.5}$$

$$\nabla \cdot u = 0 \tag{4.6}$$

where τ is the extra stress tensor, P is the pressure and u is the velocity vector. τ is given by

$$\tau = 2\eta D \tag{4.7}$$

where D is the rate of deformation tensor, η is the kinematic viscosity and depends on the shear rate $\dot{\gamma}$. The constitutive equation is represented by the Carreau model:

$$\eta(\dot{\gamma}) = \eta_0 \left[1 + (\lambda\dot{\gamma})^2\right]^{(n-1)/2} \tag{4.8}$$

where η_0 is the zero shear rate viscosity, λ is the natural time and n is the power law index. The material used in this study is a polystyrene (PS) of YANGZI-BASF, China. Its viscosity is measured on a capillary rheometer (Thermo Hake Rheoflixer) for the high shear rate domain and on an advanced rheometric expansion system (ARES, Rheometrics Corp., USA) in a parallel plate mode for the low shear rate domain (see Fig. 4.3). The parameters for the Carreau model are: η_0 = 2814 Pa.s, λ = 0.148 s and n = 0.278.

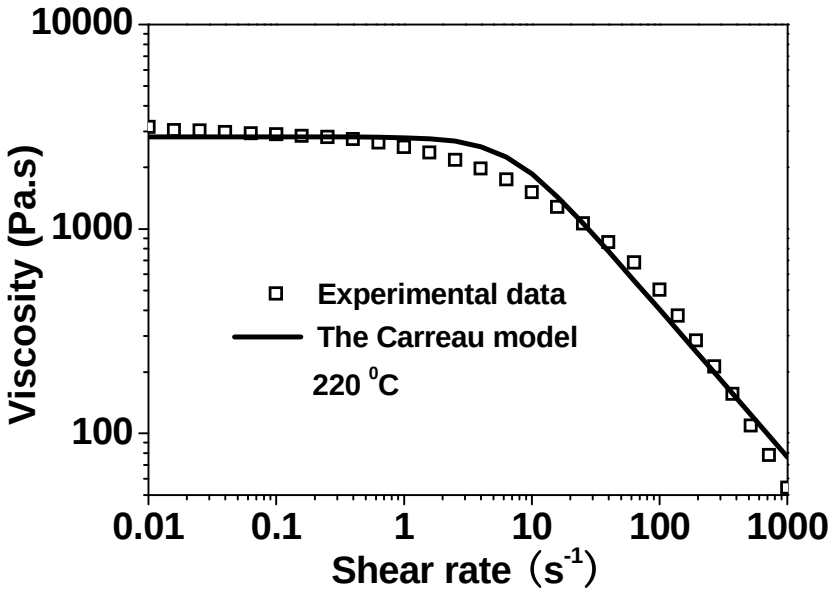

Fig. 4.3 Viscosity of polystyrene vs. shear rate at 220 °C.

The no-slip boundary conditions are imposed to the surfaces of the kneading discs and barrel bore walls. A volume flow rate is set to the inlet section and a normal stress boundary condition is applied to the outlet section. Table 4.3 lists the operating conditions for the numerical simulations and experiments. The volume throughput was calculated by dividing the mass throughput by the melt density of the PS, 970 kg/m^3.

Table 4.3 Operating conditions for the numerical simulations and experiments carried out in this work (barrel temperature: 220 °C).

Experimental No.	1	2	3	4
Screw speed (rpm)	120	150	150	150
Mass throughput (kg/h)	10.7	10.7	13.4	17.8
Volume throughput Q ($\times 10^{-6}$ m^3/s)	3.06	3.06	3.84	5.10

4.2.3 Marker Particle Tracking Analysis

To calculate the local RTD provided by each of the above eight types of kneading discs, virtual particles are launched at the same time in the flow domain. It is assumed that the marker particles are massless and non-interacting with each other.

Under these assumptions, the particles can be located by integrating the velocity vectors with respect to time. Initially, these particles are randomly distributed in an inlet vertical plane (Fig. 4.4) and their trajectories between the inlet and outlet are calculated from the velocity profiles. Along each trajectory, the residence time is computed. The residence time distribution is then obtained based on the residence time of each of these particles. The number of marker particles has to be high enough for the simulation. Fig. 4.5 shows that 1000 marker particles are not enough and that 2000 marker particles start yielding results similar to 3000 ones.

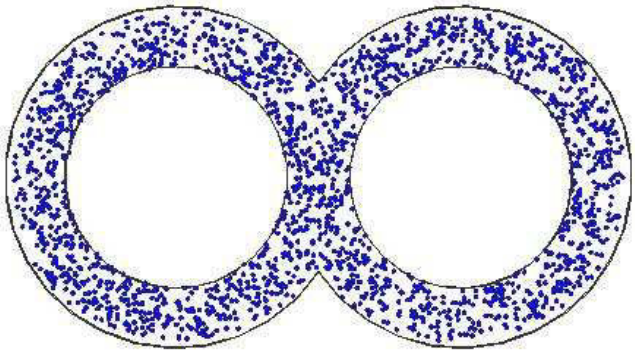

Fig. 4.4 Schematic diagram for the initial locations of 2000 virtual particles.

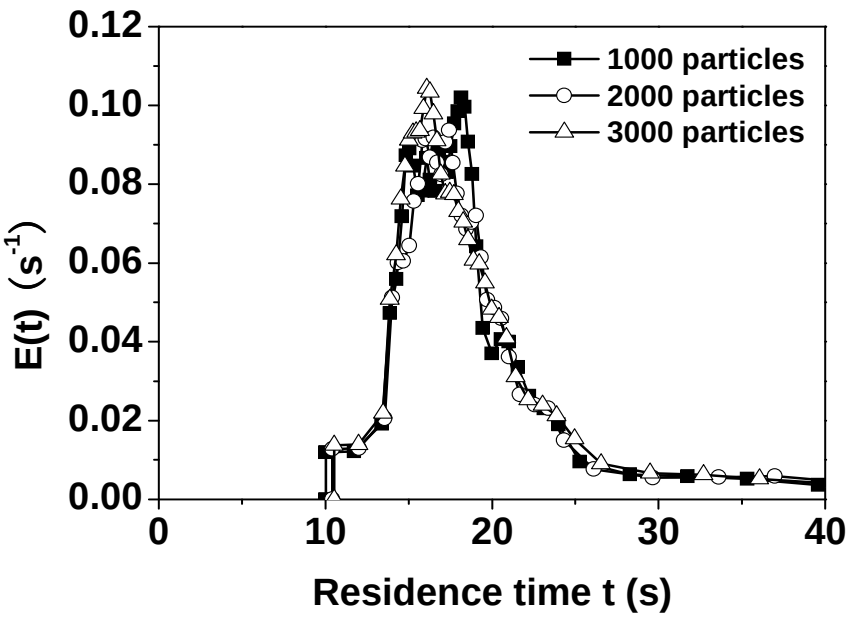

(a)

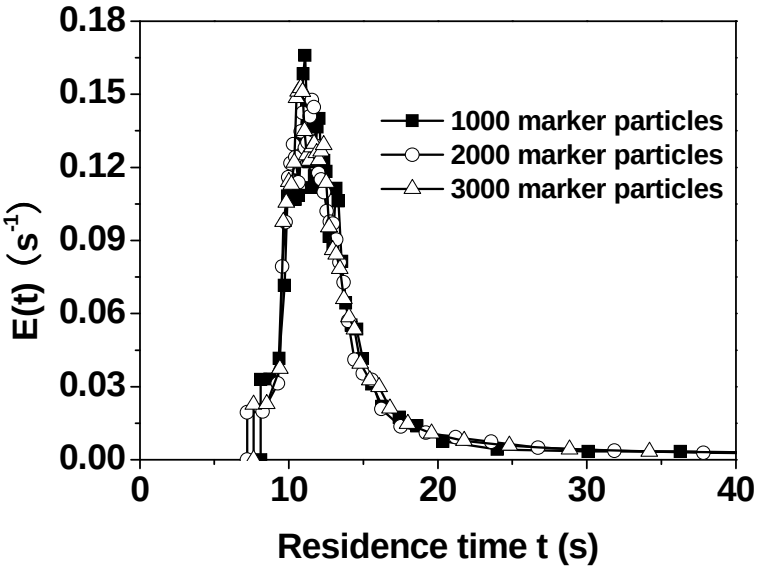

(b)

Fig. 4.5 Simulated residence time distributions with different marker particles. (a) KD2, screw speed = 120 rpm, feed rate = 10.7 kg/h; (b) KD3, screw speed = 150 rpm, feed rate = 17.8 kg/h.

Previous researchers pointed out that the initial location and orientation of interfaces had an influence on the result of mixing parameters such as the area stretch ratio η and instantaneous stretching efficiency e_η[20, 21, 28, 29]. According to Chella and Ottino, the stretch rate of the initially vertical interface perpendicular to the streamlines is faster than that of horizontal interface in the rectangular cavity flow[31]. Also they pointed out that when a large amount of the area is calculated to character the mixing performance of different mixers, the influence of initial orientation on the stretch rate is very small. Fig. 4.6 shows the effect of the number of marker particles and initial direction of interface on the arithmetic mean of the area stretch ratio and that of the instantaneous stretching efficiency in KD2. When the number of marker particles to be calculated is large such as 2000 and 3000 particles, the arithmetic means of two mixing parameters are insensitive to the initial direction and location as well as the number of marker particles. This infers that they can be used to compare the distributive mixing performance and efficiency of different types of kneading discs. Subsequently, 2000 particles with random direction are used to calculate mixing parameters.

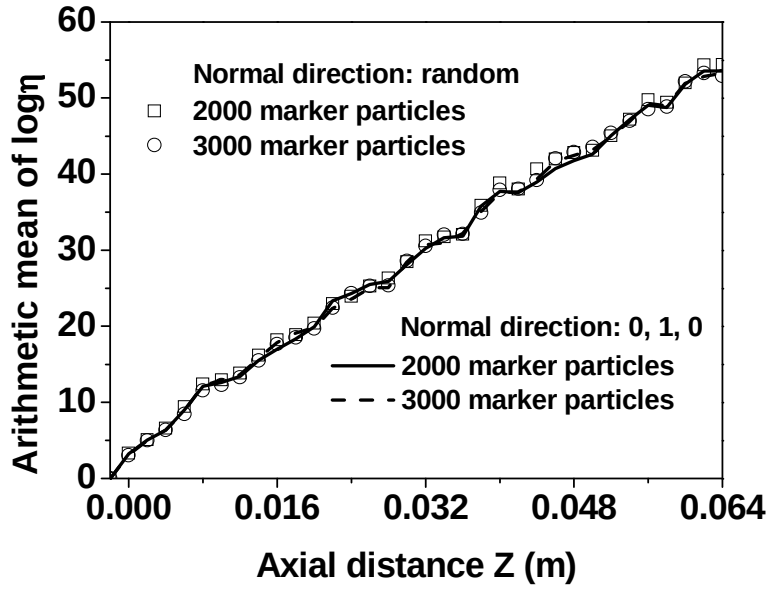

(a)

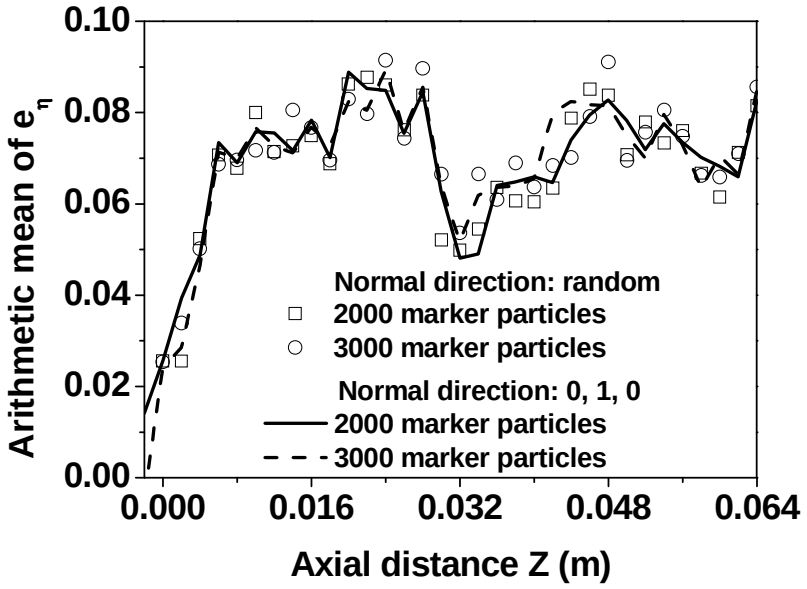

(b)

Fig. 4.6 Influence of the initial direction and location of markers, number of marker particles on (a) the arithmetic mean of logη and (b) that of e_η. KD2; screw speed = 120 rpm; feed rate = 10.7 kg/h. The normal direction is perpendicular to the surface of the marker particles. Normal direction (0, 1, 0) indicates that the surface of the marker particle is parallel to the xz plane.

4.3 Experimental

Residence time distributions are measured under the same operating conditions

as the numerical simulations. Fig. 4.7 shows the screw configuration used in this study. There are two test points as marked by probes 1 and 2. The screw elements beneath probes 1 and 2 were cylinders. The cylinders ensured full fill of the screw elements beneath probes 1 and 2 and a constant depth between the probes and the screw element surfaces. Meanwhile, using the cylinder was to make sure that the flow was fully developed in the inlet and outlet sections as it is assumed for the numerical simulations. Details about the characteristics and working principles of those probes can be found in the literatures[35, 36]. There were four identical kneading discs between probes 1 and 2, called the test zone. It was the object of the numerical simulation. However, the test zone had four pairs of identical kneading discs instead of two for the numerical simulation. The reason was that computing four pairs of kneading discs was computationally very costly. In order to overcome this problem, four pairs of kneading discs were divided into two "two pairs". It was assumed that the statistical theory for residence time distributions is applicable for calculating the residence time distribution of the four pairs from those of the two "two pairs". Based on the statistical theory[38-40], the delay time of the four pairs was twice that of the two "two pairs". $E_1(t)$ and $E_2(t)$ were measured by probes 1 and 2, respectively. Meanwhile, $E_2(t)$ was calculated by the convolution of $E_1(t)$ and $E_{12}(t)$ obtained by numerical simulations and was used to compare with the experimentally measure $E_2(t)$.

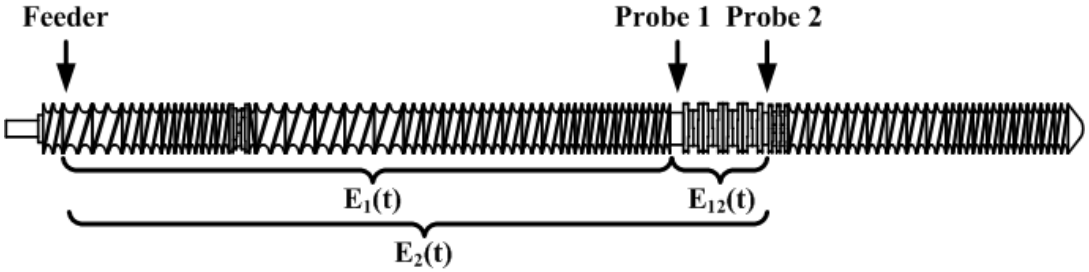

Fig. 4.7 Screw configuration and probe locations for RTD measurements.

4.4 Results

4.4.1 Experimental Validation

To gain a better understanding of the flow occurring in the kneading discs of the co-rotating twin-screw extruder, Fig. 4.8 shows the streamlines of two particles initially located at different places of the inlet. They followed different streamlines to

the exit, implying that they had different residence times. Particle one proceeded around the screws in a "figure-eight" mode, which is in agreement with the experimental results of previous researchers[41, 42]. For particle two, its motion first followed a "figure-eight" mode and then circled around one screw. It finally returned a "figure-eight" mode. The above motion modes show that as time evolved, the fluid particles underwent different degrees of shear and stress. The complex flow in the kneading discs is indicative of good mixing.

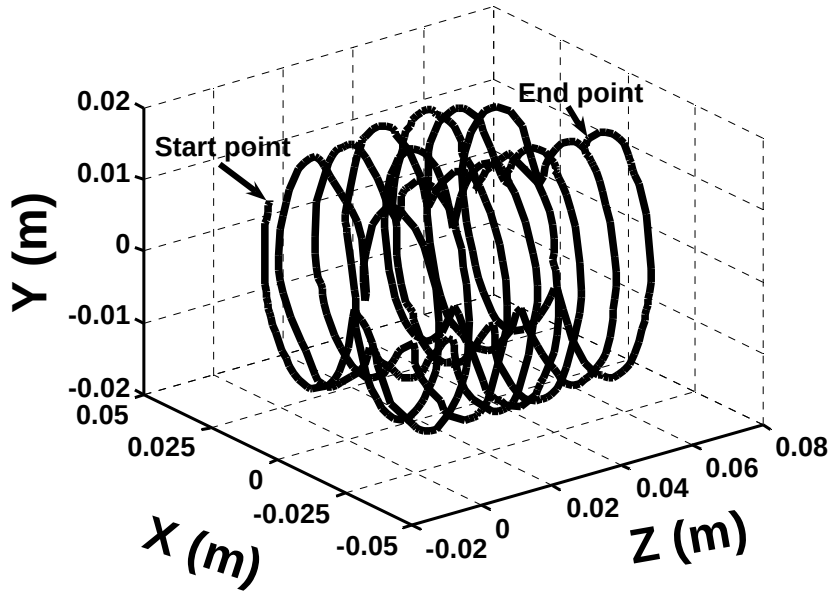

(a) Particle one

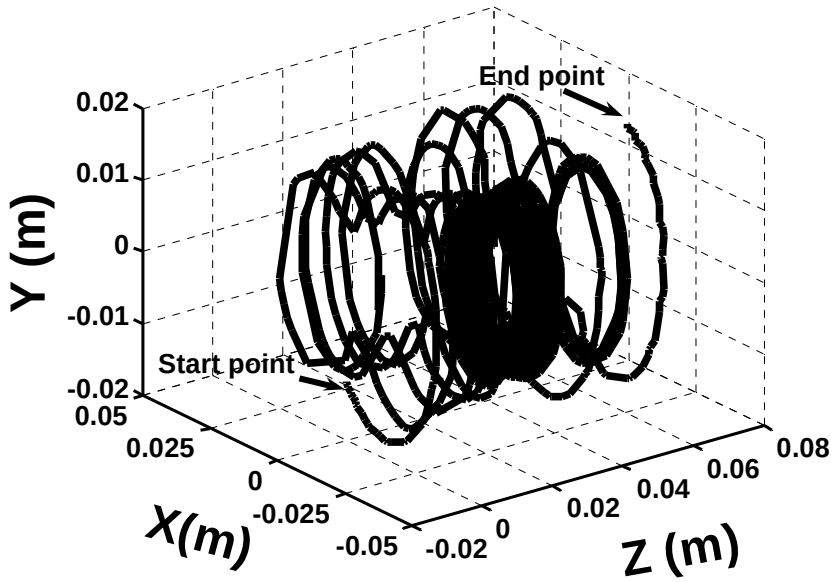

(b) Particle two

Fig. 4.8 Streamlines of two particles for KD3. Screw speed = 150 rpm; feed rate = 17.8 kg/h.

Fig. 4.9 compares the numerical local RTD results with the experimental ones for KD2. The overall trend was in good agreement. However, the former were wider than the latter. Reasons for those differences are as follows. The simulation assumed that the flow channel be fully filled and that the flow be isothermal. Those assumptions don't fully meet in practice and are the main reason for those differences. The melt density is a function of pressure and temperature, not a constant, which also lead to those differences. Meanwhile, the subtle effects of the rheology on the velocity profile could impart significant differences to mixing[20]. Fig. 4.10 compares the simulated and experimental RTD for different screw configurations. Again the 90° kneading discs has the highest axial mixing performance, but 45° and 60° kneading discs have similar axial mixing performance.

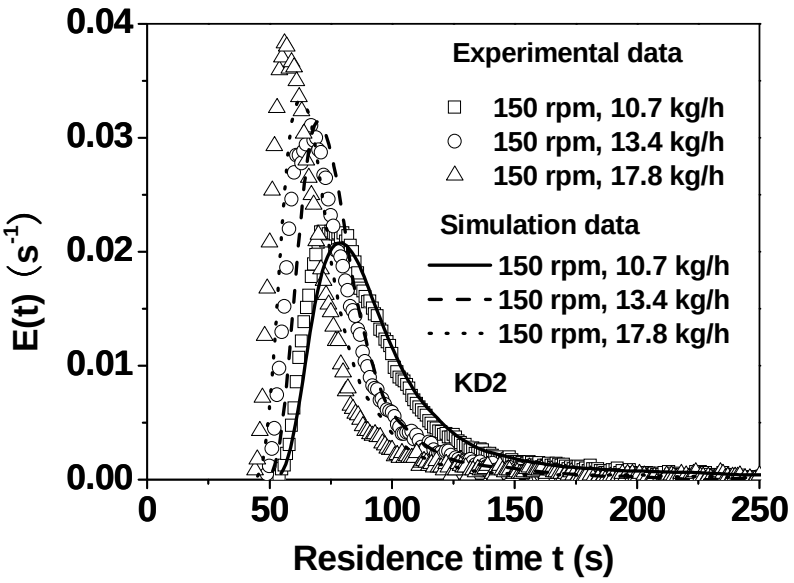

Fig. 4.9 Comparison of the local RTD between the numerical and experimental results for different feed rates.

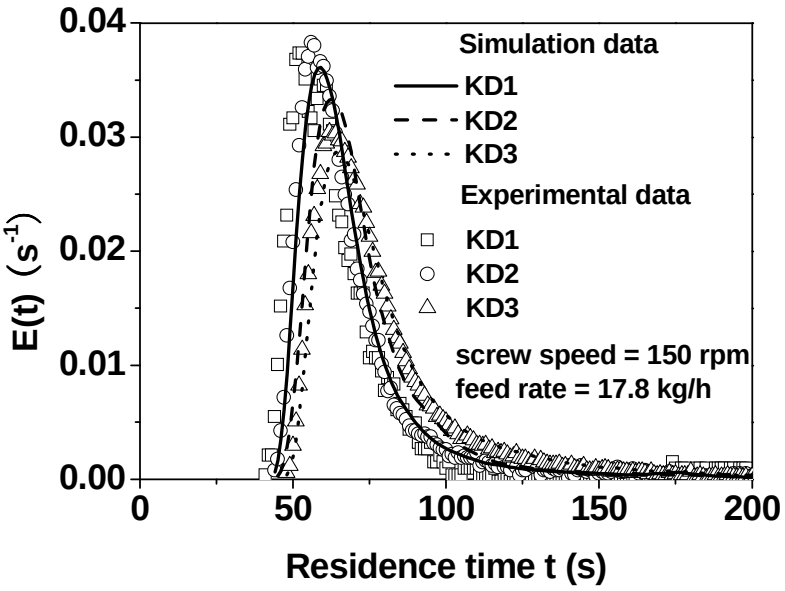

Fig. 4.10 Comparison of the local RTD between numerical and experimental results for different screw configurations.

4.4.2 Effect of Geometrical Parameters on Local Residence Time Distribution

The KD4, KD5 and KD6 have the same disc width and gap, but have different stagger angles. Fig. 4.11 shows the effect of stagger angle on the local RTD. The delay time and average residence time increased with an increase in the stagger angle. Also the 90° kneading disc provides the highest axial mixing quality.

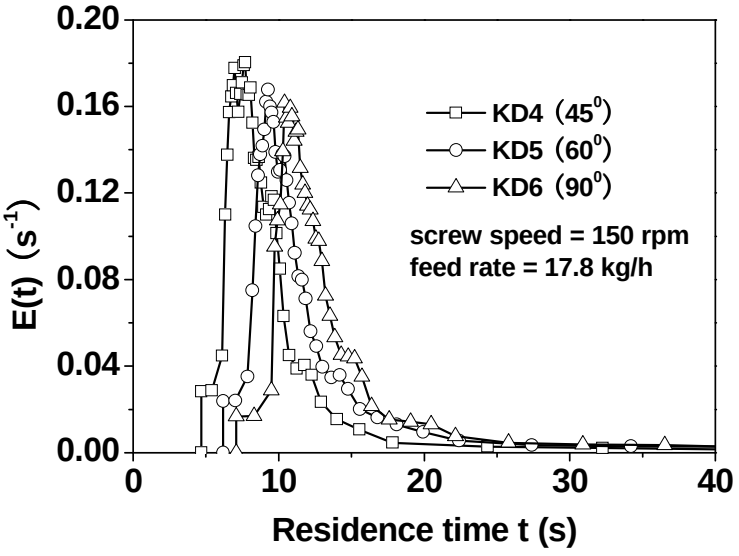

Fig. 4.11 Effect of stagger angle on the local RTD.

Fig. 4.12 shows the effects of the disc gap and width on the local RTD. The three local RTD curves are similar in delay time and shape, indicating that the KD6, KD7 and KD8 have similar axial mixing quality.

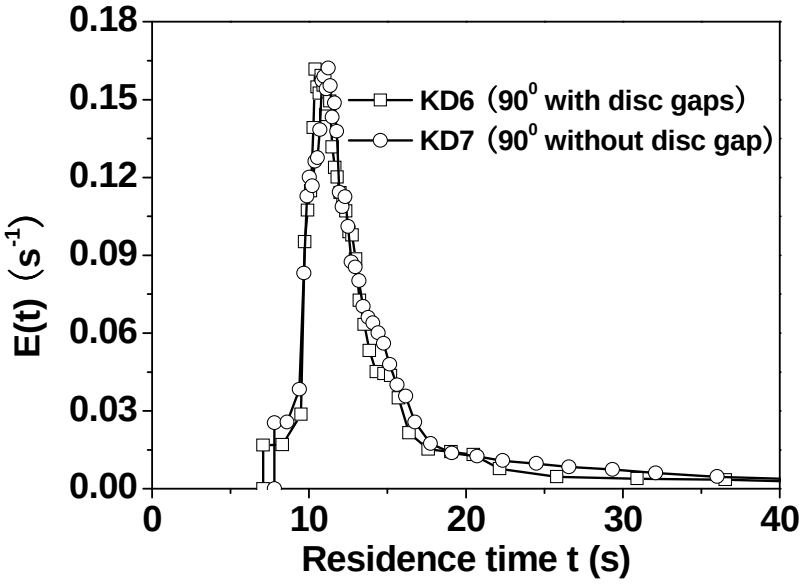

(a)

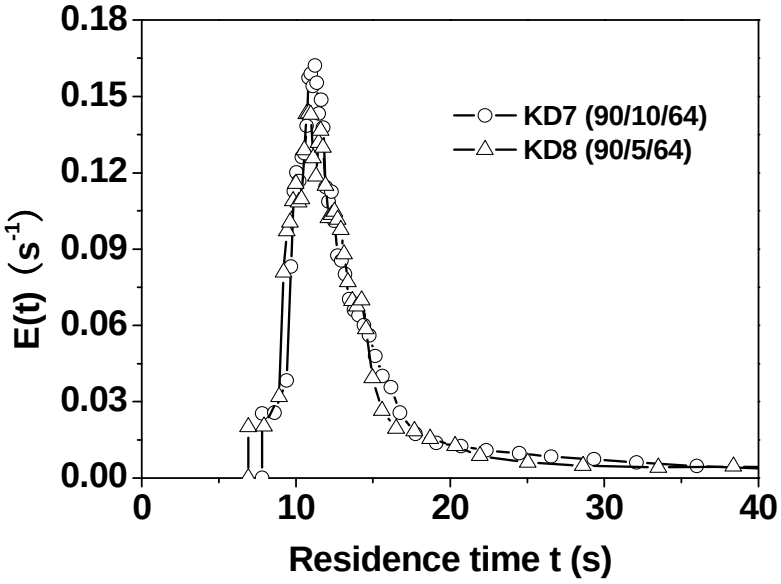

(b)

Fig. 4.12 Effects of the disc gap (a) and disc width (b) on the local RTD.

4.4.3 Distributive Mixing Performance and Efficiency

The area stretch was calculated to compare the distributive mixing performance of different types of kneading discs. An effective kneading disc requires high values

of the logarithm of the area stretch ratio over the axial distance. Distributive mixing efficiency was characterized by time-average efficiency. Fig. 4.13a shows the arithmetic mean of logη from the entry to the exit. For KD4, KD5 and KD6, it increased more or less linearly with increasing axial distance Z, indicating that η increased exponentially with Z. Among the three screw configurations, for a given axial distance the arithmetic mean of logη followed the order: KD6 > KD5 > KD4, indicating that the distributive mixing performance increased with increasing stagger angle of the kneading disc. Fig. 4.13b shows the critical value of the arithmetic mean of logη along Z for 10, 50 and 90 % marker particles for KD4, KD5 and KD6, respectively. Again it followed the order: KD6 > KD5 > KD4, regardless of the percentile of marker particles.

From Fig. 4.13a, the arithmetic mean of logη vs. Z curves fluctuated, especially at higher axial distance. This means that not all particle surfaces are stretched along Z in a steady manner. At the initial stage of mixing, it is easy to stretch the surface area and the arithmetic mean of logη increases linearly with Z. As the surface area is further stretched, area stretching becomes more difficult. Meanwhile, Ishikawa et al. pointed out that the disc gap plays an important role for mixing due to the large amount of forward and backward flow[11]. The latter may bring about stretch and shrink of surfaces. Fig. 4.13b shows that stretch and shrink of surfaces occur primarily at high area stretch ratio.

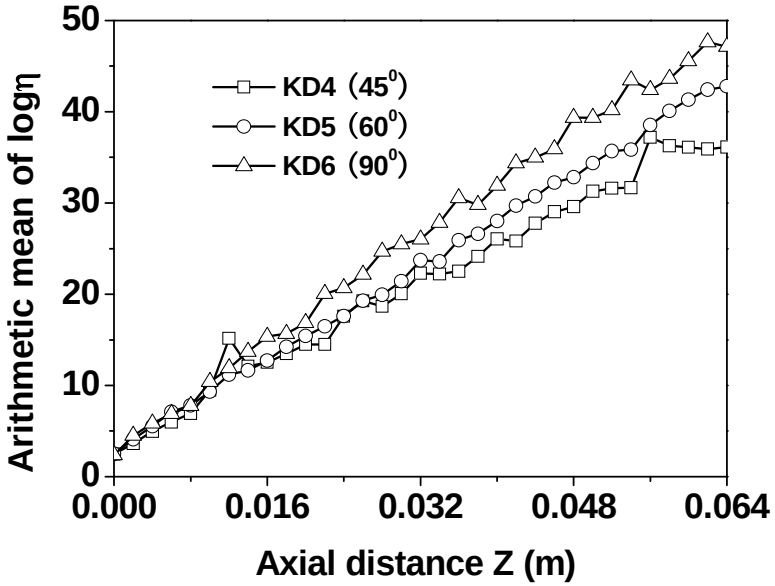

(a)

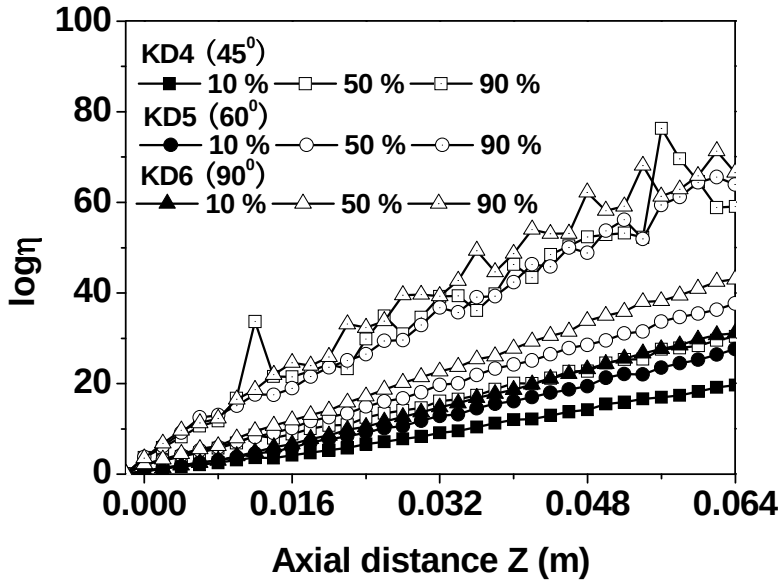

(b)

Fig. 4.13 Axial evolution of logη: (a) arithmetic mean of logη, (b) critical value of logη for given percentiles of marker particles. Screw speed: 150 rpm, feed rate: 17.8 kg/h.

Fig. 4.14a shows the effects of the disc gap and disc width on the arithmetic mean of logη as a function of Z for 90° kneading discs. The arithmetic mean of logη of a kneading disc with a gap (KD6) is higher than that of a corresponding kneading disc without disc gap (KD7). On the other hand, A kneading disc with a smaller disc width (KD7) has a higher arithmetic mean of logη than a corresponding one (KD8), indicating that the distributive mixing performance decreases with increasing disc width. This result is in agreement with that of Andersen[43]. It is also noted that unlike KD7 and KD8 whose arithmetic mean of logη increases linearly and smoothly with Z, that of KD6 also increases linearly but in a fluctuating manner. In fact each fluctuation of the arithmetic mean of logη corresponds to a passage through a gap. Fig. 4.14b shows the critical values for 10, 50, 90 % maker particles. There are no fluctuations at low percentiles such as 10 and 50 %. Fluctuations are visible only at high percentiles 90 %.

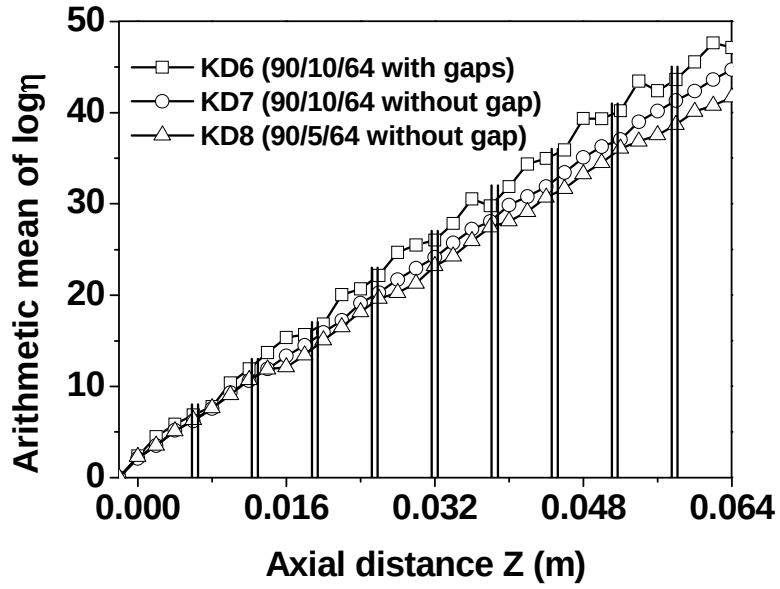

(a)

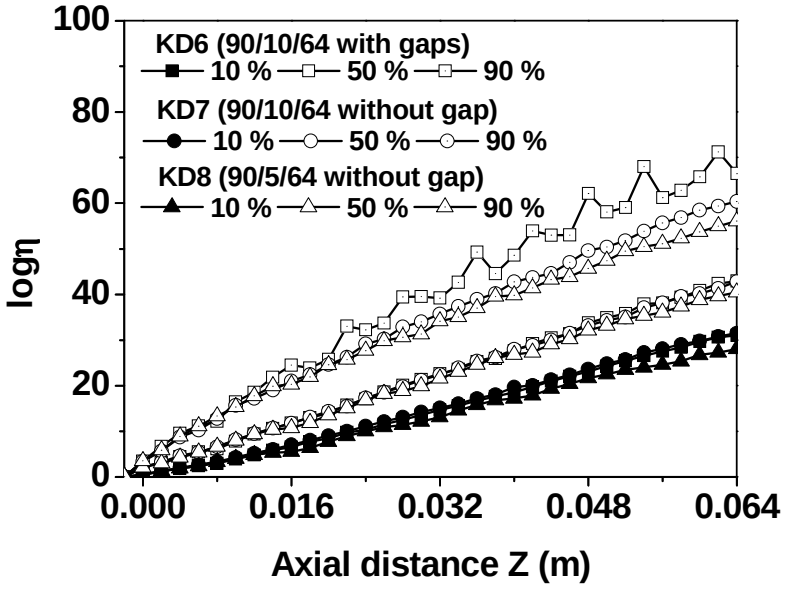

(b)

Fig. 4.14 Effect of the disc gap and disc width on the axial evolution of logη: (a) arithmetic mean of logη, (b) logη for given percentiles of marker particles. Screw speed: 150 rpm, feed rate: 17.8 kg/h. The vertical lines in Fig. 4.14(a) correspond to the locations of the disc gaps of KD6 in Fig. 4.2

In a closed system such as a batch mixer, the time-average efficiency exhibits three characteristic features: $\langle e_\eta \rangle$ decays as t^{-1} for flow with no reorientation; $\langle e_\eta \rangle$ also decays as t^{-1} but oscillates for flow with moderate reorientation; $\langle e_\eta \rangle$ oscillates without decay for flow with strong reorientation[20, 31, 32]. For an open system such as an extruder or a Kenics mixer, Z^{-1} is equivalent to t^{-1}. Fig. 4.15a shows the evolution

of the arithmetic mean of the time-average efficiency as a function of Z for KD4, KD5 and KD6. The three curves have periodic oscillations without decay as Z^{-1}, indicating that all the three kneading discs bring about strong reorientation. Among the three kneading discs, the arithmetic mean of the time-average efficiency is the highest for KD6 is highest, indicating that KD6 provides strongest reorientation. Fig. 4.15b shows the time-average efficiency as a function of Z for different percentiles of marker particles. At low percentiles such as 10 and 50%, the critical values of the time-average efficiency are similar for the three types of kneading discs. At high percentile such as 90%, KD6 yields significantly higher time-average efficiency. This indicates that at low percentiles the three types of kneading discs are similar in time-average efficiency. However, at high percentiles KD6 provides the highest time-average efficiency. It is also noted that when marker particles start moving, most of them are stretched. Nevertheless, some of them are shrunk. Therefore, they exhibit negative time-average efficiency at the initial stage. They are all stretched eventually.

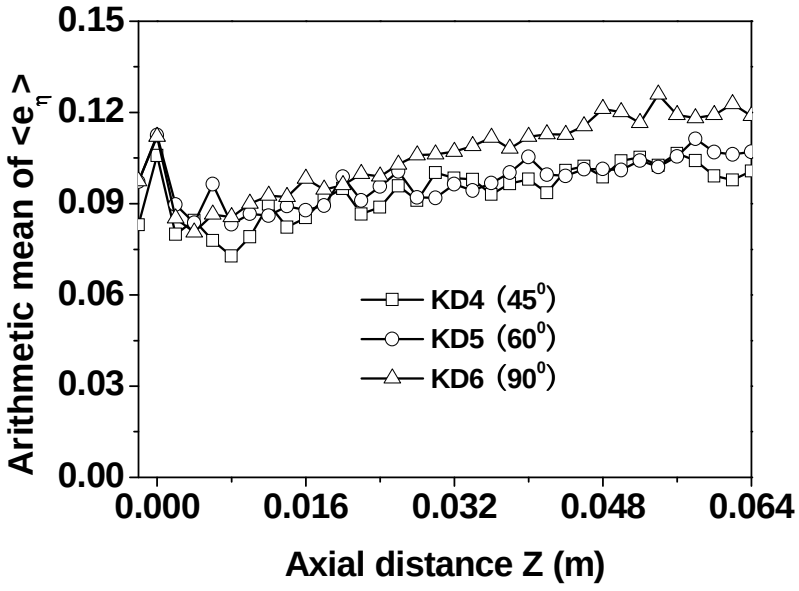

(a)

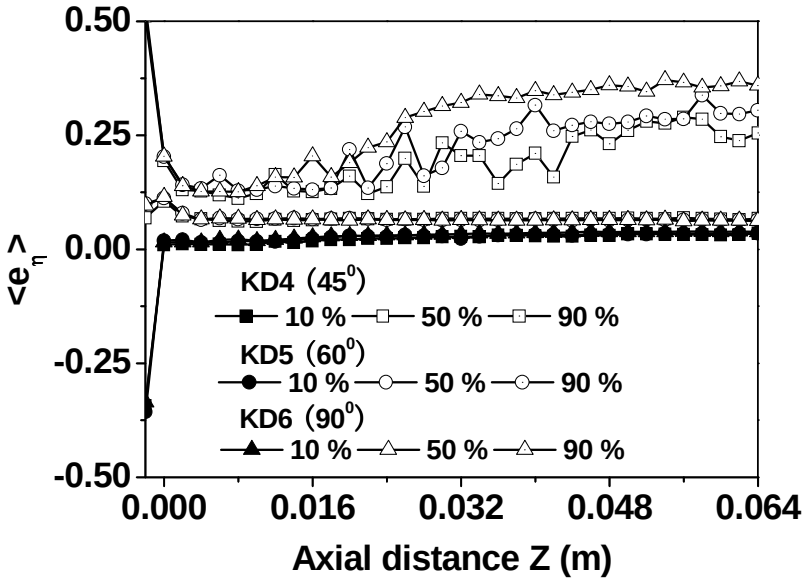

(b)

Fig. 4.15 Axial evolution of time-average efficiency <e_η>: (a) arithmetic mean of <e_η>, (b) <e_η> for given percentiles of marker particles. Screw speed: 150 rpm, feed rate: 17.8 kg/h.

As for the three 90° kneading discs (KD6, KD7 and KD8), they have similar RTD curves (see Fig. 4.12) but differ in logη (see Fig. 4.14). KD6 provides the highest logη, thus the highest distributive mixing performance. Fig. 4.16 compares these three types of kneading discs in terms of <e_η>. Clearly KD8 provides the highest mixing efficiency and not KD6. The reason is that <e_η> is not only a function of d(logη)/dt but also of D:D and RTD. Fig. 4.17 shows the evolution of $d(\log\eta)/dt$ and $(D:D)^{1/2}$ as a function of Z for KD6, KD7 and KD8, respectively. The arithmetic mean of $d(\log\eta)/dt$ is very close for the three types of kneading discs. On the other hand, the three types of kneading discs differ more or less in $(D:D)^{1/2}$, the energy dissipated. The value of $(D:D)^{1/2}$ is the lowest for KD8, indicating that the fraction of the energy dissipated for the area stretch is the highest for KD8. In sum, KD8 provides the lowest distributive mixing performance (characterized by logη) but highest mixing efficiency (characterized by <e_η>).

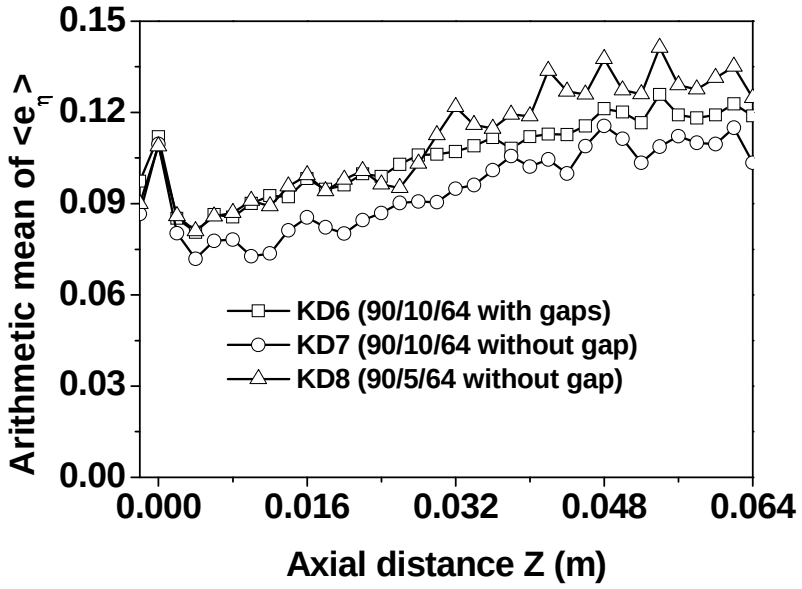

(a)

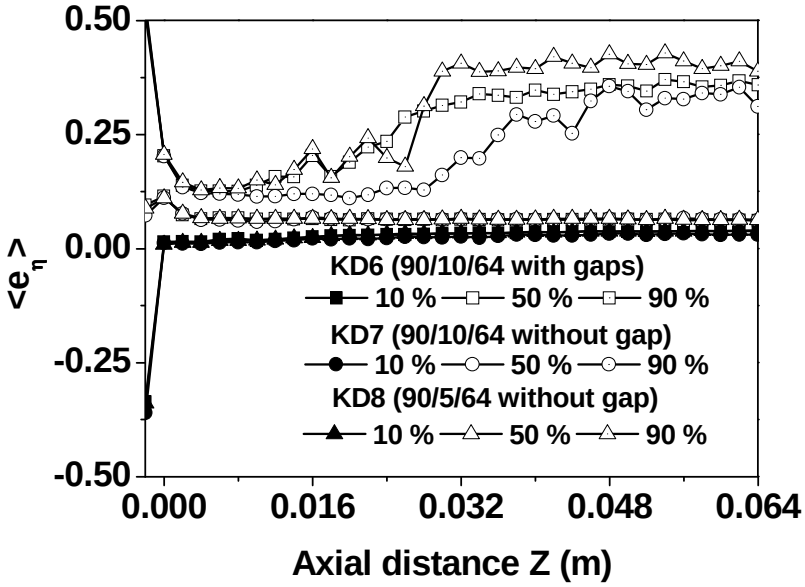

(b)

Fig. 4.16 Axial evolution of time-average efficiency $<e_\eta>$: (a) arithmetic mean of $<e_\eta>$, (b) $<e_\eta>$ for different percentiles of marker particles. Screw speed: 150 rpm, feed rate: 17.8 kg/h.

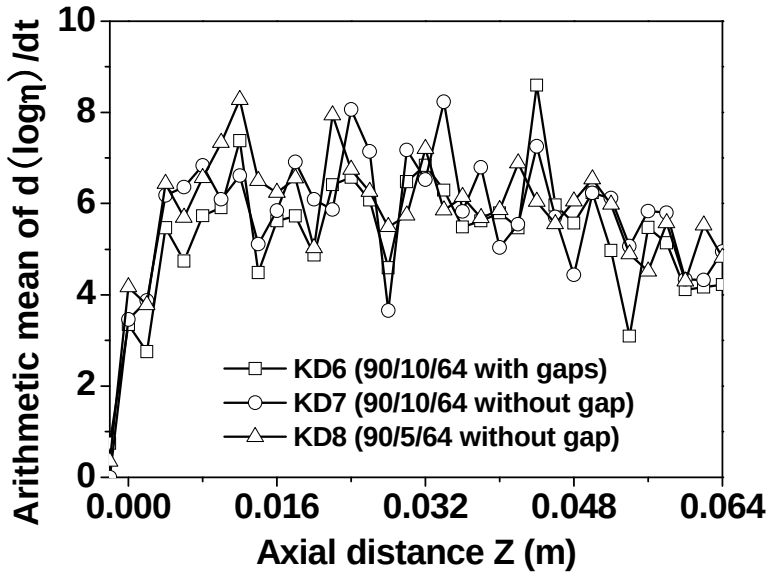

(a)

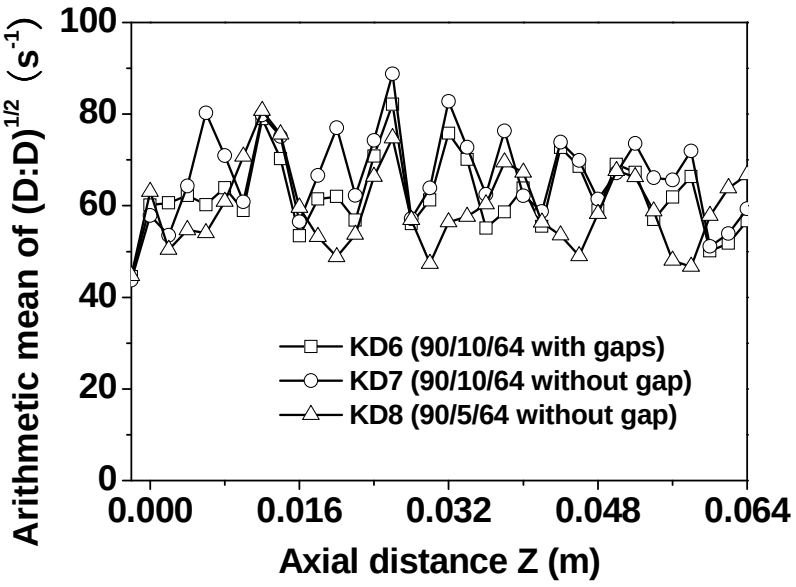

(b)

Fig. 4.17 Axial evolution of (a) the arithmetic mean of $d(\log\eta)/dt$ and (b) that of $(D:D)^{1/2}$. Screw speed: 150 rpm, feed rate: 17.8 kg/h.

4.5 Conclusion

This paper has reported on three-dimensional numerical simulations of flow and mixing in kneading discs in a co-rotating twin-screw extruder. The simulations are validated against experimentally measured local residence time distributions (RTD) using different types of kneading discs.

In addition to operating conditions, the geometry of the kneading disc may have a significant effect on the local RTD. The delay time and mean residence time increase with increasing stagger angle of the kneading disc: 45 < 60° < 90°. The axial mixing characterized by the spread of the local RTD follows the opposite trend.

The area stretch ratio η and the time-average efficiency $\langle e_\eta \rangle$ characterize the distributive mixing performance and efficiency, respectively. The former increases with increasing axial distance Z in an exponential manner for all types of kneading discs simulated in this work, indicating that they all have good distributive mixing performance. The magnitude of increase in η and $\langle e_\eta \rangle$ follows the order: 45° < 60° < 90°.

The disc gap and disc width play an important role in distributive mixing performance and efficiency. A kneading disc with a disc gap provides a higher area stretch ratio and a higher time-average efficiency than a corresponding one without disc gap. A kneading disc with a larger disc width has a lower distributive mixing performance than a corresponding one with a smaller disc width. However its distributive mixing efficiency could be higher due to lower energy dissipation. In general, kneading discs with disc gaps, small disc widths and large stagger angles provide good distributive mixing performance.

4.6 References

[1]. Baker, W.; Scott, C.; Hu, G. H. *Reactive Polymer Blending;* Hanser: Muinich, Germany, 2001.

[2]. Gao, J.; Walsh, G. C.; Bigio, D.; Briber, R. M.; Wetzel, M. D. Residence-time distribution model for twin-screw extruders. *AIChE Journal* **1999,** *45* (12), 2541-2549.

[3]. Vergnes, B.; Della Valle, G.; Delamare, L. A global computer software for polymer flows in corotating twin screw extruders. *Polymer Engineering and Science* **1998,** *38* (11), 1781-1792.

[4]. Zhu, L. J.; Narh, K. A.; Hyun, K. S. Evaluation of numerical simulation methods in reactive extrusion. *Advances in Polymer Technology* **2005,** *24* (3), 183-193.

[5]. Cassagnau, P.; Bounor-Legare, V.; Fenouillot, F. Reactive processing of thermoplastic polymers: A review of the fundamental aspects. *International Polymer Processing* **2007,** *22* (3), 218-258.

[6]. Cheng, H.; Manas-Zloczower, I. Distributive mixing in conveying elements of a ZSK-53 co-rotating twin screw extruder. *Polymer Engineering and Science* **1998,** *38* (6), 926-935.

[7]. Cheng, H.; Manas-Zloczower, I. Study of mixing efficiency in kneading discs of co-rotating twin-screw extruders. *Polymer Engineering and Science* **1997,** *37* (6), 1082-1090.

[8]. Yao, C. H.; Manas-Zloczower, I. Influence of design on dispersive mixing performance in an axial discharge continuous mixer-LCMAX 40. *Polymer Engineering and Science* **1998,** *38* (6), 936-946.

[9]. Bravo, V. L.; Hrymak, A. N.; Wright, J. D. Numerical simulation of pressure and velocity profiles in kneading elements of a co-rotating twin screw extruder. *Polymer Engineering and Science* **2000,** *40* (2), 525-541.

[10]. Bravo, V. L.; Hrymak, A. N.; Wright, J. D. Study of particle trajectories, residence times and flow behavior in kneading discs of intermeshing co-rotating twin-screw extruders. *Polymer Engineering and Science* **2004,** *44* (4), 779-793.

[11]. Ishikawa, T.; Kihara, S. I.; Funatsu, K. 3-D numerical simulations of nonisothermal flow in co-rotating twin screw extruders. *Polymer Engineering and Science* **2000,** *40* (2), 357-364.

[12]. Ishikawa, T.; Kihara, S. I.; Funatsu, K. 3-D non-isothermal flow field analysis and mixing performance evaluation of kneading blocks in a co-rotating twin srew extruder. *Polymer Engineering and Science* **2001,** *41* (5), 840-849.

[13]. Ishikawa, T.; Amano, T.; Kihara, S. I.; Funatsu, K. Flow patterns and mixing mechanisms in the screw mixing element of a co-rotating twin-screw extruder. *Polymer Engineering and Science* **2002,** *42* (5), 925-939.

[14]. Lawal, A.; Kalyon, D. M.; Li, Z. H. Computational study of chaotic mixing in co-rotating two-tipped kneading paddles: Two-dimensional approach. *Polymer Engineering and Science* **1993,** *33* (3), 140-148.

[15]. Avalosse, T. Numerical simulation of distributive mixing in 3-D flows. *Macromolecular Symposia* **1996,** *112*, 91-98.

[16]. Avalosse, T.; Rubin, Y. Analysis of mixing in corotating twin screw extruders through numerical simulation. *International Polymer Processing* **2000,** *15* (2), 117-123.

[17]. Alsteens, B.; legat, V.; Avalosse, T. Parametric study of the mixing efficiency in a kneading block section of a twin-screw extruder. *International Polymer Processing* **2004,** *19* (3), 207-217.

[18]. Avalosse, T.; Rubin, Y.; Fondin, L. Non-isothermal modeling of co-rotating and contra-rotating twin screw extruders. *Journal of Reinforced Plastics and Composites* **2002,** *21* (5), 419-429.

[19]. Connelly, R. K.; Kokini, J. L. 2-D numerical simulation of differential viscoelastic fluids in a single-screw continuous mixer: Application of viscoelastic finite element methods. *Advances in Polymer Technology* **2003,** *22* (1), 22-41.

[20]. Connelly, R. K.; Kokini, J. L. The effect of shear thinning and differential viscoelasticity on mixing in a model 2D mixer as determined using FEM with particle tracking. *Journal of Non-Newtonian Fluid Mechanics* **2004,** *123* (1), 1-17.

[21]. Connelly, R. K.; Kokini, J. K. Mixing simulation of a viscous Newtonian liquid in a twin sigma blade mixer. *AIChE Journal* **2006,** *52* (10), 3383-3393.

[22]. Breuer, O.; Chen, H. B.; Lin, B.; Sundararaj, U. Simulation and visualization of flow in a new miniature mixer for multiphase polymer systems. *Journal of Applied Polymer Science* **2005,** *97* (1), 136-142.

[23]. Ficarella, A.; Milanese, M.; Laforgia, D. Numerical study of the extrusion process in cereals production: Part I. Fluid-dynamic analysis of the extrusion system. *Journal of Food Engineering* **2006,** *73* (2), 103-111.

[24]. Ficarella, A.; Milanese, M.; Laforgia, D. Numerical study of the extrusion process in cereals production: Part II. Analysis of variance. *Journal of Food Engineering* **2006,** *72* (2), 179-188.

[25]. Jaffer, S. A.; Bravo, V. L.; Wood, P. E.; Hrymak, A. N.; Wright, J. D. Experimental validation of numerical simulations of the kneading disc section in a twin screw extruder. *Polymer Engineering and Science* **2000,** *40* (4), 892-901.

[26]. Potente, H.; Flecke, J. Analysis and modeling of the residence time distribution in intermeshing co-rotating twin screw extruders based on finite element simulations. *Journal of Reinforced Plastics and Composites* **1998,** *17* (11), 1047-1054.

[27]. Huneault, M. A. Residence time distribution, mixing and pumping in co-rotating twin screw extruders. Soc Plast Eng, Brookfield, CT, United States: 1997; pp 165-187.

[28]. Chella, R. Laminar Mixing in Miscible Fluids. In *Mixing and Compounding of polymers: Theory and Practice*, Manas-Zloczower, I., Tadmor, Z., Agassant, J. F., Eds.; Hanser: Munich, Germany, 1994; pp 1-40.

[29]. Ottino, J. M.; Ranz, W. E.; Macosko, C. W. A framework for description of mechanical mixing of fluids. *AIChE Journal* **1981,** *27* (4), 565-577.

[30]. Ottino, J. M.; Chella, R. Laminar mixing of polymeric liquids; a brief review and recent theoretical development. *Polymer Engineering and Science* **1983,** *23* (7), 357-379.

[31]. Chella, R.; Ottino, J. M. Fluid mechanics of mixing in a single-screw extruder. *Industrial and Engineering Chemistry Fundamentals* **1985,** *24* (2), 170-180.

[32]. Ottino, J. M. *The kinematics of mixing: Stretching, chaos and transport.;* Cambridge University Press: Cambridge, 1989.

[33]. Avalosse, T.; Crochet, M. J. Finite-element simulation of mixing: 1.

two-dimensional flow in periodic geometry. *AIChE Journal* **1997,** *43* (3), 577-587.

[34]. Avalosse, T.; Crochet, M. J. Finite-element simulation of mixing: 2. three-dimensional flow through a kenics mixer. *AIChE Journal* **1997,** *43* (3), 588-597.

[35]. Zhang, X. M.; Xu, Z. B.; Feng, L. F.; Song, X. B.; Hu, G. H. Assessing local residence time distributions in screw extruders through a new in-line measurement instrument. *Polymer Engineering and Science* **2006,** *46* (4), 510-519.

[36]. Zhang, X. M.; Feng, L. F.; Hoppe, S.; Hu, G. H. Local residence time, residence revolution, and residence volume distributions in twin-screw extruders. *Polymer Engineering and Science* **2008,** *48* (1), 19-28.

[37]. *POLYFLOW v3.10.0 Users Guide;* Fluent Benelux, Wavre, Belgium, 2002.

[38]. Chen, L.; Hu, G. H. Applications of a statistical theory in residence time distributions. *AIChE Journal* **1993,** *39* (9), 1558-1562.

[39]. Chen, L.; Pan, Z.; Hu, G. H. Residence time distribution in screw extruders. *AIChE Journal* **1993,** *39* (3), 1455-1464.

[40]. Chen, L.; Hu, G. H.; Lindt, J. T. Residence time distribution in non-intermeshing counter-rotating twin-screw extruders. *Polymer Engineering and Science* **1995,** *35* (7), 598-603.

[41]. Erdmenger, R. Zur Entwicklung von Schneckenverdampfern. *Chemie Ingenieur Technik* **1962,** *34* (11), 751-754.

[42]. Erdmenger, R. Mehrwellen-Schnecken in der Verfahrenstechnik. *Chemie Ingenieur Technik* **1964,** *36* (3), 175-185.

[43]. Andersen, P. Co-rotating intermeshing twin screw extruder: Berstorff's system. In *Plastics compounding: equipment and processing*, Todd, D. B., Ed.; Hanser: Munich, 1998; pp 77-136.

Chapter 5 Conclusions and Future Work

5.1 Conclusions

The incentive of this project is to develop a new instrument to measure in real time the global and partial RTD due to the lack of experimental data on partial and local axial mixing in extruders. The performance of set-up was evaluated in terms of the reproducibility and the linearity between the amplitude of the response single and the amount of the tracer. The effect of the concentration of the tracer (anthracene) in the masterbatch on the raw analogue signal and RTD was investigated in order to determine the amount of tracer. The global and partial RTD measurements were taken with various screw speeds, feed rates and screw configurations. Their residence time (delay time and average residence time) decreases with both increasing screw speed and feed rate, whatever the test location. However, the influence of screw speed on the width of RTD seemed to be only slightly affected. The RTD curves significantly narrowed with increasing feed rate, which was different from increasing screw speed.

An important aim of this work was to assess the local RTD of a kneading zone and the effect of the geometry of the latter on its RTD based on a statistical theory. In order to study the effect of different kneading discs and one special mixing element on the local RTD, the screw configurations were designed to match the in-line measurement. The results show that the local RTD of a kneading zone depended very much on the geometry (staggering angle) of the kneading discs. The local RTD of a kneading zone depended very much on the staggering angle of the kneading discs. The mean residence time and the axial mixing quality characterized by the width of the RTD following the order $30^\circ < 45^\circ \leq 60^\circ < 90^\circ <$ gear discs, indicating gear discs had the best axial mixing performance.

It was confirmed theoretically and experimentally that specific throughput Q/N, defined as a ratio of throughput (Q) over screw speed (N), was indeed a key process

parameter for controlling the dimensionless time distribution, RRD and RVD. For a given value of Q/N, the overall, partial and local RTD were different when Q and N varied. However the corresponding dimensionless RTD as well as the RRD and RVD all fell on single master curves, respectively. This is because the mean degree of fill and complete fill length were the same for a given value of Q/N.

The research work in the literature extends from the prediction of the flow field using the finite element method for numerical solution of conservation equations, to the calculation of particle trajectories for the analysis of mixing performance and the experimental verification of the model's predictions. Previous researchers compared experimental pressure, temperature and velocity along the kneading discs with predictions by numerical models. The RTD measurement validation helps understand the flow behavior and provides a novel and comprehensive approach of validating the numerical model. The distributive mixing parameters such as the area stretch ratio of material surface η, instantaneous mixing efficiency e_η and time-averaged mixing efficiency $\langle e_\eta \rangle$ are calculated using the interface tracking techniques. These parameters are then used to compare the distributive mixing performance and efficiency of different kneading discs. The disc gap and disc width play an important role in distributive mixing performance and efficiency. A kneading disc with a disc gap provides a higher area stretch ratio and a higher time-average efficiency than a corresponding one without disc gap. A kneading disc with a larger disc width has a lower distributive mixing performance than a corresponding one with a smaller disc width. However its distributive mixing efficiency could be higher due to lower energy dissipation.

5.2 Future Work

Polymer materials and extruder processing conditions (screw speed, screw configuration, barrel temperature, and die geometry) affect final product quality through the development of extruder responses (RTD, pressure, torque, product temperature, distributive and dispersive mixing) inside the barrel. Although RTD is an important parameter and has been commonly used in determining the performance of an extruder, the measurement of other response parameters such as temperature, pressure and

viscosity is necessary to control the whole extrusion processes.

The basic requirements for selecting a tracer for RTD experiments is that it should be miscible and have physical properties similar to those of the fluid under investigation, and it should be accurately detectable in small amounts, so that its introduction does not perturb the flow pattern of main stream. Macromolecular tracers should be the most ideal choice to obtain the RTD in extruders, because the tracers are chemically similar to and miscible with the polymer matrix. Therefore, the synthesis of macromolecular tracers is very significant. It is well-known that most polymer materials are two-phase/multiphase polymer blends. When the polymer materials are prepared by extrusion, the two/multi phases may be neither have the same RTD nor the same mean residence time. This finding can be obtained only when adequate macromolecular tracers are used for each of the phases.

The modeling of mixing in co-rotating twin-screw extruders is very complex, due to the complex screw configuration, material properties and the limitation of computational capabilities. In the current studies, it was assumed that extrusion processes are isothermal, that is to say, there is no heat generation and transfer, and the model based on Mesh Superposition Technology was used to simulate the dynamic motion of fluid in the twin-screw extrusion. Meanwhile, the inertia terms in the momentum equations are neglected because of high viscosity of polymer melt. These assumptions could affect the precision of the numerical simulation results. For the flow and mixing in kneading discs, a numerical simulation with three-dimensional non-Newtonian, non-isothermal and inclusion of the inertia terms is necessary.

INSTITUT NATIONAL
POLYTECHNIQUE
DE LORRAINE

AUTORISATION DE SOUTENANCE DE THESE
DU DOCTORAT DE L'INSTITUT NATIONAL
POLYTECHNIQUE DE LORRAINE

o0o

VU LES RAPPORTS ETABLIS PAR :
Monsieur Bruno VERGNES, Directeur de Recherche, Mines ParisTech, Sophia Antipolis

Monsieur Jian-Jun WANG, Professeur, Université de Zhejiang, Chine

Le Président de l'Institut National Polytechnique de Lorraine, autorise :

Monsieur ZHANG Xian-Ming

NANCY BRABOIS
2, AVENUE DE LA
FORET-DE-HAYE
BOITE POSTALE 3
F - 54501
VANDŒUVRE CEDEX

à soutenir devant un jury de l'INSTITUT NATIONAL POLYTECHNIQUE DE LORRAINE, une thèse intitulée :

"Simulation par CFD et mesure en ligne de la distribution des temps de séjour et la qualité de mélange dans une extrudeuse bi-vis"

en vue de l'obtention du titre de :

DOCTEUR DE L'INSTITUT NATIONAL POLYTECHNIQUE DE LORRAINE

Spécialité : « **Génie des Procédés et des Produits** »

Fait à Vandoeuvre, le 15 octobre 2008
Le Président de l'I.N.P.L.,
F. LAURENT

TITRE

Simulation par CFD et mesure en ligne de la distribution des temps de séjour et la qualité de mélange dans une extrudeuse bi-vis

RESUME

Aujourd'hui le développement de nouveaux matériaux polymères ayant de bonnes propriétés repose de plus en plus sur des procédés de mélange ou de compoundage de polymères au lieu de recourir à la synthèse de nouvelles molécules. L'action du mélange peut fortement influer sur la morphologie des matériaux polymères multi-constituants. Les extrudeuses bi-vis (TSE) sont souvent utilisées comme mélangeurs/réacteurs pour des procédés de mélange, de compoundage et d'extrusion réactive. Cependant, l'étude sur la qualité du mélange dans les TSE demeure un grand défi en raison de la complexité géométrique et du caractère transitoire de l'écoulement. Cette thèse a pour objet de développer un nouvel instrument en line pour mesurer en temps réel la distribution des temps de séjour (DTS) qui caractérise la performance du mélange axial et la capacité de convoyage de différents types d'éléments de vis basées sur l'analyse de l'écoulement transitoire et l'évaluation systématique de la théorie de mélange dans les TSE. Le mélange distributif des polymères fondus est caractérisé par la génération de l'aire des interfaces, un paramètre difficile à mesurer expérimentalement. Alors on fait appel à des simulations numériques de type CFD.

MOTS-CLES

CFD ; extrudeuse bi-vis ; distribution des temps de séjour ; qualité du mélange.

TITLE

CFD simulation and online measurement of the residence time distribution and mixing in twin screw extruders

ABSTRACT

The development of new materials with improved properties seems to rely nowadays more on blending and compounding than on the synthesis of chemically new polymers. Mixing may have a great effect on the morphology and structure of multi-component polymer materials. Twin-screw extruders (TSE) are widely used as mixers/reactors for blending, compounding, and reactive processing. This work aimed at developing a new instrument to measure in real time the residence time distribution (RTD) which characterizes the axial mixing and transport abilities of different screw elements based on the analysis of the transient flow pattern and systematic evaluation of mixing theory in TSE. Distributive mixing of polymer melts is characterized by the generation of interfacial area, which is experimentally much more difficult to measure. This 3D numerical simulation based on CFD is adopted.

KEY WORDS

CFD; twin screw extruder; residence time distribution; mixing.